The Dissertation Committee for Abdalrahman D. Alsulaili Certifies that this is the approved version of the following dissertation:

Impact of Bromide, NOM, and Prechlorination on Haloamine Formation, Speciation, and Decay During Chloramination

Committee:

Gerald E. Speitel Jr., Co-Supervisor

Lynn E. Katz, Co-Supervisor

Howard M. Liljestrand

Desmond F. Lawler

C. Buddie Mullins

Impact of Bromide, NOM, and Prechlorination on Haloamine Formation, Speciation, and Decay During Chloramination

by

Abdalrahman D. Alsulaili, B.S.; M.S.

Dissertation

Presented to the Faculty of the Graduate School of

The University of Texas at Austin

in Partial Fulfillment

of the Requirements

for the Degree of

Doctor of Philosophy

The University of Texas at Austin

December, 2009

Dedication

Dedicated to my parents

Acknowledgements

I would first like to thank my supervising professors Dr. Gerald E. Speitel Jr. and Dr. Lynn E. Katz. It has been a privilege to work with such brilliant and wonderful advisors. Their guidance and patience have helped me grow both scientifically and professionally. I am especially thankful for Dr. Katz's friendly encouragement. I would also like to thank my dissertation committee for their guidance and wisdom. I would like to thank Dr. Liljestrand for being available and willing to consult with me during some experimental challenges.

I am also thankful for the pioneering work and continued support of Dr. Greg Pope. His kindness in demonstrating experimental methodologies was critical to my success. I have also made many good friends in EWRE. I thank the research groups of Dr. Speitel, Dr. Katz, and Dr. Lawler for all the help they have provided, but I especially thank Shane, Hector, Patrick, and Andrew.

A special thanks to Kuwait University for the scholarship to attend the University of Texas at Austin. I gratefully thank my parents for instilling in me the values of integrity and discipline. The support and patience of my wife and daughters was remarkable, especially during these last months.

Abdalrahman Alsulaili
November 23, 2009

Impact of Bromide, NOM, and Prechlorination on Haloamine Formation, Speciation, and Decay During Chloramination

Publication No._____

Abdalrahman Daham Alsulaili, Ph.D.

The University of Texas at Austin, 2009

Co-Supervisor: Gerald E. Speitel Jr.

Co-Supervisor: Lynn E. Katz

The Chlorine-Ammonia Process was developed recently as a preoxidation process to minimize the formation of bromate during ozonation of the waters containing a significant bromide concentration. Chlorine is added first, followed by ammonia 5-10 minutes later, with the goal of sequestering bromide in monobromamine before the subsequent ozonation step. The goal of this research was to improve the Chlorine-Ammonia Process by introducing a very short prechlorination step (i.e., 30 seconds before addition of ammonia) to minimize overall disinfection by-product formation. Also, in this strategy, formation of a powerful halogenating agent, HOBr, is minimized and bromochloramine (NHBrCl) is used predominantly instead of monobromamine to sequester bromide during ozonation. To support this improved approach to bromide sequestration, this study examined the formation and decay of bromochloramine as a function of operating conditions, such as pH and Cl_2/N ratio, and refined a chemical

kinetic model to predict haloamine concentrations over time. Two natural organic matter (NOM) sources were used in this study (Lake Austin, Texas and Claremore Lake, Oklahoma) to study the effect of NOM on monochloramine and total chlorine decay after 30 seconds of prechlorination. The rate of the reaction between haloamines and fast and slow sites on the NOM was estimated. A kinetics model was developed to model total chlorine decay after a short prechlorination time. The model is based on the Unified Haloamine Kinetic Model developed by Pope (2006). Pope`s model failed to model the initial monochloramine concentration after 30 seconds prechlorination time as well as the monochloramine and total chlorine decay over time. The modified model shows an excellent prediction of monochloramine and total chlorine decay after 30 seconds prechlorination time at pH range of 6.5-8.0 and over a carbonate buffer concentration range of 2-10 mM. The model includes a new bromochloramine decay scheme via the reaction with monochloramine and with itself. In addition, new rate constants for the reaction of HOCl with bromide ion and reaction of HOBr with monochloramine were added. The hypobromous acid formation rate was found to be an acid-catalyzed reaction, which confirms the finding of Kumar et al. (1987). A new value of the acid catalysis effect of hydrogen ion was estimated. New terms were introduced to the hyprobromous acid formation rate including the acid catalysis effect of bicarbonate, carbonic acid, and ammonium ion. In addition, the reaction of HOBr with monochloramine to form bromochloramine was found to be an acid-catalyzed reaction, and a new value of the rate constant was estimated.

Table of Contents

List of Tables x

List of Figures xii

CHAPTER 1: Introduction 1

1.1. background 1

1.2. research tasks 4

1.3. Dissertation Structure 5

CHAPTER 2: Literature Review 7

2.1. introduction 7

2.2. chloramine chemistry 7

2.3. Factors Affecting monochloramine and total chlorine decay 9

2.4. Bromamine chemistry 10

2.5. bromochloramine Chemistry 12

2.6. effect of nom on monochloramine and total chlorine decay 13

2.7. effect of mode of chloramine addition 15

2.8. the reaction scheme 17

2.9. summary 18

CHAPTER 3: General Acid Catalysis of Hypobromous Acid Formation 20

3.1. Introduction 20

3.2. Materials and methods 23

3.3. results and discussion 29

3.4. Conclusions 43

CHAPTER 4: Modeling Monochloramine and Total Chlorine Decay After a Short Prechlorination Time in the Presence of Bromide 44

4.1. introduction 44

4.2. Materials and Methods 49

4.3. Kinetics model 54

4.4. Results and discussion 55

4.5. Conclusion 70

CHAPTER 5: Effect of NOM on Monochloramine and Total chlorine Decay.....72

5.1. Introduction.....72

5.2. Materials and Methods.....73

5.3. Results and discussion 81

5.4. Effect of NOM on Haloamine decay 95

5.5. Conclusion 96

CHAPTER 6: Conclusions and Engineering Significance 98

6.1. Conclusions.....98

6.2. Engineering significance.....100

Appendix -1: Brønsted p and q estimation 108

Appendix -2: Experimental Result and Model Prediction.....109

References.....122

Vita 127

List of Tables

2-1: Carbonate acid catalysis effect. 8

2-2: Hypobromous acid formation rate. 11

Table 2-3: NOM reactions. 14

Table 2-4: Unified Haloamine Kinetic Model (Pope, 2006) 18

Table 3-1: Unified Haloamine Kinetic Model (Pope, 2006) 21

Table 3-2: Molar Absorpitivities of HOBr, OBr^- and OCl^- at different wavelengths..... 26

3-3: Equilibrium constants for HOCl and HOBr 26

Table 3-4: Experimental matrix for hydrogen ion and bicarbonate acid catalysis effect on k_{11}. 26

Table 3-5: Experimental matrix for general acid catalysis effect on k_{11} at low pH 28

Table 3-6: Apparent rate constant for reaction 11 vs. different carbonate concentration at pH 9.0 31

Table 3-7: Apparent rate constant for reaction 11 vs. different pH (8.05-9.75). 34

Table 3-8: Initial monochloramine concentration and the apparent rate constant for reaction 11 at low pH range (6.55 and 7.10) 35

Table 3-9: Summary of measured and predicted acid catalysis effect for the oxidation of bromide by hypochlorous acid. 37

Table 3-10: p/q values for Brønsted plot from different sources 39

Table 3-11: Initial measured monochloramine concentration vs predicted monochloramine concentration at low pH range (6.50-8.05) 41

Table 3-12: Measured k_{11} vs. model prediction, pH range (6.55-9.75) carbonate buffer range (4-20 mM) 42

Table 4-1: The Modified Unified Haloamine Kinetic Model V 1.0 47

Table 4-2: Experimental matrix. 53

Table 4-3: The Modified Unified Haloamine Kinetic Model V 1.1 61

Table 4-4: Estimated value for k_{13} and k_{26} 63

Table 5-1: Water quality characteristics for Lake Austin and Claremore Lake 73

Table 5-2: Experimental matrix for NOM 79

Table 5-3: Modified Unified Haloamine Kinetic Model V.1.1 80

Table 5-4: TOX results for Lake Austin water 83

Table 5-5: Measured and predicted initial total chlorine and monochloramine concentration 87

Table 5-6: Reaction of NOM in the chloramination model 90

Table 5-7: Measured and predicted TOX concentration 95

Table 5-8: Modified Unified Haloamine Kinetic Model V.2 97

List of Figures

Figure 1-1: Reaction scheme for bromate formation during conventional ozonation (Pinkernell and von Gunten, 2001) 2

Figure 1-2: Operative Reaction Schemes for Different Bromate Control Strategies 3

Figure 1-3: Phases of research objectives 4

Figure 21-: Effect of chloramination addition mode in the bromate and THMS formation (Kransar (2007)) 17

Figure 3-1: Effect of carbonate buffer in the hyprobromus acid formation rate 31

Figure 3-2: Apparent rate constant for reaction 11 vs. bicarbonate concentration at pH 9.0 32

Figure 3-3: Effect o pH in the hyprobromous acid formation rate 33

Figure 3-4: Apparent rate constant for reaction 11 vs. hydrogen ion concentration at 4 mM carbonate concentration 34

Figure 3-5: Apparent rate constant for reaction 11 vs. carbonic acid concentration 36

3-6: Brønsted plot for catalysis terms of rate constant k_{11} with 95% confidence region shown 38

Figure 3-7: Effect of pH in the free chlorine decay rate 40

Figure 3-8: Effect of carbonate buffer in the free chlorine decay rate 40

Figure 3-9: Measured k_{11} vs. model prediction (lines) , pH range (6.55-9.75) carbonate buffer range (4-20 mM) 42

Figure 4-1: Model prediction (a) Monochloramine decay and (b) Total chlorine decay at (pH = 6.55, $TOTCO_3$= 7 mM, Br^-=1000 µg/L, Cl_2/N=3/1, 30 seconds prechlorination time) 48

Figure 4-2: Model prediction (a) Monochloramine decay and (b) Total chlorine decay at (pH = 8.05, $TOTCO_3$= 10 mM, Br-=1000 µg/L, Cl_2/N=3/1, 30 seconds prechlorination time) 48

Figure 4-3: Model prediction of Bromochloramine formation and decay in organic free water ($TOTCl_2$= 2 mg/L , Cl_2/N=3/1 , $TOTCO_3$=4 mM, Br-=1 mg/L , T=22^oC, and pH=7). 51

Figure 4-4: Model prediction of Bromamine + Bromochloramine formation and decay in organic free water ($TOTCl_2$= 2 mg/L, Cl_2/N=3/1 , $TOTCO_3$=4mM, Br-=1mg/L , T=22^oC, and pH=7). 51

Figure 4-5: Monochloramine and total chlorine decay ($TOTCO_3$= 4 mM, Cl_2/N=3/1, 30 seconds prechlorination time) (a) pH=6.55 and Br^-=100 µg/L, (a) pH=6.55 and Br-=1000 µg/L, (a) pH=8.05 and Br^-=100 µg/L , and (a) pH=8.05 and Br^-=1000 µg/L 57

Figure 4-6: Monochloramine and total chlorine decay (pH = 8.05, $TOTCO_3$= 4 mM, Br^- =1000 µg/L, Cl_2/N=3/:1) (a) pre ammonia addition (b) 30 seconds prechlorination 59

Figure 4-7: Monochloramine and total chlorine decay (pH = 6.55, $TOTCO_3$= 2 mM, Br-=1000 µg/L, Cl_2/N=3/1, 30 seconds prechlorination time) 63

Figure 4-8: k_{13} as a function of bicarbonate concentration at pH 8.05 65

Figure 4-9: k_{26} as a function of bicarbonate concentration at pH 8.05 65

Figure 4-10: k_{13} as a function of carbonic acid concentration at pH 6.55 66

Figure 4-11: k_{26} as a function of carbonic acid concentration at pH 6.55 66

Figure 4-12: Model fitting (a) Monochloramine decay and (b) Total chlorine decay (pH = 8.05, $TOTCO_3$= 10 mM, Br-=1000 µg/L, Cl_2/N=3/1, 30 seconds prechlorination time) 67

Figure 4-13: Model fitting (a) Monochloramine decay and (b) Total chlorine decay (pH = 6.55, $TOTCO_3$= 7 mM, Br-=1000µg/L, Cl_2/N=3/1, 30 seconds prechlorination time) ... 68

Figure 4-14: Monochloramine decay over time at pH 6.55 and different carbonate buffer concentration..... 69

Figure 4-15: Monochloramine and total chlorine decay (pH = 6.55, $TOTCO_3$= 4 mM, Br-=1000 µg/L, Cl_2/N=1/1, 30 seconds prechlorination time) (dash lines represent model prediction)..... 70

Figure 5-1: NOM reaction schematic in the presence of free chlorine, free bromine and haloamines 81

Figure 5-2: Total reactive site determination for Lake Austin NOM. 82

Figure 5-3: Total reactive site determination for Claremore Lake NOM. 82

Figure 5-4: Monochloramine and total chlorine decay (pH = 6.55, TOTCO3= 4mM, Br-=1000µg/L, Cl_2/N=3/1, 30 seconds prechlorination time) (dash lines represent model results)..... 85

Figure 5-5: Model fitting (pH = 7.0, TOTCO3= 4mM, Br-=1000µg/L, /=3/1, NOM= 5 mg/L as C, and , 30 seconds prechlorination time) (dash lines represent model results) (a) total chlorine with Lake Austin NOM, (b) monochloramine with Lake Austin NOM, (c) total chlorine with Claremore Lake NOM, and (d) monochloramine with Claremore Lake NOM, ... 91

Figure 5-6: (a) Total chlorine decay and (b) monochloramine decay (pH = 6.5, TOTCO3= 4mM, Br-=1000µg/L, Cl_2/N=3/1, 5 mg/L as C Lake Austin NOM, 30 seconds prechlorination time) (dash lines represent model prediction) 92

Figure 5-7: (a) Total chlorine decay and (b) monochloramine decay (pH = 8.0, TOTCO3= 4mM, Br-=1000µg/L, Cl_2/N=3/1, 5 mg/L as C Lake Austin NOM, 30 seconds prechlorination time) (dash lines represent model prediction) 92

Figure 5-8 Model prediction (pH = 6.5, $TOTCO_3$= 4 mM, Br-=1000 µg/L, Cl_2/N=3/1, and , Lake Austin NOM, 30 seconds prechlorination time) (dash lines represent model prediction) (a) total chlorine with 2 mg/L NOM, (b) monochloramine with 2 mg/L NOM, (c) total chlorine with 5 mg/L NOM, (d) monochloramine with 5 mg/L NOM, (e) total chlorine with 10 mg/L NOM, (f) monochloramine with 10mg/L NOM 93

Figure 5-9: (a) Total chlorine decay and (b) monochloramine decay (pH = 6.5, $TOTCO_3$= 4 mM, Br-=1000 µg/L, Cl_2/N=3/1, 5 mg/L as C Claremore Lake NOM, 30 seconds prechlorination time) (dash lines represent model prediction) 94

Figure 5-10: Monochloramine and total chlorine decay (pH = 6.55, TOTCO3= 4mM, Br^- =1000µg/L, Cl_2/N=3/1, 30 seconds prechlorination time) 96

Figure 6-1: model prediction for bromide speciation (pH=7.0, Br^- =100 µg/L, NOM=4 mg/L, Cl_2/N=3/1) (a) 30 seconds prechlorination time, (b) 5 minutes prechlorination time, (c) Preformed monochloramine, and (d) Simultaneous chlorine and ammonia addition 102

Figure 6-2: model prediction for bromide speciation (Simultaneous chlorine and ammonia addition ,pH=7.0, Br=100 µg/L, NOM=4 mg/L) (a) $TOTCl_2$= 2mg/L and Cl_2/N = 3/1, (b) $TOTCl_2$= 3 mg/L and Cl_2/N = 3/1 (c) $TOTCl_2$= 2 mg/L and Cl_2/N = 5/1, and (d) $TOTCl_2$= 2 mg/L and Cl_2/N = 1/1 104

Figure 6-3: model prediction for bromide speciation (Simultaneous chlorine and ammonia addition ($TOTCl_2$= 2 mg/L, Br=100 µg/L, NOM=4 mg/L) (a) pH-7.0 and Cl2/N = 3/1, (b) pH=7.0 and Cl_2/N = 5/1 and (c) pH=6.5 and Cl_2/N = 3/1 105

Figure 6-4: Effect of chloramine addition mode on bromate and THMs formation (pH=7.0, Cl_2/N= 4/1 and bromide = 200 µg/L) (Krasner et al., 2007) 107

CHAPTER 1: Introduction

1.1. BACKGROUND

The popularity of ozone and chloramines as disinfectants for drinking water has increased over the past 20 years because of their effectiveness as disinfectants and the reduction in halogenated Disinfection By-Product (DBP) formation associated with their use. Unfortunately, ozonation of waters containing bromide can produce undesirable concentrations of bromated, which is regulated at a Maximum Concentration Level (MCL) of 10 µg/L. Violation of the bromate MCL is of particular concern during ozonation when bromide concentrations are high or high ozone levels are required for inactivation of highly resistant pathogens. Amy *et al*. (1994) found an average concentration of 100 µg/L in source waters in the U.S. with a range of 0 to 2.3 mg/L.

Bromate formation during conventional ozonation can occur through several pathways as summarized in Figure 1-1. The oxidation of bromide occurs through formation of several key intermediates. In most pathways, $HOBr/OBr^-$ is a key intermediate, while in one pathway, commonly referred to as the indirect/direct pathway and shown along the top of Figure 1-1, $HOBr/OBr^-$ is not an intermediate.

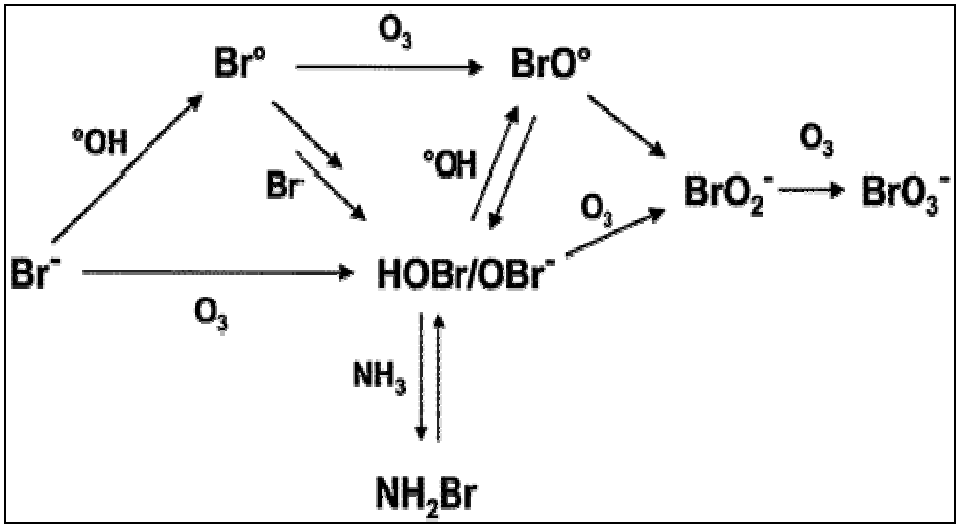

Figure 1-1: Reaction scheme for bromate formation during conventional ozonation (Pinkernell and von Gunten, 2001)

Different strategies have been used to control bromate formation during ozonation. Figure 1-2 (a) shows a strategy in which pH reduction shifts the $HOBr/OBr^-$ equilibrium toward the less reactive HOBr. This minimizes the direct ozone pathway. Figure 1-2 (b) shows ammonia addition for bromate control. Addition of ammonia leads to formation of bromamine species. This reduces the availability of $HOBr/OBr^-$ interaction with either hydroxyl radicals or ozone in the direct and direct/indirect pathway. Figure 1-2 (c) shows the *Chlorine-Ammonia Process* for bromate control. Addition of $HOCl/OCl^-$ followed by ammonia prior to ozonation also leads to reductions in the free bromide concentration and to the formation of bromamine species; however, in this process there is believed to be a significant reduction in Br^- oxidation to Br^o. One concern with the *Chlorine-Ammonia Process* is that significant formation of other halogenated DBPs is possible. Figure 1-2 (d) shows an alternative to this process that has the potential of minimizing the formation of $HOBr/OBr^-$, and reducing the indirect pathway through the formation of bromine-substituted haloamines. This latter process consists of introducing a prechloramination step, perhaps involving a very short period of

prechlorination (e.g., 30 seconds), such that the same level of bromate control can be achieved with less exposure to free chlorine and bromine, and thereby less DBP formation. The process has the potential to reduce overall DBP formation by sequestering Br in bromine-substituted haloamines prior to ozonation.

Application of any of these strategies requires a quantitative understanding of the underlying reaction chemistry. One aspect of that chemistry of primary importance in selecting among the *Chlorine Ammonia Process* and the short prechlorination is the chemistry associated with haloamine formation and decay.

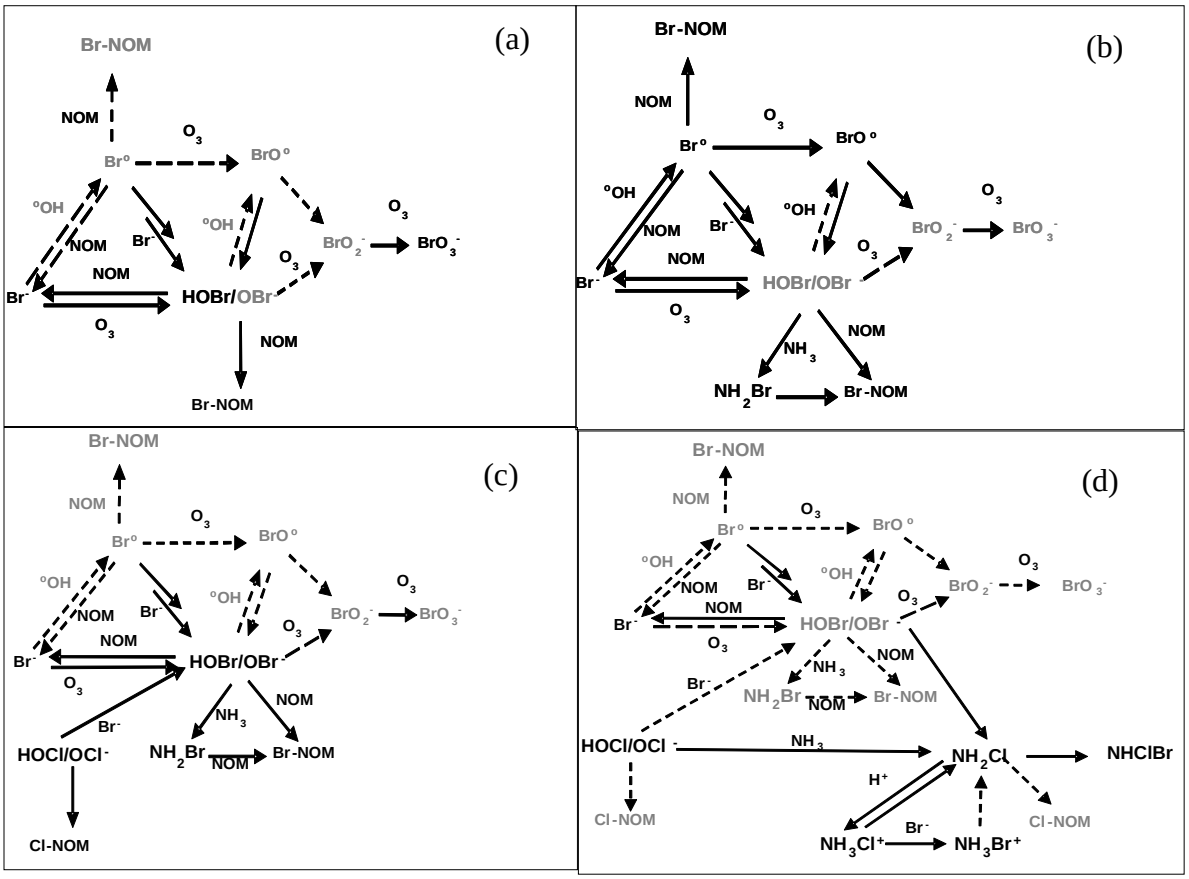

Figure 1-2: Operative Reaction Schemes for Different Bromate Control Strategies (Dashed lines and gray lettering indicate minor pathways and species, respectively)

1.2. RESEARCH TASKS

A logical approach to developing a model that describes and predicts bromate formation during ozonation is to initially address pre-ozonation chemistry and secondly incorporate reactions with ozone as shown in Figure 1-3 . Specifically, the first phase of research should focus on understanding the formation and the decay of haloamines in buffered, ultra pure water and in water containing Natural Organic Matter (NOM). The second phase of the research should then focus on understanding the decay of haloamines and formation of bromate during ozonation. This dissertation focuses on the first phase.

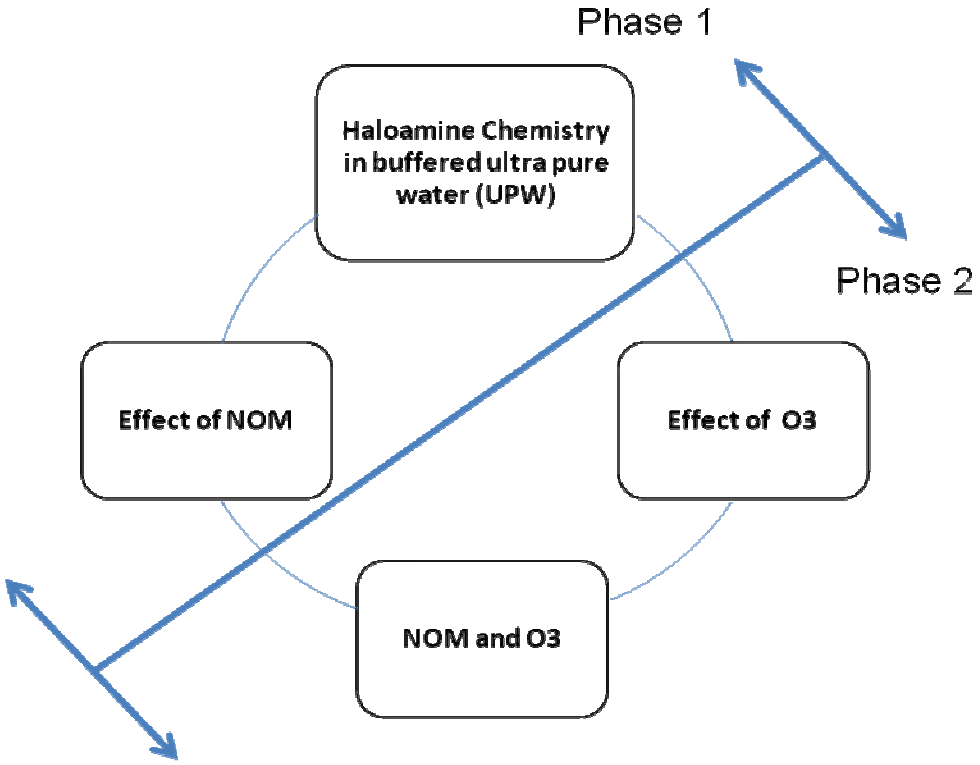

Figure 1-3: Phases of research objectives

A significant amount of research has been conducted that describes the formation and decay of monochloramine in the presence and absence of NOM. However, significantly less attention has been given to the impact of bromide in these systems.

Recently, Pope (2006) assimilated much of this literature into a unified model that describes haloamine formation and decay for preformed monochloramines and after long prechlorination periods (i.e., 5 minutes). However, the model is still limited in its ability to predict haloamine decay after a short prechlorination period and with high carbonate concentrations. The research conducted in this dissertation addresses several key questions related to extending this model:

1. What are the kinetics of haloamine formation and decay after a short prechlorination period in the presence of bromide in water free of NOM?

2. What are the kinetics of haloamine formation and decay after a short prechlorination period in the presence of bromide and NOM?

3. How can operating conditions be manipulated to decrease the concentration of free bromide and increase the formation rate of bromine-substituted haloamines?

The results from this research include the development of a Modified Unified Haloamine Kinetic Model that has a) the potential of predicting the impact of various chlorine and ammonia addition strategies prior to ozonation; and, b) and elucidates the key role of bromochloramine in controlling bromate formation during ozonation.

1.3. DISSERTATION STRUCTURE

The literature review can be found in Chapter 2. The following three chapters are devoted to experimental results and discussion and are written in manuscript format for journal papers (to be submitted). Chapter 3 focuses on the formation of HOBr from

oxidation of bromide ion by HOCl. Chapter 4 focuses on modeling the total chlorine and monochloramine decay after a short time of prechlorination period in the presence of bromide ion. Chapter 5 focuses on the impact of NOM on the decay of total chlorine and monochloramine decay after a short prechlorination period in the present of bromide ion. Chapter 6 provides conclusions and engineering significance of this work.

CHAPTER 2: Literature Review

2.1. INTRODUCTION

This research explores the use of a prechloramination strategy to control bromate formation, as well as overall DBP formation during ozonation, by using bromochloramine (NHBrCl) to sequester bromide during ozonation. The chemistry associated with bromate formation and control strategies to reduce bromate formation are complex and involve a number of reactions to describe chloramine formation and decay, the reactions between chlorine and ammonia, and the reactions between bromide ion and chlorine and chloramines. In addition, the reaction of NOM with chloramines, and free chlorine and bromine must characterized. Variations in prechloramination strategies adds further complexity to the reaction scheme, which must be characterized in order to describe and predict the reaction products as a function of water chemistry and operating conditions. This chapter provides a review of previous literature that describes these reactions.

2.2. CHLORAMINE CHEMISTRY

The reactions describing the decay of monochloramine and dichloramine in water free of bromide have been characterized previously in the literature. Valentine et al. (1992) proposed a reaction scheme for the chlorination of ammonical water (water that contains ammonia). In this study, they measured the decay of monochloramine and dichloramine under different conditions. Vikesland et al. (2001) modified the Valentine monochloramine model to account for the presence of bromide by including nitrite-monochloramine and bromide-monochloramine reactions. The resulting model did not

track the concentrations of bromine containing haloamines, which are important in understanding and modeling the total chlorine decay.

The reaction between hypochlorous acid and ammonia to form monochloramine (reaction 1 in Table 2-4) was studied by Margerum et al. (1978), Morris and Isaac (1983), and Qiang and Adams (2004). They reported almost the same value for the rate constant at 25^{o}C 3x10^{6} $M^{-1}s^{-1}$. Therefore, this reaction seems well characterized.

Monochloramine hydrolysis (reaction 5 in Table 2-4) is known to be acid catalyzed, which means the presence of hydrogen ions results in more rapid formation of dichloramine. Acid catalysis can also be achieved by other species whose catalytic effect exceeds that of the hydrogen ion. Thus, species such as carbonic acid, bicarbonate ion and ammonium ion must be considered in the overall rate of dichloramine formation. While the impact of acid catalysis on dichloramine formation has been studied by Valentine and Jafvert (1988) and Vikesland et al. (2004), they reported different values for the acid catalysis effect of carbonic acid and bicarbonate as, shown in Table (2-1). The differences are due to the different methods they used to quantify the acid catalysis constant of each species. Valentine and Jafvert found the acid catalysis effect of phosphate systems, and used it to predict the acid catalysis coefficients of carbonate system by using a Linear Free Energy Relationship. Vikesland et al. ran experiments under different carbonate concentrations to find these rate constants. Vikesland's acid catalysis coefficients are used in this study because they are developed from experimental data.

2-1: Carbonate acid catalysis effect.

	Valentine and Jafvert (1988)	Vikesland et al. (2004)
H_2CO_3	2700 $M^{-2}h^{-1}$	40,000 $M^{-2}h^{-1}$
HCO_3^-	7.2 $M^{-2}h^{-1}$	800 $M^{-2}h^{-1}$

Leao and Selleck (1983) proposed the mechanism for the decay of dichloramine as shown in reactions (8-10 in Table 2-4), which include an intermediate specie that contains one nitrogen atom. Leao and Selleck found that the dichloramine decay is OH^- catalyzed, producing an unstable intermediate and stable products such as H^+ and Cl^-.

No spectrophotometric evidence of an intermediate has been observed, which supports the hypothesis that this intermediate must exist at a very low concentration. Therefore, only the ratio of reactions (9 and 10 in Table 2-4) is important.

Jafvert and Valentine (1987) studied the decomposition of dichloramine in the presence of excess ammonia. Jafvert and Valentine (1987) used Leao and Selleck's mechanism and determined a rate constant for reaction 8 as well as a fitted value of the ratio of reactions 9 and 10.

2.3. FACTORS AFFECTING MONOCHLORAMINE AND TOTAL CHLORINE DECAY

The literature review identified different factors that can affect the decay of monochloramine, as well as total chlorine. These include:

- pH
- Buffer concentration
- Temperature
- Chlorine to ammonia ratio
- Bromide concentration
- Mode of chloramines addition

As pH decreases and buffer concentration increases, the rate of decay of monochloramine and total chlorine will increase due to the effect of acid catalysis on

monochloramine auto decomposition (reaction 5) (Valentine and Jafvert 1988, Valentine et al. 1992 and Vikesland et al. 2001).

Vikesland et al. (2001) showed that temperature has a very large effect on monochloramine stability over the range of 4-30^{o}C. Monochloramine decay will increase as temperature increases. For example, the half-life of monochloramine will decrease from 300 h to 75 h when the temperature increases from 4^{o}C to 30^{o}C at pH 7.5. Also, they showed that monochloramine stability will increase as the chlorine to ammonia ratio increases.

The presence of bromide in the water will increase the decay of monochloramine because the monochloramine will react with the bromide ion to form bromochloramine Trofe *et al*. (1980) (reaction 14 in Table 4-2), which will react with monochloramine and cause faster decay.

2.4. BROMAMINE CHEMISTRY

The presence of bromide in drinking water results in an additional set of reactions that must be considered in developing a model for the proposed prechloramination strategy. The reaction between the chlorine (I) and bromide ion is the most important mechanism in generating bromine (I) (Wong and Davidson, 1977). The oxidation of the bromide ion by hypochlorous acid has been studied by Farkas et al. (1949), Bousher (1987), and Kumar et al. (1987). They all found rate constants on the same order of magnitude (1550 to 6840 $M^{-2}s^{-1}$) at 25^{o}C. Kumar also studied the oxidation of bromide by hypochlorous acid and hypochlorite and showed that both reactions are general acid catalyzed, which means that the presence of hydrogen ions results in a more rapid formation of hypobromous acid. Acid catalysis can also be achieved by other species whose catalytic effect exceeds that of the hydrogen ion. Thus, species such as carbonic acid, the bicarbonate ion and the ammonium ion must be considered in the overall rate of

hypobromous acid formation. Kumar showed that the rate of bromide oxidation by hypochlorite is six orders of magnitude less than the rate of oxidation by hypochlorous acid, so the main bromide ion oxidation pathway will involve oxidation by hypochlorous acid (reaction 1). This reaction plays an important role, especially at a short prechlorination time (less than 0.5 min), because at this short time with a pH above the neutral, not all of the bromide will be oxidized. Finding the rate constant of hypobromous acid formation will help to determine the fraction of bromide that is oxidized during a 30-second prechlorination time. The literature reports three different values for the rate constant for the reaction between hypochlorous acid and bromide ions that forms hypobromous acid (reaction 11) (Table 2-4). Because of the large discrepancy among these values, it will be necessary to evaluate the kinetics associated with reaction 11 in this research by conducting experiments over a range of prechlorination times and pH values.

2-2: Hypobromous acid formation rate.

Rate constant at 25°C ($M^{-1}s^{-1}$)	Reference
2950	Farkas et al. (1949)
6838	Bousher et al. (1986)
1550	Kumar and Margerum (1987)

Gazda and Margerum (1994) studied the reaction of monochloramine with hypobromous acid and its conjugate base to form bromochloramine (reaction 13), and they found that the rate of the reaction of monochloramine and hypobromous acid to form bromochloramine is 2.86×10^5 $M^{-1}s^{-1}$. Gazda and Margerum's experiments covered the pH range of 9.42 to 11.36, and in this range OBr^- is the dominant species for the $HOBr/OBr^-$ system. However, this high pH is not representative of typical drinking water treatment conditions. Also, they used a high concentration of carbonate buffer (25 mM),

which is unrealistic for natural waters. Therefore, more experiments are needed here to understand this reaction under ozonation treatment conditions and a realistic range of carbonate buffer concentrations.

Lei et al. (2004) investigated bromamine decomposition in aqueous solutions (reactions 16-19). Lei et al. showed the catalysis effect of ammonia, the hydrogen ion, the carbonate buffer, and the phosphate buffer. Also, in this study, the pH ranged from 8.98 to 9.43, which is very high for ozonation treatment conditions. Lei et al. (2004) used a simplified description of the mechanism for bromamine decomposition rather than developing a model based on the complete description of the mechanism. Their simplified description of the mechanism made two key assumptions. First, the concentrations of HOBr and NBr_3 were assumed to be negligible. Second, hydrolysis of dibromamine was assumed to be slow.

2.5. BROMOCHLORAMINE CHEMISTRY

Bromochloramine can form from reactions of monochloramine with bromide or HOBr. Trofe *et al*. (1980) proposed the following reaction scheme:

$$NH_2Cl + H^+ \leftrightarrow NH_3Cl^+$$

$$NH_3Cl^+ + Br^- \rightarrow NH_3Br^+ + Cl^-$$

$$NH_3Br^+ + NH_2Cl \rightarrow NHBrCl + NH_4^+$$

Also, bromochloramine can form from the reaction of HOBr or OBr^- with monochloramine (Gazda and Margerum *et al.* 1994).

Information on bromochloramine decay is limited. Valentine (1983) proposed that NHBrCl decomposes in a base to regenerate OBr^- as a final product by the reaction below:

$$2NHBrCl + OH^- \rightarrow N_2 + 3H^+ + 2\ Cl^- + Br^- + OBr^-$$

A more detailed assessment of bromochloramine decay kinetics is needed in this research because of the practical importance of bromochloramine in controlling the formation of bromate and other DBPs.

The preceding studies have considered the reactions between chloramine-chloramine and bromamine-bromamine species individually, but have not included studies that address the reaction chemistry between the bromamine-chloramine species. These reactions are likely to be important at the lower pH range of interest in natural waters (i.e., pH 6.5-8).

2.6. EFFECT OF NOM ON MONOCHLORAMINE AND TOTAL CHLORINE DECAY

Qualls and Johnson (1983) studied the consumption of chlorine by fulvic acid. Fulvic acid was used to represent of NOM. Qualls and Johnson divided the consumption of chlorine by NOM into two reactions: a fast reaction which occurred in less than 30 seconds, and a slower reaction that continued throughout the experiments.

The application of this process to natural waters must also include the impact of NOM on the kinetics and effectiveness of the prechloramination strategy. Vikesland et al. (1998) studied the effect of NOM on the decomposition of monochloramine. Vikesland et al. found that the addition of NOM caused an increase in monochloramine destruction relative to laboratory grade water controls.

Duirk and Valentine (2005) studied the effects of six different NOM sources on monochloramine loss. Duirk and Valentine determined the total reactive sites on each NOM structure by adding free chlorine to water that contained NOM, and monitoring the residual free chlorine for approximately one month. Duirk and Valentine divided the total reactive sites found using this approach into two types of sites: fast sites which reacted

directly with monochloramine, and slow sites which reacted with free chlorine derived from monochloramine hydrolysis.

Duirk and Valentine (2006) studied the formation of dichloroacetic acid from the reaction of monochloramine with NOM. Duirk and Valentine found that NOM can be oxidized by an active chlorine species (monochloramine and hypochlorous acid) to form dichloroacetic acid.

Duirk and Valentine (2007) studied bromide oxidation and formation of dihaloacetic acids in chloraminated water. Their model did not differentiate among bromide-containing haloamines. Therefore, the work on haloamine reactions with NOM needs to be extended by conducting more detailed studies of the interaction between NOM and bromine-containing haloamines. Table 2-3 summarizes the known reactions of NOM in water that contains bromide.

Table 2-3: NOM reactions.

Reaction	Reference
$NH_2Cl + DOC_1 \rightarrow$ Products $+ DOC_{OX}$	Duirk and Valentine (2006)
$HOCl + DOC_1 \rightarrow$ Products $+ DOC_{OX}$	Duirk and Valentine (2006)
$Br(I) + DOC_2 \rightarrow DOC_{OX} + Br^-$	Duirk and Valentine (2007)

Morris (1978) showed that HOBr is a more powerful halogen than HOCl. Symons (1993) agreed with Morris and found that the reaction incorporating bromine into NOM was faster that those incorporating chlorine. Nokes et al. (1999) modeled the formation of bromine-substituted THMs in chlorinated drinking water. Nokes et al. found that the ratio of the rate constant of bromination to chlorination of the NOM was 9.

Echigo and Minear (2006) studied the reaction of HOBr with NOM in water treatment processes. Echigo and Minear used a stop-flow technique in their work and found that there are two types of reactive sites for the reaction of HOBr with NOM. Fast reactive sites range from (0.26 to 0.92 µmol.(mg C)$^{-1}$ at pH 7.0. The reaction between HOBr and the fast reactive sites took place in the first second, with an apparent second order rate constant range from $5.4x10^5$ to $1.4x10^6$ $M^{-1}s^{-1}$. In addition, they found that bromination is the major pathway during the reaction between HOBr and NOM, compared to oxidation-reduction reactions that do not yield organic bromines.

Echigo and Minear found that bromination was the dominant pathway over the chlorination pathway in the reaction with the fast sites, even when the lag time of HOBr formation is taken into account. This calculation is based on the Kumar's rate constant for the reaction of HOCl with bromide to form HOBr, which is underestimated, according to results shown in Chapter 3 of this dissertation. Echigo and Minear found that the rate constant of the reaction of HOBr with the slow sites k_2[site2] range from $9.0x10^{-3}$ to $2.7x10^{-2}$.

Chang et al. (2001) found that the ratio of applied chlorine to bromide dosage played an important role in the formation and speciation of DPBs. At a lower chlorine to bromide ratio, $CHBr_3$ was the dominant THMs specie. The same trend was observed with HAAs, dibromoacetic acid will be dominant at a lower chlorine to bromide ratio.

2.7. EFFECT OF MODE OF CHLORAMINE ADDITION

Different chloramine addition modes (prechlorination, pre-ammonia, or simultaneous chlorine and ammonia addition) lead to different bromate and THMs formation levels. Krasner et al. (2007) studied the effect of the chloramine addition mode on THM and bromate formation in a pilot study (2.25-gpm facility). As shown in Figure

2-1, prechlorination yielded the lowest bromate concentration, and as the lag time between the chlorine and ammonia decreased, the THMs concentration decreased.

Buffle et al. (2004) developed the Chlorine-Ammonia process to minimize the formation of bromate during ozonation of water that contains a significant bromide concentration. In the Chlorine-Ammonia process, chlorine is added first and after 5-10 minutes, ammonia is added. This process controls the bromate formation, but as a result of the prechlorination time, DPBs as THMs will be formed. Krasner et al. (2007) showed that reducing prechlorination time from five minutes to one minute will reduce THM formation from 28 µg/L to 16 µg/L, while bromate formation in both cases is 2 µg/L. Symons *et al*. (1998) studied the effects of delayed ammonia addition (versus preformed chloramines) and mixing intensity to simulate the less-than-perfect conditions that might be encountered at full scale. A 30-second delay between chlorine and ammonia addition produced no significant effect on DBP concentrations or speciation after 48 hours of incubation; in particular, no discernable impact on HAA formation was evident. Therefore, the formation kinetics appear slow enough such that a very short period of free chlorine exposure will have no effect on DXAA concentrations at the longer time frames of regulatory interest.

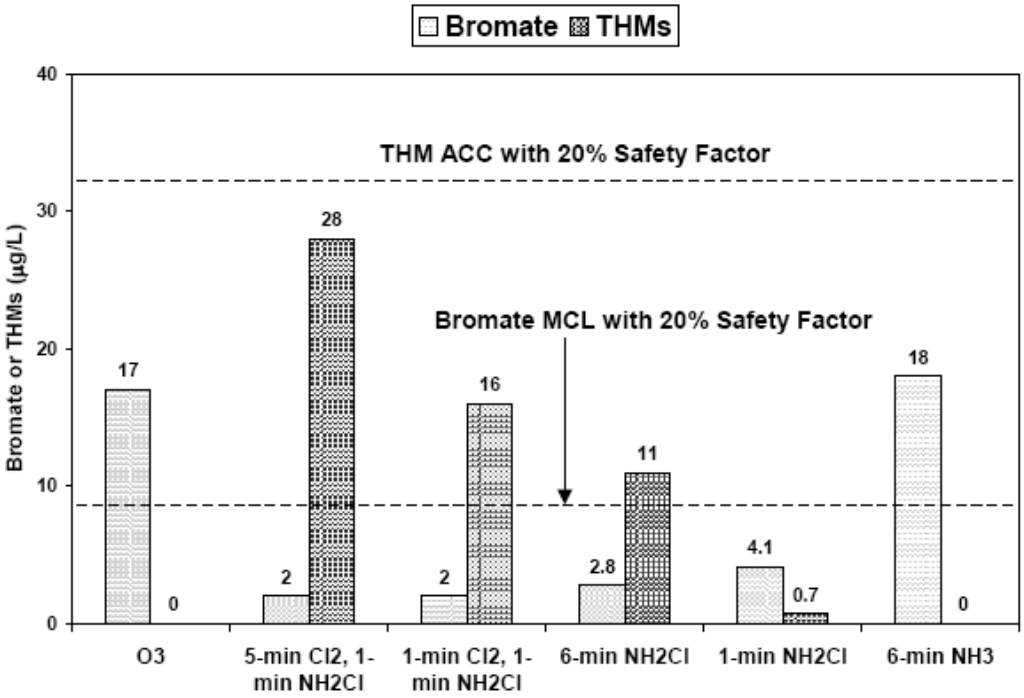

Figure 2-1: Effect of chloramination addition mode in the bromate and THMS formation (Kransar (2007))

2.8. THE REACTION SCHEME

The reaction scheme that will be used in this research is based on the Unified Haloamine Kinetic Model of Pope (2006), which incorporates the monochloramine decay model developed by Vikesland el al. (2001), the bromamine decomposition model developed by Lei et al. (2004), the bromochloramine formation and decay reactions developed by Gazda and Margerum 1994, Trofe et al. 1980, Bousher et al. 1986, and various equilibrium expressions (Table 2-4).

Table 2-4: Unified Haloamine Kinetic Model (Pope, 2006)

No.	Reaction
1	$HOCl + NH_3 \rightarrow NH_2Cl + H_2O$
2	$NH_2Cl + H_2O \rightarrow NH_3 + HOCl$
3	$NH_2Cl + HOCl \rightarrow NHCl_2 + H_2O$
4	$NHCl_2 + H_2O \rightarrow NH_2Cl + HOCl$
5	$NH_2Cl + NH_2Cl \rightarrow NHCl_2 + NH_3$
6	$NHCl_2 + NH_3 \rightarrow NH_2Cl + NH_2Cl$
7	$NH_2Cl + NHCl_2 \rightarrow N_2 + 3H + 3Cl^-$
8	$NHCl_2 + H_2O \rightarrow NOH + 2HCl$
9	$NOH + NHCl_2 \rightarrow N_2 + HOCl + HCl$
10	$NOH + NH_2Cl \rightarrow N_2 + H_2O + HCl$
11	$HOCl + Br^- \rightarrow HOBr + Cl^-$
12	$HOBr + NH_3 \rightarrow NH_2Br + H_2O$
13	$HOBr + NH_2Cl \rightarrow NHBrCl + H_2O$
14	$NH_2Cl + NH_2Cl + Br^- \rightarrow NHBrCl + Cl^- + NH_3$
15	$NHBrCl + NHBrCl + H_2O \rightarrow N_2 + HOBr + HBr + 2HCl$
16	$NH_2Br + NH_2Br \rightarrow NHBr_2 + NH_3$
17	$NHBr_2 + NH_3 \rightarrow NH_2Br + NH_2Br$
18	$NHBr_2 + NHBr_2 \rightarrow N_2 + 3H^+ + 3\,Br^-$
19	$NH_2Br + NHBr_2 + H_2O \rightarrow N_2 + HOBr + 3H^+ + 3\,Br^-$
20	$HOCl \leftrightarrow H^+ + OCl^-$
21	$NH_4^+ \leftrightarrow NH_3 + H^+$
22	$HOBr \leftrightarrow OBr^- + H^+$
23	$H_2CO_3 \rightarrow HCO_3^- + H^+$
24	$HCO_3^- \rightarrow CO_3^{2-} + H^+$

2.9. SUMMARY

A review of literature describing the underlying chemistry associated with the proposed prechloramination strategy for ozone disinfection indicates that there are a number of reactions that are not adequately described. Determination of the rates of

these reactions is essential to developing both a conceptual understanding and a practical model for predicting the impact of water chemistry and operational variables on ozonation with a prechloramination.

CHAPTER 3: General Acid Catalysis of Hypobromous Acid Formation

3.1. INTRODUCTION

Chlorination of waters containing bromide will result in its oxidation to bromine. The extent of bromine formation can vary widely depending on the bromide concentration, water quality parameters, and treatment conditions. Once formed, bromine can react with NOM to form bromine-substituted DBPs, which in general have relatively higher genotoxicity and carcinogencity than chlorine-substituted DBPs (Plewa et al., 2004, and Li et al., 2002). In addition, the presence of bromine during chloramine formation reactions may lead to the formation of significant concentrations of bromamines, bromochloramine or both. The reaction between chlorine and the bromide ion is the most important mechanism in generating bromine (Wong and Davidson, 1977).

The oxidation of bromide ion to HOBr by hypochlorous acid has been studied by Farkas et al. (1949), Bousher (1987), and Kumar et al. (1987). The values of the rate constant determined for this reaction varied among the studies, but they were all in the same order of magnitude (1550 to 6840 $M^{-1}s^{-1}$) at 25°C. Each of these different rate constants was applied to reaction 11 in the Unified Haloamine Kinetic Model (Pope, 2006), shown in Table 3-1, to model the initial monochloramine concentration after 30 seconds of prechlorination for waters containing 1000 µg/L bromide and 2 mg/L chlorine. The model failed to predict the experimentally observed monochloramine concentration regardless of which value of the rate constant was applied, illustrating the need for further study of the reaction rate for bromide oxidation.

Table 3-1: Unified Haloamine Kinetic Model (Pope, 2006)

No.	Reaction	Rate constant at 25 °C	Reference
1	$HOCl + NH_3 \rightarrow NH_2Cl + H_2O$	$3.07 \times 10^6\ M^{-1}S^{-1}$	Qiang and Adams (2004)
2	$NH_2Cl + H_2O \rightarrow NH_3 + HOCl$	$2.1 \times 10^{-5}\ M^{-1}S^{-1}$	Morris and Isaac (1981)
3	$NH_2Cl + HOCl \rightarrow NHCl_2 + H_2O$	$2.8 \times 10^2\ M^{-1}S^{-1}$	Margerum et al. (1978)
4	$NHCl_2 + H_2O \rightarrow NH_2Cl + HOCl$	$6.4 \times 10^{-7}\ S^{-1}$	Margerum et al. (1978)
5	$NH_2Cl + NH_2Cl \rightarrow NHCl_2 + NH_3$	k_5, pH dependent	Vikesland et al. (2001)
6	$NHCl_2 + NH_3 \rightarrow NH_2Cl + NH_2Cl$	$6.1 \times 10^4\ M^{-2}S^{-1}$	Hand and Margerum (1983)
7	$NH_2Cl + NHCl_2 \rightarrow N_2 + 3H + 3Cl^-$	$1.5 \times 10^{-2}\ M^{-1}S^{-1}$	Leao (1981)
8	$NHCl_2 + H_2O \rightarrow NOH + 2HCl$	$1.1 \times 10^2\ M^{-1}S^{-1}$	Jafvert and Valentine (1987)
9	$NOH + NHCl_2 \rightarrow N_2 + HOCl + HCl$	$2.8 \times 10^4\ M^{-1}S^{-1}$	Leao (1981)
10	$NOH + NH_2Cl \rightarrow N_2 + H_2O + HCl$	$8.3 \times 10^3\ M^{-1}S^{-1}$	Leao (1981)
11	$HOCl + Br^- \rightarrow HOBr + Cl^-$	$1.55 \times 10^3\ M^{-1}s^{-1}$	Kumar and Margerum (1987)
12	$HOBr + NH_3 \rightarrow NH_2Br + H_2O$	$7.5 \times 10^7\ M^{-1}S^{-1}$	Wajon and Morris (1980)
13	$HOBr + NH_2Cl \rightarrow NHBrCl + H_2O$	$2.86 \times 10^5\ M^{-1}S^{-1}$	Gazda and Margerum (1994)
14	$OBr^- + NH_2Cl \rightarrow NHBrCl + OH$	$2.2 \times 10^4\ M^{-1}S^{-1}$	Gazda and Margerum (1994)
15	$NH_2Cl + NH_2Cl + Br^- \rightarrow NHBrCl + Cl^- + NH_3$	k_{15} pH dependent	Trofe et al. (1980)
16	$NHBrCl + NHBrCl + H_2O \rightarrow N_2 + HOBr + HBr + 2HCl$	$17\ M^{-1}S^{-1}$	Valentine (1983) and Pope (2006)
17	$NH_2Br + NH_2Br \rightarrow NHBr_2 + NH_3$	pH dependent	Lei et al. (2004)
18	$NHBr_2 + NH_3 \rightarrow NH_2Br + NH_2Br$	pH dependent	Lei et al. (2004)
19	$NHBr_2 + NHBr_2 \rightarrow N_2 + 3H^+ + 3\ Br^-$	pH dependent	Lei et al. (2004)
20	$NH_2Br + NHBr_2 + H_2O \rightarrow N_2 + HOBr + 3H^+ + 3\ Br^-$	$8.9\ M^{-1}S^{-1}$	Lei et al. (2004)
21	$HOCl \leftrightarrow H^+ + OCl^-$	$pK_a = 7.5$	Connick and Chia (1959)
22	$NH_4^+ \leftrightarrow NH_3 + H^+$	$pK_a = 9.3$	Snoeyink and Jenkins (1980)
23	$HOBr \leftrightarrow OBr^- + H^+$	$pK_a = 8.8$	Haag and Hoigne (1983)
24	$H_2CO_3 \rightarrow HCO_3^- + H^+$	$pK_a = 6.3$	Snoeyink and Jenkins (1980)
25	$HCO3^- \rightarrow CO_3^{2-} + H^+$	$pK_a = 10.3$	Snoeyink and Jenkins (1980)

$k_5 = k_{H^+}[H^+] + k_{H2CO3}[H_2CO_3] + k_{HCO3}[HCO_3] + k_{H2PO4}[H_2PO_4^-] + k_{H3P}[H_3PO_4]$

$k_{15} = 1.4 \times 10^6\ M^{-2}S^{-1}\ [NH_2Cl][Br^-][H^+]$

$k_{17} = 0.5\ M^{-1}S^{-1} + 5 \times 10^8\ M^{-2}S^{-1}\ [H^+] + 2900\ M^{-2}S^{-1}\ [NH_4^+] + 540\ M^{-2}S^{-1}\ [HCO_3^-]$

$k_{18} = 1M^{-1}S^{-1} + 1 \times 10^9\ M^{-2}S^{-1}\ [H^+] + 190\ M^{-2}S^{-1}\ [NH_4^+] + 180\ M^{-2}S^{-1}\ [HCO_3^-]$

$k_{19} = 6.2M^{-1}S^{-1} + 8.3 \times 10^4\ M^{-2}S^{-1}\ [OH^-] + 3.2 \times 10^3\ M^{-2}S^{-1}\ [CO_3^{2-}]$

NOH is the unidentified monochloramine auto-decomposition intermediate.

Kumar et al. also studied the oxidation of bromide by hypochlorite, and they showed that the reaction of either hypochlorous acid or hypochlorite ion with bromide follows general acid catalysis. This means that the presence of hydrogen ions or other acidic species results in more rapid formation of hypobromous acid. Because the catalytic effect of other acids such as carbonic acid, bicarbonate and ammonium often exceeds that of the hydrogen ion, these species must be considered in the overall rate of hypobromous acid formation. Kumar et al. showed that the rate of bromide oxidation by hypochlorite is six orders of magnitude less than that of hypochlorous acid, so the main bromide ion oxidation pathway is oxidation by hypochlorous acid. Moreover, this reaction is expected to play an important role at short prechlorination times (less than 0.5 min), because not all of the bromide will be oxidized, especially at pH values in the middle to upper end of the range commonly encountered in practice. Defining the rate constant for reaction 11 more precisely will yield more accurate predictions of the percentage of bromide that is oxidized within these short time frames.

3.2. MATERIALS AND METHODS

To determine the appropriate kinetic expression for Reaction 11, a series of batch kinetic experiments were conducted over a range of solution conditions including pH, total carbonate concentration, and initial bromide concentration. While the goal of the experimental design was to provide conditions that would allow independent determination of each of the species contributing to acid catalysis, it was recognized that this could not be achieved for all of the species.

3.2.1. Materials

Aldrich 4% minimum available chlorine, a reagent grade sodium hypochlorite, was used as the source of HOCl and OCl^-. Solid KBr was used as the source of the bromide ion. NH_4Cl was used as the source of ammonia. An ammonia dosing solution was prepared to have 3.33 g/L as N. Millipore ultra pure water was used in preparing all the solutions. The pH was adjusted by NaOH and HCl, and sodium carbonate was used to buffer the solutions. An ORION® 920A meter with ORION Combination H/ATC probe were used to measure the pH, and an Agilent 8453 UV spectrophotometer was used to measure the absorbance.

For the total chlorine dosing solution and standard curve, the exact concentration of the chlorine dosing solution was measured prior to dosing using Standard Method 4500-Cl B (APHA, 1998), and by spectrophotometry at a wavelength of 292 nm and molar absorptivity of 362 $M^{-1}cm^{-1}$ for OCl^- (Furman and Margerum 1998) after rasing the pH with NaOH.

For the monochloramine standard curve, preformed monochloramine was created by mixing aqueous ammonium chloride (NH_4Cl) and sodium hypochlorite (NaOCl) solutions. These solutions were formulated so that approximately equal volumes of the two, when combined, produced the desired Cl_2/N ratio (3/1 mass ratio). Both solutions

were adjusted to pH 9 with HCl and/or NaOH. Prior to creating preformed chloramines, the concentration of the chlorine solution was measured as described above. The volume of ammonium chloride solution added was adjusted to ensure the correct Cl_2/N ratio. The chlorine solution was added slowly to the ammonium chloride solution with constant mixing in an ice bath at 1°C. After 15 minutes of mixing, the concentration of the monochloramine solution was measured using Standard Method 4500-Cl B and by spectrophotometry using a molar absorptivity of 461 $M^{-1}cm^{-1}$ at λ_{max} of 243 nm for NH_2Cl (Kumar *et al.,* 1986) prior to dosing the samples. Two measurements were made. If these measurements differed by more than 0.1 mg/L a second pair was made. If the second pair of measurements differed by more than 0.1 mg/L the solution was discarded and remixed. An average of the two appropriate measurements was used in the calculations. All solutions were mixed with Millipore ultra pure water. This procedure was used successfully in previous chloramination research (Symons *et al*., 1998).

3.2.2. Methods

Kumar et al. (1987) showed that the rate of bromide oxidation by hypochlorite is six orders of magnitude less than that of hypochlorous acid, so the main bromide ion oxidation pathway is oxidation by hypochlorous acid. In the first series of experiments, the reaction of bromide ion with hypochlorous acid to form HOBr (reaction 11 in Table 3-1) was isolated by adding chlorine and bromide into the system, but excluding ammonium.

Sodium carbonate was added to Millipore ultra pure water to buffer the solution in an Erlenmeyer flask, which was covered with foil to prevent any light from accelerating the decay of the chlorine. The pH was adjusted to the target pH (pH 8.5 to pH 9.75) using HCl and NaOH. These high pHs were selected to be at least one pH unit higher than the equilibrium constant of $HOCl/OCl^-$ system, so this reaction can be

measured directly using UV spectrophotometry. The chlorine was added, and the pH was readjusted as necessary. Bromide was then added to the solution. A 10-cm cell was used in the UV spectrophotometry. The decay of OCl^- and the formation of HOBr and OBr- were calculated by measuring the absorbance at the wavelengths shown in Table 3-2. To resolve the overlapping spectra of HOBr, OBr^-, and OCl^-, three equations were solved simultaneously, as shown in the equations below, where Abs is the absorbance at specific wavelength, a is the molar absorptivity in $M^{-1}cm^{-1}$, b is the length of the cell in cm, and C is the concentration of different species in M. The concentration of HOCl was assumed to be very low at the pH used in these experiments (one pH unit or more away from the equilibrium constant of the $HOCl/OCl^-$ system), as a result of the lower equilibrium constant of the $HOCl/OCl^-$ system. Table 3-3 shows the equilibrium constants of $HOCl/OCl^-$ and $HOBr/OBr^-$. The concentration of HOCl is one to two orders of magnitude less than the concentration of OCl^- at pH 8.5 and pH 9.0, respectively. However, the oxidation of bromide by HOCl is still expected to be the dominant pathway for bromide oxidation given the significantly higher rate constant. Experiments with different pH (8.5-9.75) and different carbonate buffer concentrations (4-20 mM) were run to estimate the general acid catalysis effect on reaction 11. Table 3-4 shows the experimental matrix.

$$Abs@260\ nm = a_{HOBr@260nm}\, b\, C_{HOBr} + a_{OBr@260nm}\, b\, C_{OBr} + a_{OCl@260nm}\, b\, C_{OCl}$$
$$Abs@292\ nm = a_{HOBr@292nm}\, b\, C_{HOBr} + a_{OBr@292nm}\, b\, C_{OBr} + a_{OCl@292nm}\, b\, C_{OCl}$$
$$Abs@329\ nm = a_{HOBr@329nm}\, b\, C_{HOBr} + a_{OBr@329nm}\, b\, C_{OBr} + a_{OCl@329nm}\, b\, C_{OCl}$$

Table 3-2: Molar Absorpitivities of HOBr, OBr^- and OCl^- at different wavelengths

Species	Absorptivity, a (M^{-1} cm^{-1})		
	260 nm	292 nm	329 nm
HOBr	85 [a]	50 [a]	25 [a]
OBr^-	25 [d]	85 [d]	332 [c]
OCl^-	102 [d]	362 [b]	110 [d]

[a] Wajon and Morris (1982) , [b] Furman and Margerum (1998), [c] Troy and Margerum 1991, and [d] this work

3-3: Equilibrium constants for HOCl and HOBr

Equilibrium	pKa at 25°C	Ref.
HOCl ↔ OCl- + H+	7.5	Connick and Chia (1959)
HOBr ↔ OBr- + H+	8.8	Haag and Hoigne (1983)

Table 3-4: Experimental matrix for hydrogen ion and bicarbonate acid catalysis effect on k_{11}.

Exp. No.	pH	Chlorine (mg/L as Cl_2)	Bromide (mg/L as Br)	Carbonate buffer (mM)
1	8.50	10	5	4
2	8.75	10	5	4
3	9.00	10	5	4
4	9.25	10	5	4
5	9.50	10	5	4
6	9.75	10	5	4
7	9.00	10	5	10
8	9.00	10	5	20

The Unified Haloamine Kinetic Model (Table 3-1) was used to fit the data and estimate the rate constant for hypobromous acid formation (Equation 11) for each of the different conditions shown in Table 3-4, and these constants were then used to estimate the acid-catalyzed rate constants. Because no ammonia was present only Reaction 11 and

equilibrium reactions 21, 23, 24, and 25 in Table 3-1 were operative for this series of experiments. The model consists of a system of ordinary differential equations for the rate expressions as well as algebraic expressions for the equilibrium expressions that describe the reactive system. The model was solved using the software package Scientist ®3.0 by Micromath Research, which uses Gear's Method to solve simultaneous differential equations. The rate constant was estimated by least squares fitting in Scientist ®3.0 using a modified Powell algorithm to minimize the unweighted sum of the squares of the residual error between the predicted and experimentally observed values. Upper and lower bounds were placed on the estimated parameter so as not to exceed reasonable estimates. The lower and upper bounds for k_{11} were set to 300 and 30,000 $M^{-1}s^{-1}$ respectively. These bounds were selected to be about one order of magnitude away from the rate constants measured by Farkas et al. (1949), Bousher et al. (1987), and Kumar et al. (1987).

The next series of experiments focused on estimating the general acid catalysis effect on the rate constant for the hypobromous acid formation (reaction 11 in Table 3-1) at lower pH. Experiments were conducted over the pH range of most interest in practice (pH 6.55- 8.05). For pH 6.55-8.05, the apparent rate constant for Reaction 11 is very large for two main reasons. First, the reaction of HOCl with Br^- is acid catalyzed, and as the pH decreases the concentration of hydrogen ion will increase. Second, at a lower pH, the ratio of HOCl to the total free chlorine concentration increases. Because the reaction rate is more rapid than at high pH, the same direct spectrophotometric technique used in the first series of experiments to estimate the rate constant could not be used for the lower pH range. Rather, an indirect technique was used by adding ammonia to the mixture of chlorine and bromide 30 seconds after chlorine addition to essentially quench the hypobromous acid formation reaction. Quenching is accomplished because any

remaining free chlorine (that did not react with bromide ion to form HOBr) will rapidly react with ammonia to form monochloramine. The rate constant for monochloramine formation, from the reaction of HOCl and NH_3, is $3.07x10^6$ $M^{-1}s^{-1}$ (Qiang and Adams 2004), which is three orders of magnitude larger than the hypobromous acid formation rate constant; therefore, the addition of ammonia effectively shuts down hypobromous acid formation. Monochloramine is the dominant chloramine species at the typical water treatment conditions used in this series of experiments. The measured initial monochloramine concentration was used in conjunction with the Unified Haloamine Kinetic Model to estimate the hypobromous acid concentration just prior to ammonia addition. The model was also used to determine an apparent k_{11} for each of the different conditions shown in Table 3-5, and these constants were then used to estimate the acid-catalyzed rate constant for H^+. The initial monochloramine concentration depends on the amount of free chlorine that remains after the reaction with the bromide ion to form hypobromous acid. Table 3-5 summarizes the experimental matrix for general acid catalysis effect on k_{11} at low pH.

Table 3-5: Experimental matrix for general acid catalysis effect on k_{11} at low pH

Exp. No.	pH	Chlorine (mg/L as Cl_2)	Bromide (mg/L as Br)	Cl_2/N	Carbonate buffer (mM)
1	6.55	2	1	3/1	4
2	7.10	2	1	3/1	4
3	8.05	2	1	3/1	4
4	6.55	2	1	3/1	4
5	8.05	2	1	3/1	7
6	8.05	2	1	3/1	7
7	8.05	2	1	3/1	10

Sodium carbonate was added to Millipore ultra pure water to buffer the solution in a 2-L Erlenmeyer flask covered with foil. Bromide was added and continuously mixed

for five minutes, then chlorine was added, and ammonia was added 30 seconds later to get the target Cl_2/N ratio shown in Table 3-5. This Cl_2/N ratio was based on the initial chlorine concentration; therefore, the actual Cl_2/N ratio at the start of the chloramination step was lower. The exact ammonia concentration added was used in the modeling, so no inaccuracies were introduced. The monochloramine concentration was measured about 2 minutes after ammonia addition to ensure that the ammonia was completely mixed and reacted with the free chlorine. Under the conditions of these experiments, monochloramine is quite stable for 5 minutes, so the slight delay in measuring the initial monochloramine concentration had no impact on the estimation of the rate constant for bromide oxidation.

Monochloramine was measured using spectrophotometry at a wavelength of 655 nm using Hach Monochlor F Reagent Powder Pillows with Hach Method 10171. Monochloramine standards of approximately 0, 0.5, 1, 2, and 3.5 mg/L as Cl_2 analyzed in triplicate prior to running the samples. This analytical technique only measures monochloramine (Chang and Blatchley 1999).

3.3. RESULTS AND DISCUSSION

The oxidation of bromide by hypochlorous acid (reaction 11 in Table 3-1) is general acid catalyzed. Thus, the overall value of k_{11} will vary depending on the concentration of acidic species. In drinking water applications, these species include hydrogen ion, bicarbonate, carbonic acid, and ammonium ion (when present) as shown in the equation below.

$$k_{11} = k_{H_2O} + k_{H^+}[H^+] + k_{HCO_3^-}[HCO_3^-] + k_{H_2CO_3}[H_2CO_3] + k_{NH_4^+}[NH_4^+]$$

By selecting various data sets from those presented in Table 3-4 and 3-5, it was possible to estimate the contribution of each of these species to the overall rate constant, k_{11}. Apparent values of k_{11} were obtained by fitting the rate data to TOTBr (HOBr and OBr^-) production for the experiments shown in Table 3-4 and by fitting initial monochloramine concentration for the experiments shown in Table 4-5.

3.3.1. Effect of water and bicarbonate

The carbonic acid system is the most common acid/base system in natural waters. Bicarbonate is the dominant carbonate species over the pH range found in natural waters, and at pH 9 it represents 97% of the total aqueous carbonate in fresh water systems. By examining rate data from experiments conducted at pH 9.0 in the absence of ammonia, it was possible to isolate the acid catalysis effect of water and bicarbonate. This isolation is due to the low concentration of both H^+ and carbonic acid at this pH. Based on these assumptions, the equation for k_{11}can be written as shown below.

$$k_{11} = k_{H_2O} + k_{HCO_3^-}[HCO_3^-]$$

The Unified Haloamine Kinetic Model and Scientist ®3.0 were used to fit the formation of total bromine over time as described in Section 3.2.2. Figure 3-1 shows the experimental results and the model fits for a series of experiments conducted over a range of total carbonate concentrations at pH 9.0.

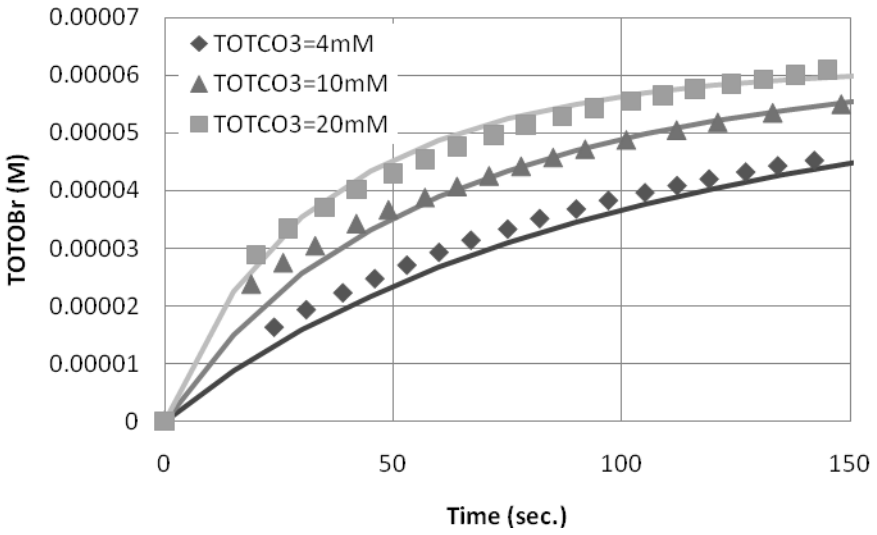

Figure 3-1: Effect of carbonate buffer in the hyprobromus acid formation rate (pH= 9.0, total OCl =0.137 mM, Bromide = 0.063 mM (points are experimental results and lines are the model fit)

Table 3-6 and Figure 3-2 show the fitted apparent rate constant for Reaction 11 at pH 9.0 and different carbonate concentrations. The slope of the line in Figure 3-2 represents the acid catalysis effect of bicarbonate (k_{HCO3}) and the intercept represents the acid catalysis effect of the water (k_{H2O}). The values of 1517 $M^{-1}s^{-1}$ for k_{H2O} and $3.00x10^5$ $M^{-2}s^{-1}$ for k_{HCO3}- suggest that the effect of carbonate is significant for total carbonate concentrations as low as 1 mM at this pH.

Table 3-6: Apparent rate constant for reaction 11 vs. different carbonate concentration at pH 9.0

Carbonate concentration (mM)	Apparent rate constant for reaction 11 ($M^{-1}s^{-1}$)
4	2676
10	4300
20	7190

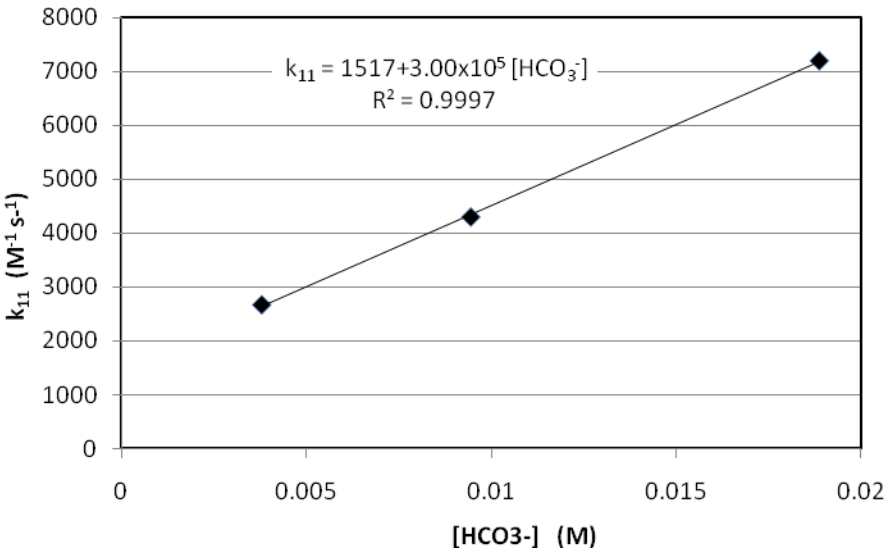

Figure 3-2: Apparent rate constant for reaction 11 vs. bicarbonate concentration at pH 9.0

3.3.2. Effect of hydrogen ion

Data from experiments conducted over pH values ranging from 8.05-9.75 were used to study the effect of the hydrogen ion on the formation rate of hyprobromous acid (reaction 11 in Table 3-1). Figure 3-3 shows the effect of pH on the formation rate of hyprobromous acid and the model fit.

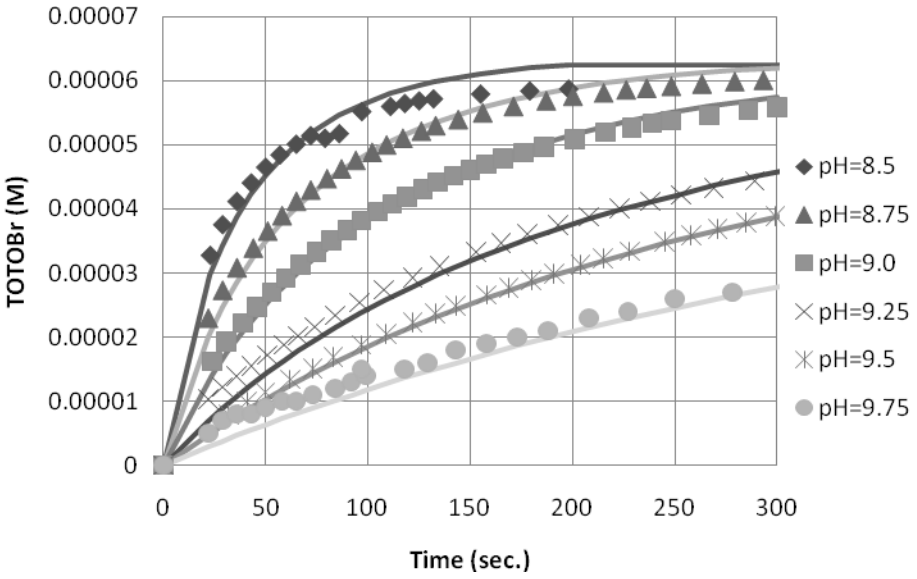

Figure 3-3: Effect o pH in the hyprobromous acid formation rate (total OCl =0.137 mM, Bromide = 0.063 mM total carbonate = 4mM (points are experiments results and lines are the model fit)

Table 3-7 shows the fitted apparent rate constant for Reaction 11 at 4 mM carbonate concentration over the pH range of 8.05-9.75. Over the elevated pH range of these experiments, the carbonic acid concentration was insignificant and, therefore, could be ignored in the data analysis. The water and bicarbonate acid catalysis terms estimated in the first set of experiments were incorporated into the expression for k_{11}, as shown below.

$$k_{11} = 1517 + 3x10^5[HCO_3^-] + k_H[H^+]$$

$$k_{11} - 1517 - 3x10^5[HCO_3^-] = k_H[H^+]$$

The fit of the rate expression model to the data is shown in Figure 3-4, where the slope of the best-fit line provides an estimate of the acid catalysis effect of hydrogen ion (k_H). The value of $2.83x10^{10}M^{-2}s^{-1}$ for k_H suggests that the effect of hydrogen ion is significant for pH as high as pH 8.5.

Table 3-7: Apparent rate constant for reaction 11 vs. different pH (8.05-9.75).

pH	Apparent rate constant for reaction 11 ($M^{-1}s^{-1}$)
8.05	2940
8.50	2776
8.75	2721
9.00	2676
9.25	2619
9.50	2539
9.75	2427

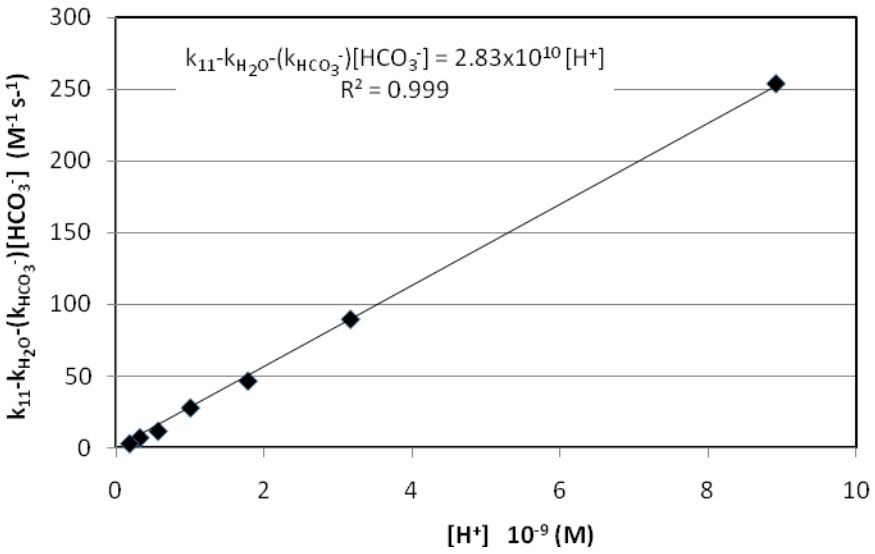

Figure 3-4: Apparent rate constant for reaction 11 vs. hydrogen ion concentration at 4 mM carbonate concentration.

3.3.3. Effect of carbonic acid

To study the effect of carbonic acid on the reaction rate, experiments were run at lower pH (6.55 -8.05) and 4mM and 7mM carbonate concentration. Under these

conditions, the rate of Reaction 11 is too fast to measure directly using UV spectrophotometry. An indirect technique was used by adding ammonia to the mixture of chlorine and bromide after 30 seconds of chlorine exposure to stop the reaction by forming monochloromine, which was then measured to infer the concentrations of HOBr and HOCl at the time of ammonia addition as shown in the equation below.

$$[TOTOBr]_{30\ sec.} = [TOTOCl]_o - [TOTOCl]_{30\ sec.}$$

Table 3-8 summarizes the apparent rate constant and the measured initial monochloramine concentration for different pH and carbonate buffer concentrations. As seen in this table, the apparent rate constants are significantly higher at lower pH.

Table 3-8: Initial monochloramine concentration and the apparent rate constant for reaction 11 at low pH range (6.55 and 7.10)

pH	total carbonate (mM)	Measured initial monochloramine (mg/L as Cl_2)	Apparent rate constant* ($M^{-1}s^{-1}$)
6.55	4	1.05	11,000
7.10	4	1.15	5,030
8.05	4	1.62	2,940
6.55	7	0.87	11,800

*Apparent rate constant for reaction 11 in Table 3-1

Acidity constants for and concentrations of H_2CO_3 are typically reported in terms of a mixed acidity constant or the mixed concentration that includes CO_2(aq). Because this mixed concentration, $H_2CO_3^*$, represents the sum of H_2CO_3 and CO_2(aq), it is necessary to calculate the actual concentration of carbonic acid rather than use values estimated from mixed acidity constants. The concentration of the carbonic acid was calculated by multiplying the total carbonate concentration by α_o (the ratio of $H_2CO_3^*$ concentration to the total carbonate buffer concentration) and then dividing the result by

630. The value of 630 is the ratio of the actual concentration of H_2CO_3 to the apparent concentration of $H_2CO_3^*$ (Snoeyink and Jenkins (1980).

The apparent rate constants for k_{11} reported in Table 3-8 were used to estimate the acid catalysis effect of carbonic acid. Incorporating the previously estimated effects of water, bicarbonate, and hydrogen ion, the expression for k_{11} is shown below.

$$k_{11} = 1517 + 2.83x10^{10}[H^+] + 3.00x10^5[HCO_3^-] + k_{H_2CO_3}[H_2CO_3]$$

$$k_{11} - 1517 - 2.83x10^{10}[H^+] - 3.00x10^5[HCO_3^-] = k_{H_2CO_3}[H_2CO_3]$$

The fit of the rate expression model to the data is shown in Figure 3-5, where the slope of the line represents the acid catalysis effect of carbonic acid ($k_{H_2CO_3}$).

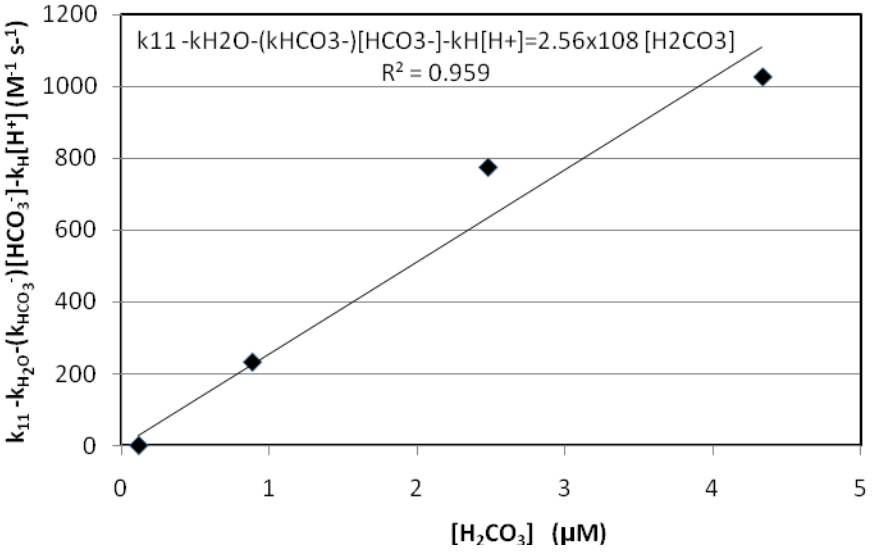

Figure 3-5: Apparent rate constant for reaction 11 vs. carbonic acid concentration

The data in Table 3-8 and Figure 3-5 suggest that the increase in the rate constant at lower pH is primarily due to H^+, as increasing the concentration of total carbonate from 4 mM to 7 mM only increased k_{11} by 7 percent, and the maximum contribution of carbonic acid (as represented by $k_{H2CO3}[H_2CO_3]$) to k_{11} is approximately 1000 $M^{-1}s^{-1}$)

3.3.4. Brønsted plot and the effect of ammonium ion

The Brønsted relationship was used to determine if the catalysis rate constants listed in Table 3-9 correlated with the acid dissociation equilibrium constants for the carbonate system and to predict the acid catalysis of the ammonium ion. The Bronsted-Relationship is:

$$\log\left(\frac{k_i}{p}\right) = \log(C_A) + \alpha \log\left(\frac{k_a q}{p}\right)$$

p is the number of equivalent acidic protons in the acid, and q is the number of equivalent basic sites in its conjugate base. It is important to recognize that the equivalency of the sites includes symmetry considerations (Espenson, 1981). The parameter α indicates the degree of proton transfer ability and the C_A is a proportionality constant.

The Brønsted relationship is shown in Figure 3-6 for the results summarized in Table 3-9. The measured acid catalysis effect of H_2O, H^+, H_2CO_3 and HCO_3^- correlated very well with their acid dissociation equilibrium constants. This correlation gives more confidence in the measured acid catalysis effect. Therefore, the Brønsted relationship can be used with some confidence to predict the acid catalysis effect of ammonium ion (k_{NH4}).

Table 3-9: Summary of measured and predicted acid catalysis effect for the oxidation of bromide by hypochlorous acid.

Catalyst	pKa	p	q	log(Kaq/p)	log(k_ip)	k_i (M^{-2} s^{-1})	
						measured	predicted
H_2O	15.42[e]	2	1	-15.72	1.14	27.33*	
HCO_3^-	10.30	1	3	-9.82	5.48	3.00×10^5	
NH_4^+	9.30	4	1	-9.90	5.01		4.06×10^5
H_2CO_3	6.35	2	2	-6.35	8.11	2.56×10^8	
H^+	-1.72[e]	3	1	1.24	9.97	2.83×10^{10}	

[e] from Kumar and Margerum 1987

*k_i for H_2O calculated by dividing k_{H2O} (1517 $M^{-1}s^{-1}$) by the water molarity, 55.5 M

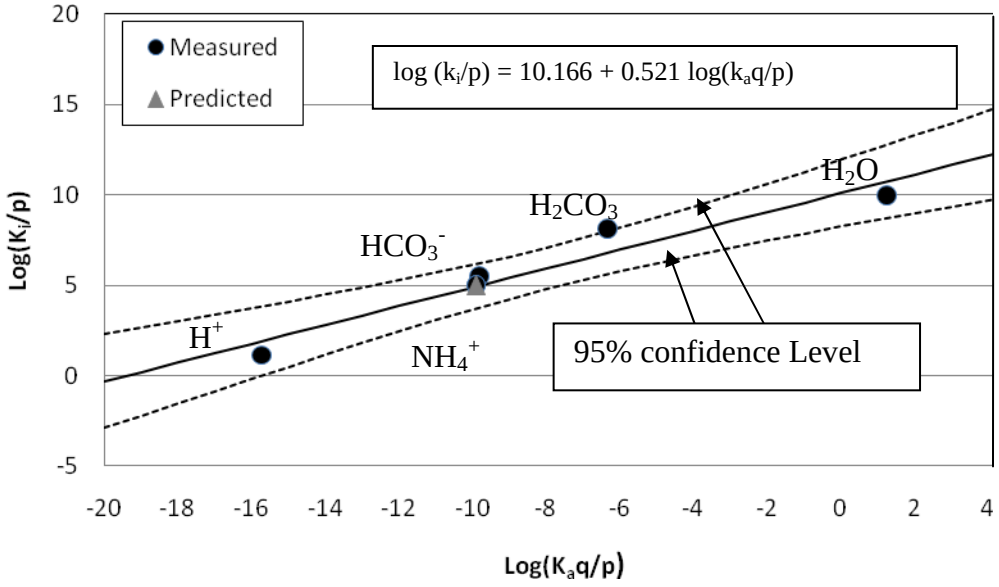

3-6: Brønsted plot for catalysis terms of rate constant k_{11} with 95% confidence region shown

It should be noted that the literature reports different values of p and q for the species shown in Table 3-9, as illustrated in Table 3-10. This difference in p and q values will affect the correlation between acid catalysis effects and the acid dissociation equilibrium constant, as well as the value of the acid catalysis effect estimated from Brønsted plot. To offer clarity on the approach used in this research, Appendix I shows the calculation of p and q for the different species in this research.

Table 3-10: p/q values for Brønsted plot from different sources

Species	Valentine and Jafvert (1988)	Lei et al. (2004)	This work
H^+	1/1	3/2	3/1
HCO_3^-	1/2	1/3	1/3
H_2CO_3	2/1	2/3	2/2
NH_4^+	N.A.	4/4	4/1
H_2O	N.A.	2/3	2/1

N.A. : Not Available

3.3.5. Modeling

The final expression for the rate constant associated with Reaction 11 in Table 3-1 is shown below:

$$k_{11}=1517+2.83x10^{10}[H^+] + 3.0x10^5[HCO_3^-] + 2.56x10^8[H_2CO_3] + 4.06x10^5[NH_4^+]$$

This expression was verified by incorporating it into the Unified Haloamine Kinetic Model and predicting TOTOCl (HOCl and OCl^-) decay as a function of time. The model accurately predicted TOTOCl decay for systems containing 4 mM total carbonate over the pH range of 8.5-9.75, as shown in Figure 3-7. The model also showed excellent predictions for TOTOCl decay over time at pH 9.0 for varying carbonate concentrations (4-20 mM), as shown in Figure 3-8. It should be noted that data from experiments at pH 6.55 and 7 mM carbonate buffer and at pH 8.05 and 7mM and 10 mM carbonate buffer were not used in the calibration of k_{11} above further verifying the predictive capabilities of this model.

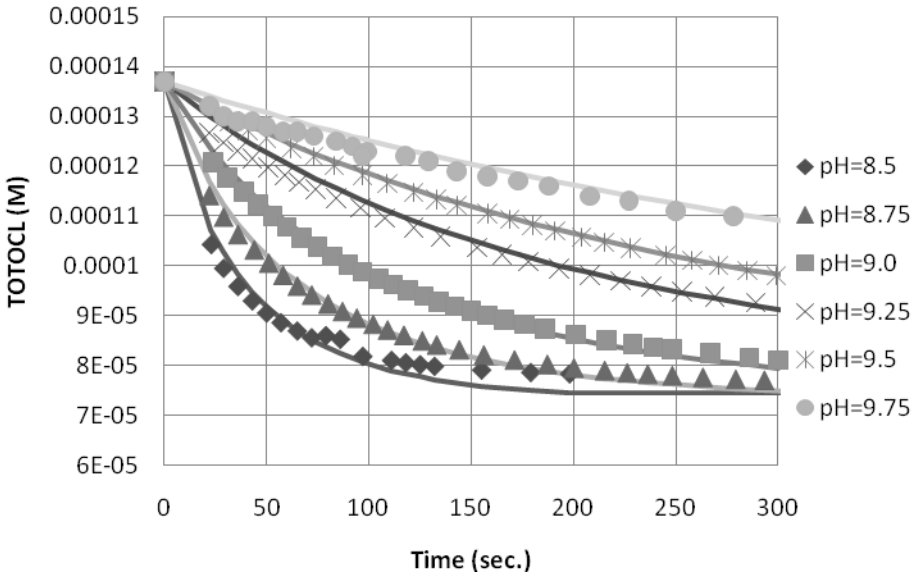

Figure 3-7: Effect of pH in the free chlorine decay rate (TOTOCl = 0.137 mM, Bromide = 0.063 mM total carbonate = 4mM (points are experimental results and lines are the model prediction)

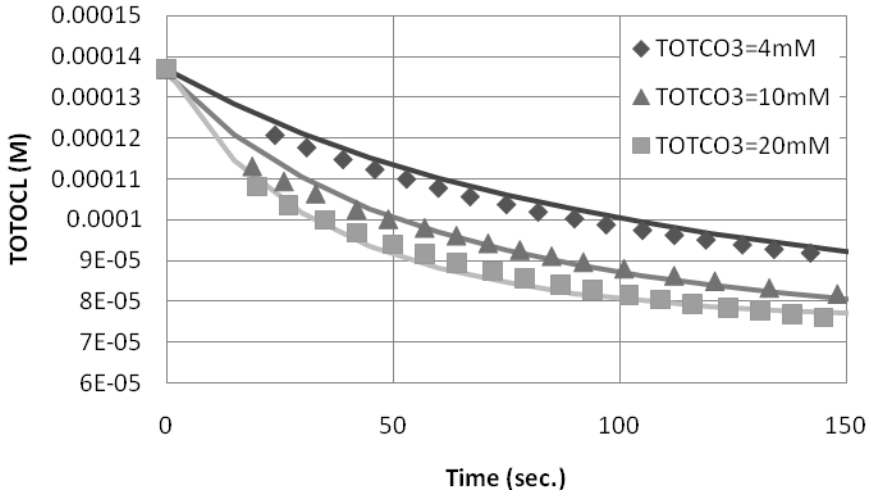

Figure 3-8: Effect of carbonate buffer in the free chlorine decay rate (TOTOCl = 0.137 mM, Bromide = 0.063 mM total carbonate = 4mM (points are experimental results and lines are the model prediction)

In addition, the model provided excellent predictions of the initial monochloramine concentration in the experiments in which ammonia was added after a 30 second prechlorination period as shown in Table 3-11.

Table 3-11: Initial measured monochloramine concentration vs predicted monochloramine concentration at low pH range (6.50-8.05)

pH	total carbonate (mM)	Measured initial monochloramine (mg/L as Cl_2)	Predicted initial monochloramine (mg/L as Cl_2)	% Error
6.55	4	1.05	1.10	4.76
7.10	4	1.15	1.13	-1.74
8.05	4	1.62	1.57	-3.08
6.55	7	0.87	0.91	4.60
8.05	7	1.49	1.54	3.36
8.05	10	1.46	1.48	1.36

3.3.6. Summary

The estimated acid catalysis effect of the water (1517 $M^{-1}s^{-1}$) agreed very well with the value estimated by Kumar et al. (1987) (1548 $M^{-1}s^{-1}$); however, the estimated acid catalysis effect of the hydrogen ion ($2.83x10^{10}M^{-2}s^{-1}$) is four orders of magnitude higher than the value estimated by Kumar et al. ($1.3x10^{6}M^{-2}s^{-1}$). As shown in Figure 3-9, the acid catalysis effect of hydrogen ion will be the dominant parameter in k_{11} at pH less than 7.5, which suggests that Kumar et al. underestimated the effect of hydrogen ion. In addition, Kumar et al. only estimated the acid catalysis effect of water and the hydrogen ion, while in this research the acid catalysis effect of bicarbonate, carbonic acid, and ammonium ion was estimated. Also, the estimated k_{11} at high pH (9.00-9.75) (k_{11} about 2600 M^{-1} s^{-1}) agreed well with the one estimated by Farkas et al. (1949) (k_{11}= 2950 M^{-1} s^{-1}), presumably because their experiments were run at high pH (above pH 10). The value of k_{11} was on the same order of magnitude as the value reported by Bousher et al. (1987) except at the lowest pH (6.55), most likely due to the high pH range that Bousher et al. used in their experiments. The rate constants reported by Farkas et al. (1949) and Bousher et al. (1987) did not account for the acid catalysis effect on this reaction. The incorporation of acid catalysis into the rate constant expression for k_{11} provides an

excellent match with experimental results (error less than 2.1 %) over a wide range of pH (6.55-9.75) and carbonate buffer concentration (4-20 mM), as shown in Figure 3-9 and Table 3-12.

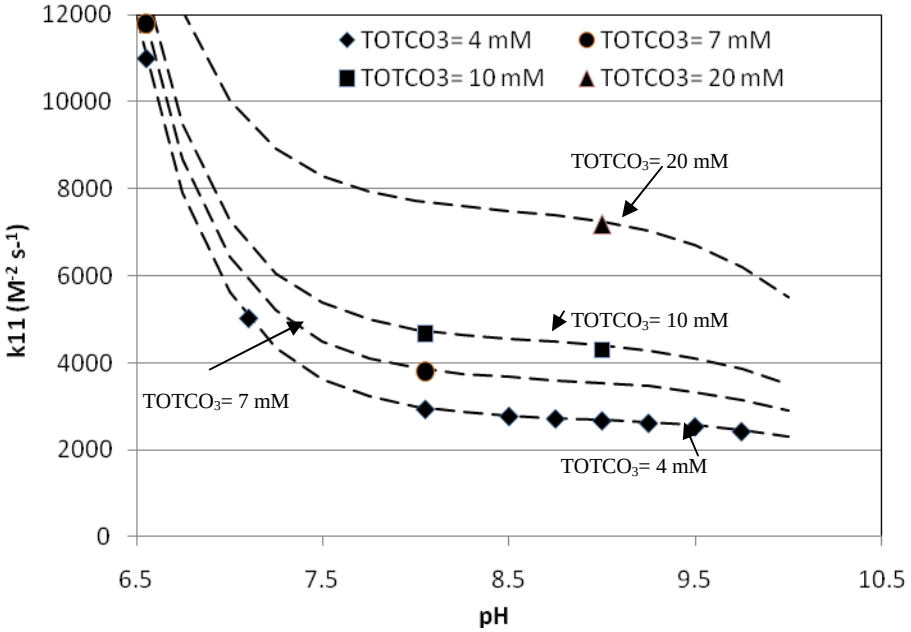

Figure 3-9: Measured k_{11} vs. model prediction (lines) , pH range (6.55-9.75) carbonate buffer range (4-20 mM)

Table 3-12: Measured k_{11} vs. model prediction, pH range (6.55-9.75) carbonate buffer range (4-20 mM)

pH	Carbonate buffer (mM)	Measured k_{11} ($M^{-1}s^{-1}$)	Predicted k_{11} ($M^{-1}s^{-1}$)	Error %
8.5	4	2776	2786	0.36
8.75	4	2721	2730	0.34
9	4	2676	2679	0.13
9.25	4	2619	2625	0.22
9.5	4	2539	2542	0.10
9.75	4	2427	2429	0.10
9	10	4300	4381	1.88
9	20	7190	7217	0.38
6.55	4	11000	10858	-1.29
7.1	4	5030	5022	-0.15
8.05	4	2940	2968	0.95
6.55	7	11800	11881	0.69
8.05	7	3800	3867	1.76
8.05	10	4670	4766	2.06

3.4. CONCLUSIONS

The hypobromous acid formation rate was found to be an acid-catalyzed reaction, which confirms the finding of Kumar et al., 1987. A new value of the acid catalysis effect of hydrogen ion was estimated. New terms were introduced to the hyprobromous acid formation rate including the acid catalysis effect of bicarbonate, carbonic acid, and ammonium ion. In addition, the hypobromous acid formation rate played a very important role in initial formation of monochloramine after a short prechlorination step. The new rate constant for the reaction of HOCl with bromide ion to form hypobromous acid proposed by this study was incorporated in the Unified Haloamine Kinetic Model and provides excellent prediction for TOTOBr formation, TOTOCl decay, and initial monochloramine concentration after 30 seconds of prechlorination. Thus, the Modefied Unified Haloamine Kinetic Model V.1.0 is now capable of providing accurate predictions during the initial stages of chloramination processes with different prechlorination periods. The following chapter addresses model improvements for extended periods of time (i.e., six to seven hours following ammonia addition).

CHAPTER 4: Modeling Monochloramine and Total Chlorine Decay After a Short Prechlorination Time in the Presence of Bromide

4.1. INTRODUCTION

The widespread presence of bromide in source waters is well documented. For example, Amy *et al*. (1994) found an average concentration of 100 µg/L in source waters in the U.S., with a range of 0 to 2.3 mg/L. Disinfection of waters containing bromide will result in its oxidation to bromine. The extent of bromine formation can vary widely depending on the bromide concentration, water quality parameters, and disinfection conditions. The concentration of bromide in the water can have significant impacts on disinfection processes such as chloramination. For example, the concentration of bromide affects the initial concentration of monochloramine formed after chlorine and ammonia addition as well as the decay of monochloramine and total chlorine over time.

Chloramination is widely used as a method of disinfection for drinking water due to its potential for reducing the concentration of disinfection-by-products (DBPs). The process can be incorporated into drinking water treatment in either a pre-chloramination step or as a primary disinfectant. Numerous studies have examined the potential for DBP formation from chloramination Krasner et al. (2007) and Shuo and Valentine (2006), and a number of studies have focused on identifying brominated DBPs that are formed from the oxidation of bromide (Echigo and Minear, 2006 and Chang et al., 2001). More recently, the use of pre-chloramination strategies has been examined for its potential for minimizing bromate formation (Krasner et al., 2007 and Buffle et al., 2004) when ozone is used as the primary disinfectant. Such strategies require predictive tools for optimizing the chlorine and ammonia concentrations and time periods for addition of the chemicals. The Unified Haloamine Kinetic Model developed by Pope (2006) and modified in

Chapter 3 provides this type of predictive tool. In particular, the model is capable of accounting for bromine-substituted haloamines, which may serve as the predominant species for sequestering bromide. This model incorporates the complex chemistry associated with haloamine formation and decay.

The reactions describing the decay of monochloramine and dichloramine in water free of bromide have been characterized previously in the literature. Jafvert and Valentine (1992) proposed a reaction scheme for the chlorination of water containing ammonia. Addition of bromide increases the complexity of this model due to the formation and decay of free bromine and bromamine species. Vikesland et al. (2001) modified their model to account for the presence of bromide by including nitrite-monochloramine and bromide-monochloramine reactions. The resulting model did not track the concentrations of brominates-substituted haloamines, which are important in understanding and modeling total chlorine decay and important for prechloramination strategies. Indeed, short prechloramination strategies proposed for reducing bromate formation during ozonation add further complexity to the reaction scheme because at higher pH and short prechlorination times (30 seconds), not all of the bromide will be oxidized to HOBr. Thus, a better description of bromine-substituted haloamine chemistry is required. Pope, (2006) developed the Unified Haloamine Kinetic Model, which incorporates the monochloramine decay model developed by Vikesland el al. (2001), the bromamine decomposition model developed by Lei et al. (2004), the bromochloramine formation and decay reactions developed by Gazda and Margerum (1994), Trofe et al. (1980), Bousher et al. (1986), and various equilibrium expressions.

In Chapter 3, a new version of the model was named the Modified Unified Haloamine Kinetic Model V. 1.0 (Table 4-1). The major modification to the previous version of the model was the incorporation of an acid-catalyzed rate constant for the

reaction involving oxidation of bromide by hypochlorous acid (Reaction 11 in Table 4-1). This reaction plays a very important role in haloamine speciation at short prechlorination time (30 seconds) especially at higher pH (pH>7.0) because at these conditions not all of the bromide will be oxidized to HOBr. The acid-catalyzed rate constant for this reaction incorporated carbonic acid, bicarbonate and ammonium as well as the proton:

$$k_{11}=1517+2.83x10^{10}[H^+] + 3.0x10^5[HCO_3^-] + 2.56x10^8[H_2CO_3] + 4.06x10^5[NH_4^+]$$

Because Reaction 11 determines the concentration of HOBr formed, the remaining concentration of bromide, and the remaining concentration of HOCl after 30 seconds, accurate estimation of the rate constant is essential for determining the remaining concentration of HOCl available to react with ammonia to form monochloramine. The results presented in Chapter 3 demonstrated the revised model's ability to predict initial monochloramine concentrations; however, the model fails to predict the decay of monochloramine and total chlorine over longer time periods as shown in Figure 4-1 and Figure 4-2.

Table 4-1: The Modified Unified Haloamine Kinetic Model V 1.0

No.	Reaction	Rate constant at 25 °C	Reference
1	$HOCl + NH_3 \rightarrow NH_2Cl + H_2O$	$3.07 \times 10^6\ M^{-1}S^{-1}$	Qiang and Adams (2004)
2	$NH_2Cl + H_2O \rightarrow NH_3 + HOCl$	$2.1 \times 10^{-5}\ M^{-1}S^{-1}$	Morris and Isaac (1981)
3	$NH_2Cl + HOCl \rightarrow NHCl_2 + H_2O$	$2.8 \times 10^2\ M^{-1}S^{-1}$	Margerum et al. (1978)
4	$NHCl_2 + H_2O \rightarrow NH_2Cl + HOCl$	$6.4 \times 10^{-7}\ S^{-1}$	Margerum et al. (1978)
5	$NH_2Cl + NH_2Cl \rightarrow NHCl_2 + NH_3$	k_5, pH dependent	Vikesland et al. (2001)
6	$NHCl_2 + NH_3 \rightarrow NH_2Cl + NH_2Cl$	$6.1 \times 10^4\ M^{-2}S^{-1}$	Hand and Margerum (1983)
7	$NH_2Cl + NHCl_2 \rightarrow N_2 + 3H + 3Cl^-$	$1.5 \times 10^{-2}\ M^{-1}S^{-1}$	Leao (1981)
8	$NHCl_2 + H_2O \rightarrow NOH + 2HCl$	$1.1 \times 10^2\ M^{-1}S^{-1}$	Jafvert and Valentine (1987)
9	$NOH + NHCl_2 \rightarrow N_2 + HOCl + HCl$	$2.8 \times 10^4\ M^{-1}S^{-1}$	Leao (1981)
10	$NOH + NH_2Cl \rightarrow N_2 + H_2O + HCl$	$8.3 \times 10^3\ M^{-1}S^{-1}$	Leao (1981)
11	$HOCl + Br^- \rightarrow HOBr + Cl^-$	pH dependent	This study
12	$HOBr + NH_3 \rightarrow NH_2Br + H_2O$	$7.5 \times 10^7\ M^{-1}S^{-1}$	Wajon and Morris (1980)
13	$HOBr + NH_2Cl \rightarrow NHBrCl + H_2O$	$2.86 \times 10^5\ M^{-1}S^{-1}$	Gazda and Margerum (1994)
14	$OBr^- + NH_2Cl \rightarrow NHBrCl + OH$	$2.2 \times 10^4\ M^{-1}S^{-1}$	Gazda and Margerum (1994)
15	$NH_2Cl + NH_2Cl + Br^- \rightarrow NHBrCl + Cl^- + NH_3$	k_{15} pH dependent	Trofe et al. (1980)
16	$NHBrCl + NHBrCl + H_2O \rightarrow N_2 + HOBr + HBr + 2HCl$	$17\ M^{-1}S^{-1}$	Valentine (1983) and Pope (2006)
17	$NH_2Br + NH_2Br \rightarrow NHBr_2 + NH_3$	pH dependent	Lei et al. (2004)
18	$NHBr_2 + NH_3 \rightarrow NH_2Br + NH_2Br$	pH dependent	Lei et al. (2004)
19	$NHBr_2 + NHBr_2 \rightarrow N_2 + 3H^+ + 3\ Br^-$	pH dependent	Lei et al. (2004)
20	$NH_2Br + NHBr_2 + H_2O \rightarrow N_2 + HOBr + 3H^+ + 3\ Br^-$	$8.9\ M^{-1}S^{-1}$	Lei et al. (2004)
21	$HOCl \leftrightarrow H^+ + OCl^-$	$pK_a = 7.5$	Connick and Chia (1959)
22	$NH_4^+ \leftrightarrow NH_3 + H^+$	$pK_a = 9.3$	Snoeyink and Jenkins (1980)
23	$HOBr \leftrightarrow OBr^- + H^+$	$pK_a = 8.8$	Haag and Hoigne (1983)
24	$H_2CO_3 \rightarrow HCO_3^- + H^+$	$pK_a = 6.3$	Snoeyink and Jenkins (1980)
25	$HCO3- \rightarrow CO_3^{2-} + H^+$	$pK_a = 10.3$	Snoeyink and Jenkins (1980)

$k_5 = k_{H+}[H^+] + k_{H2CO3}[H_2CO_3] + k_{HCO3}[HCO_3] + k_{H2PO4}[H_2PO_4^-] + k_{H3P}[H_3PO_4]$

$k_{11} = 1517 M^{-1}s^{-1} + 2.83 \times 10^{10}\ M^{-2}S^{-1}[H^+] + 3.0 \times 10^5\ M^{-2}S^{-1}[HCO_3^-] + 2.56 \times 10^8\ M^{-2}S^{-1}[H_2CO_3] + 4.06 \times 10^5\ M^{-2}S^{-1}[NH_4^+]$

$k_{14} = 1.4 \times 10^6\ M^{-2}S^{-1}[NH_2Cl][Br^-][H^+]$

$k_{17} = 0.5\ M^{-1}S^{-1} + 5 \times 10^8\ M^{-2}S^{-1}[H^+] + 2900\ M^{-2}S^{-1}[NH_4^+] + 540\ M^{-2}S^{-1}[HCO_3^-]$

$k_{18} = 1 M^{-1}S^{-1} + 1 \times 10^9\ M^{-2}S^{-1}[H^+] + 190\ M^{-2}S^{-1}[NH_4^+] + 180\ M^{-2}S^{-1}[HCO_3^-]$

$k_{19} = 6.2 M^{-1}S^{-1} + 8.3 \times 10^4\ M^{-2}S^{-1}[OH^-] + 3.2 \times 10^3\ M^{-2}S^{-1}[CO_3^{2-}]$

NOH is the unidentified monochloramine auto-decomposition intermediate.

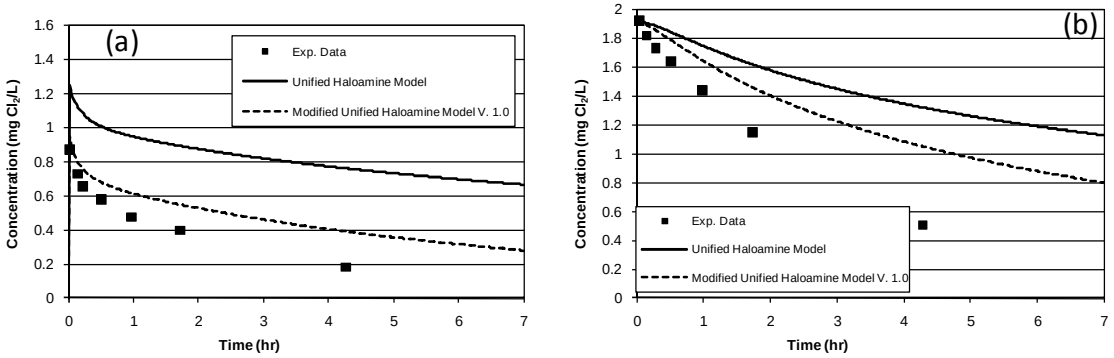

Figure 4-1: Model prediction (a) Monochloramine decay and (b) Total chlorine decay at (pH = 6.55, $TOTCO_3$= 7 mM, Br^-=1000 µg/L, Cl_2/N=3/1, 30 seconds prechlorination time)

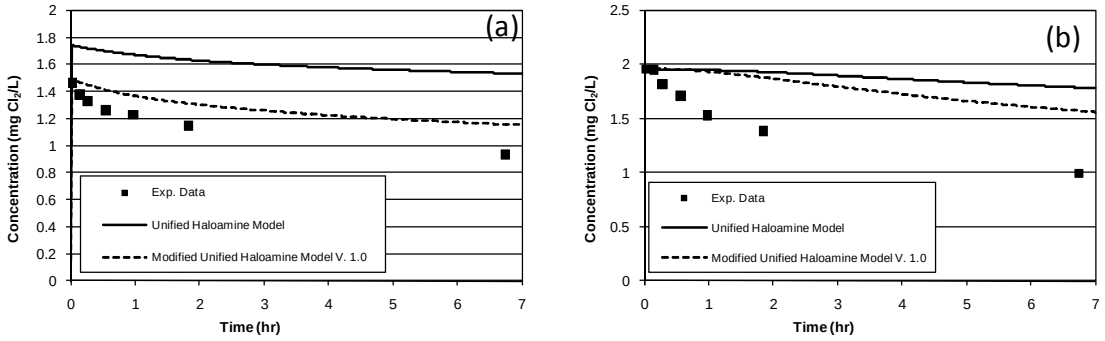

Figure 4-2: Model prediction (a) Monochloramine decay and (b) Total chlorine decay at (pH = 8.05, $TOTCO_3$= 10 mM, Br-=1000 µg/L, Cl_2/N=3/1, 30 seconds prechlorination time)

In this chapter the Unified Haloamine Kinetic Model is further modified to more accurately predict monochloramine and total chlorine concentration profiles following short prechlorination times in the presence of bromide. In contrast to previous research that focused on capturing monochloramine data only ((Vikesland et al., 1998, Duirk et al., 2005), this research evaluates the predictive capababilities of the model for both monochloramine decay and total chlorine decay. In addition, prior research examined systems in which preformed monochloramine was initially added to the system. In this research, prechlorination followed by ammonia addition was studied. The short

prechlorination time (30 seconds) adds complexity because, under many of the conditions studied (high pH), not all of the bromide ion will be oxidized to HOBr.

4.2. MATERIALS AND METHODS

Experiments were conducted over a large range of solution conditions to provide sufficient data sets to independently calibrate and verify changes to the Modified Unified Haloamine Kinetic Model. The experimental matrix was selected to study the effects of pH, carbonate buffer concentration, bromide concentration, and Cl_2/N ratio on the decay of monochloramine and total chlorine.

4.2.1. Materials

Aldrich 4% minimum available chlorine, a reagent grade sodium hypochlorite, was used as the source of HOCl and OCl^-. Solid KBr was used as the source of the bromide ion. NH_4Cl was used as the source of ammonia. Ammonia dosing solutions were prepared to provide 3.33 g/L as N. Millipore ultra pure water was used in preparing all the solutions. The pH was adjusted by addition of NaOH or HCl, and sodium carbonate was used to buffer the solutions. An ORION® 920A pH meter was used with an ORION Combination H/ATC probe to measure pH, and an Agilent 8453 UV spectrophotometer was used for all spectrophotometric measurements.

For the total chlorine dosing solution and standard curve, the exact concentration of the chlorine dosing solution was measured prior to dosing using Standard Method 4500-Cl B (APHA, 1998) and by spectrophotometry. The pH of each sample was increased to 11 with NaOH, and the absorbance at a wavelength of 292 nm was used to determine the concentration of OCl^- assuming a molar absorptivity of 362 $M^{-1}cm^{-1}$ (Furman and Margerum, 1998) .

For the monochloramine standard curve, preformed monochloramine was created by mixing aqueous ammonium chloride (NH_4Cl) and sodium hypochlorite (NaOCl) solutions. These solutions were formulated so that approximately equal volumes of the two, when combined, produced the desired Cl_2/N ratio (3/1 mass ratio). Both solutions were adjusted to pH 9 with HCl and/or NaOH. Prior to creating preformed chloramines, the concentration of the chlorine solution was measured as described above. The volume of ammonium solution added was adjusted to ensure the correct Cl_2/N ratio. The chlorine solution was added slowly to the ammonium solution with constant mixing in an ice bath at 1°C. After 15 minutes of mixing, the concentration of the monochloramine solution was measured using Standard Method 4500-Cl B and by spectrophotometry using a molar absorptivity of 461 $M^{-1}cm^{-1}$ at λ_{max} of 243 nm for NH_2Cl (Kumar *et al.*, 1986) prior to dosing the samples. Two measurements were made. If these measurements differed by more than 0.1 mg/L a second pair was made. If the second pair of measurements differed by more than 0.1 mg/L the solution was discarded and remixed. An average of the two appropriate measurements was used in the calculations. All solutions were mixed with Millipore ultra pure water. This procedure was used successfully in previous chloramination research (Symons *et al*., 1998).

4.2.2. Methods

The first step in developing a method for modeling monochloramine and total chlorine concentrations is to study the effect of chloramine addition mode on bromamine speciation. Figure 4-3 and Figure 4-4 show model results from the Unified Haloamine Model developed by Pope (2006) for 5 minutes of prechlorination time, 30 seconds of prechlorination time and preformed monochloramine. The results indicate that the two prechlorination times yield almost identical bromochloramine and total bromamine concentration profiles. Therefore, all experiments were run using a 30 second

prechlorination time such that the same level of bromate and DBP formation control was achieved using a minimum free chlorination time step.

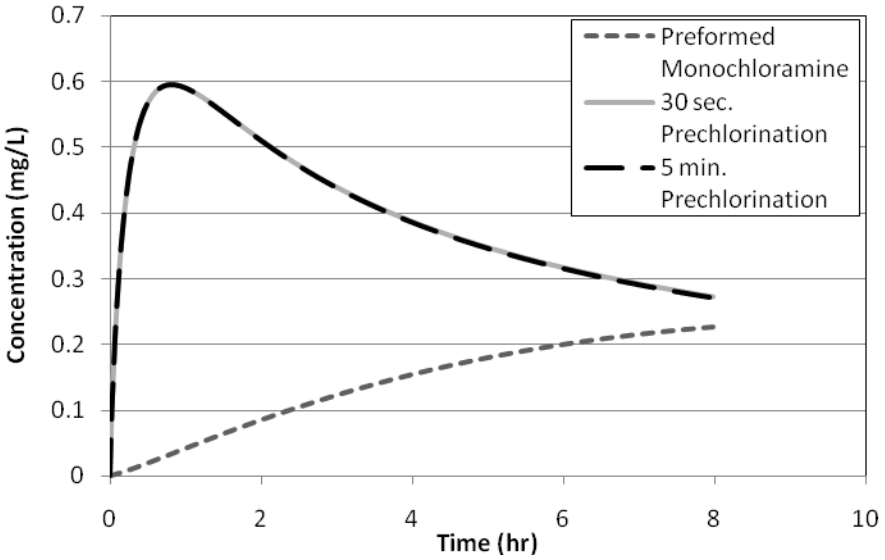

Figure 4-3: Model prediction of Bromochloramine formation and decay in organic free water ($TOTCl_2$= 2 mg/L , Cl_2/N=3/1 , $TOTCO_3$=4 mM, Br-=1 mg/L , T=22°C, and pH=7).

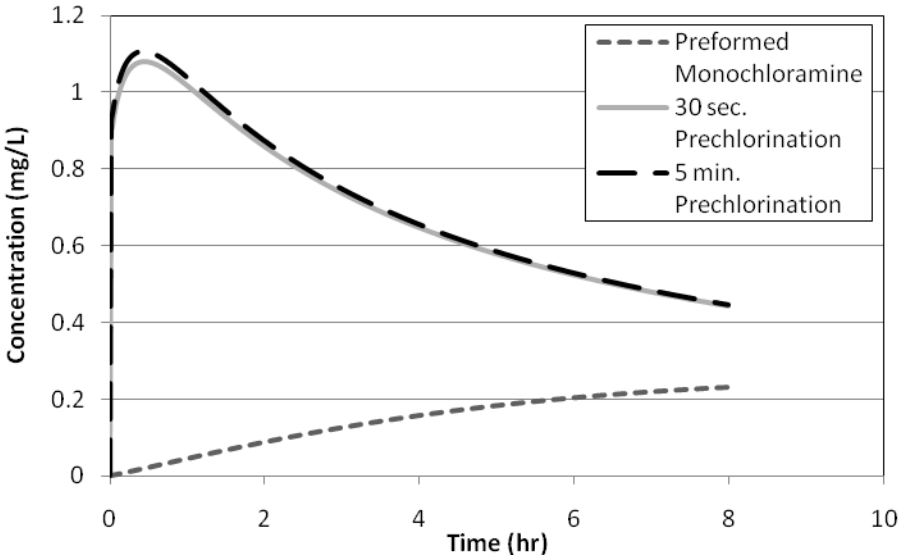

Figure 4-4: Model prediction of Bromamine + Bromochloramine formation and decay in organic free water ($TOTCl_2$= 2 mg/L, Cl_2/N=3/1 , $TOTCO_3$=4mM, Br-=1mg/L , T=22°C, and pH=7).

Sodium carbonate was added to Millipore ultra pure water to buffer the solution in a 2-L Erlenmeyer flask covered with foil. Bromide was added and continuously mixed for five minutes, then chlorine was added, and then ammonia was added 30 seconds later to get the target Cl_2/N ratio. This Cl_2/N ratio was based on the initial chlorine concentration; therefore, the actual Cl_2/N ratio at the start of the chloramination step was lower. The exact ammonia concentration added was used in the modeling, so no inaccuracies were introduced. This solution was then proportioned into 250-mL brown glass bottles that were capped with Teflon-lined septa with zero headspace, which were then incubated in the dark until the time of the analysis.

The total chlorine residual was measured using spectrophotometry to measure total chlorine at a wavelength of 530 nm using Hach DPD (N,N-diethyl-p-phenylenediamine). The Hach Total Chlorine Reagent Powder with the Hach DPD test Method 8167 is adapted from Standard Method 4500-Cl. Standards of approximately 0, 0.5, 1.5, 2.5, and 3.5 mg/L as Cl_2 were analyzed in triplicate prior to the samples to prepare the standard curve. The standards were created from the chlorine dosing solution, which was prepared with Aldrich 4% minimum available chlorine, reagent grade sodium hypochlorite. First, the exact concentration of the dosing solution was measured using Standard Method 4500-Cl B, and by spectrophotometry at a wavelength of 292nm and molar absorptivity of $362 M^{-1}cm^{-1}$ for OCl^-. Then, a primary dilution standard (PDS) was created by diluting the dosing solution to a concentration of 100 mg/L as Cl_2 with ultra pure water. Finally, the standards were prepared by diluting the DPS to the desirable concentration with ultra pure water.

The total chlorine measurement includes free chlorine (HOCl and OCl^-), free bromine (HOBr and OBr^-), chloramines (monochloramine and dichloramine), bromamines (monobromamine and dibromamine), and bromochloramine. Under typical

drinking water treatment conditions (neutral pH and Cl_2/N ratios 3-5/1), virtually all chlorine and bromine are present as combined chlorine and bromine.

The monochloramine residual was also measured using spectrophotometry to measure monochloramine at a wavelength of 655 nm using Hach Monochlor F Reagent Powder Pillows with Hach Method 10171. Monochloramine standards of approximately 0, 0.5, 1, 2, and 3.5 mg/L as Cl_2 were analyzed in triplicate prior to the samples to prepare the standard curve. This measurement only measures monochloramine (Chang and Blatchley 1999).

4.2.3. Experimental matrix

Batch experiments were conducted over a range of pH, bromide concentrations, Cl_2/N ratios, and carbonate concentrations. Table 4-2 summarizes the experimental matrix.

Table 4-2: Experimental matrix.

No.	pH	Cl_2/N ratio	Bromide(µg/L)	Carbonate buffer (mM)
1	6.55	3/1	1000	2
2	6.55	3/1	1000	4
3	6.55	3/1	1000	7
4	6.55	3/1	1000	10
5	6.55	3/1	1000	15
6	7.10	3/1	1000	4
7	8.05	3/1	1000	4
8	8.05	3/1	1000	7
9	8.05	3/1	1000	10
10	6.55	3/1	100	4
11	6.55	1/1	1000	4
12	8.05	3/1	100	4

4.3. KINETICS MODEL

The Modified Unified Haloamine Kinetic Model V.1.0 (Table 4-1) was used as the starting point for the modeling done in this chapter. The modified model is based on the Unified Haloamine Kinetic Model developed by Pope (2006), and incorporates the monochloramine decay model developed by Vikesland el al. (2001), the bromamine decomposition model developed by Lei et al. (2004), the bromochloramine formation and decay reactions developed by Gazda and Margerum (1994), Trofe et al. (1980), and Bousher et al. (1986), and various equilibrium expressions.

The oxidation of bromide by hypochlorous acid (Reaction 11, Table 4-1) plays a very important role in haloamine speciation, especially with a short prechlorination time (30 seconds) and a pH above neutral. Under these conditions, not all of the bromide will be oxidized to HOBr. Chapter 3 focused on an improved description of the reaction kinetics for Reaction 11. The resulting rate expression is:

$$k_{11}=1517+2.83x10^{10}[H^+] + 3.0x10^5[HCO_3^-] + 2.56x10^8[H_2CO_3] + 4.06x10^5[NH_4^+]$$

Addition of the rate expression for Reaction 11 to Pope's model resulted in the Modified Unified Haloamine Model V 1.0. Additional modifications, however, are required to more accurately predict the decay of monochloramine and total chlorine concentrations over time.

The model consists of a system of ordinary differential equations for the rate expressions as well as algebraic expressions for the relevant equilibrium that describe the reactive system. Model results were obtained by solving the equations using the software package Scientist ®3.0, which uses Gear's Method to solve simultaneous differential equations. Least squares fitting in Scientist ®3.0 was performed using a modified Powell algorithm to minimize the unweighted sum of the squares of the residual error between the predicted and experimentally observed values to estimate specific parameters in the

model. Upper and lower bounds were placed on each estimated parameter so as not to exceed reasonable estimates.

4.4. RESULTS AND DISCUSSION

The inability of the Modified Unified Haloamine Kinetic Model V.1.0 (Table 4-1) to predict either monochloramine decay or total chlorine decay for water containing bromide and undergoing 30 seconds of prechlorination (see Figure 4-1 or 4-2) suggests that the model required further refinement. To this end, experiments were conducted to identify model reactions that required modification.

4.4.1. Bromochloramine formation

Results from experiments conducted using a 30-second prechlorination period with two different concentrations of bromide, at two different pH values were used to identify reactions to be studied for model improvement. The data presented in Figure 4-5 show that, as expected, as the bromide concentration increased, the initial monochloramine concentration decreased due to the oxidation of bromide into HOBr by the free chlorine. This bromide ion oxidation decreased the available free chlorine to react with the ammonia to form monochloramine. Figure 4-5 (a) shows the monochloramine and total chlorine decay at pH 6.6 with a bromide concentration of 100 µg/L, total carbonate buffer concentration of 4mM, and 30 seconds of prechlorination. Figure 4-5 (b) shows the monochloramine and total chlorine decay with the same conditions except for the bromide concentration, which was increased to 1000 µg/L. Of particular interest in these two figures is that the initial difference between total chlorine and monochloramine in the 100 µg/L bromide case is 0.3 mg/L as Cl_2, while at 1000 µg/L bromide case the difference increased to 1.05 mg/L as Cl_2. The same trend for pH 8.05 is shown in Figure 4-5 (c) and Figure 4-5 (d); however, the differences between total

and monochloramine are not as significant. At 100 µg/L bromide almost all of the total chlorine was monochloramine, and the difference between total chlorine and monochloramine concentration was less than 0.1 mg/L as Cl_2 while at 1000 µg/L bromide, the difference increased to 0.3 mg/L as Cl_2.

Differences between total chloramine and total chlorine are attributed to the concentrations of the other haloamine species. The working hypothesis for the Unified Haloamine Kinetic Model is that bromochloramine represents a significant species in these systems. As a result, the decay of monochloramine and total chlorine would be expected to increase as bromide concentration increases, due to the reaction of monochloramine with HOBr to form bromochloramine. NHBrCl then decays through reaction with itself and/or with monochloramine. As shown in Figure 4-5 (a) at pH 6.6 and 100 µg/L bromide, the decay of monochloramine and total chlorine over six hours was 0.15 and 0.1 mg/L as Cl_2, respectively. Under the same conditions, but using 1000 µg/L of bromide, the total decay of monochloramine and of the total chlorine over six hours increased by over an order of magnitude to 0.6 and 1.0 mg/L as Cl_2 , respectively (Figure 4-5 (b)). This significant increase in monochloramine decay over time at higher bromide concentration is due to the increased concentration of HOBr available for reaction with monochloramine to form bromochloramine.

As shown in Figure 4-5 (c) and Figure 4-5 (d) at pH 8.05, when the bromide concentration increased from 100 to 1000 µg/L, the total decay of monochloramine over six hours only increased from 0.1 to 0.37 mg/L as Cl_2, while the total decay of total chlorine over six hours increased from 0.17 to 0.6 mg/L as Cl_2. Differences between the results at the two pH values suggest that the reaction of monochloramine with HOBr (Reaction 13) is an acid catalyzed reaction. Thus, these data suggest that modification to the rate constant for Reaction 13 is required to account for general acid catalysis.

It was also assumed that the reaction with HOBr (Reaction 13) dominates over the reaction of monochloramine with OBr^- (Reaction 14) based on the results of Gazda and Margerum (1994), which showed that the reaction of HOBr with monochloramine is one order of magnitude faster than the reaction of OBr^- with monochloramine. In addition, the typical pH in water treatment is below pH 9.0, and HOBr will be dominant at such pH conditions. Therefore, only the acid catalysis effect on Reaction 13 was studied in this research.

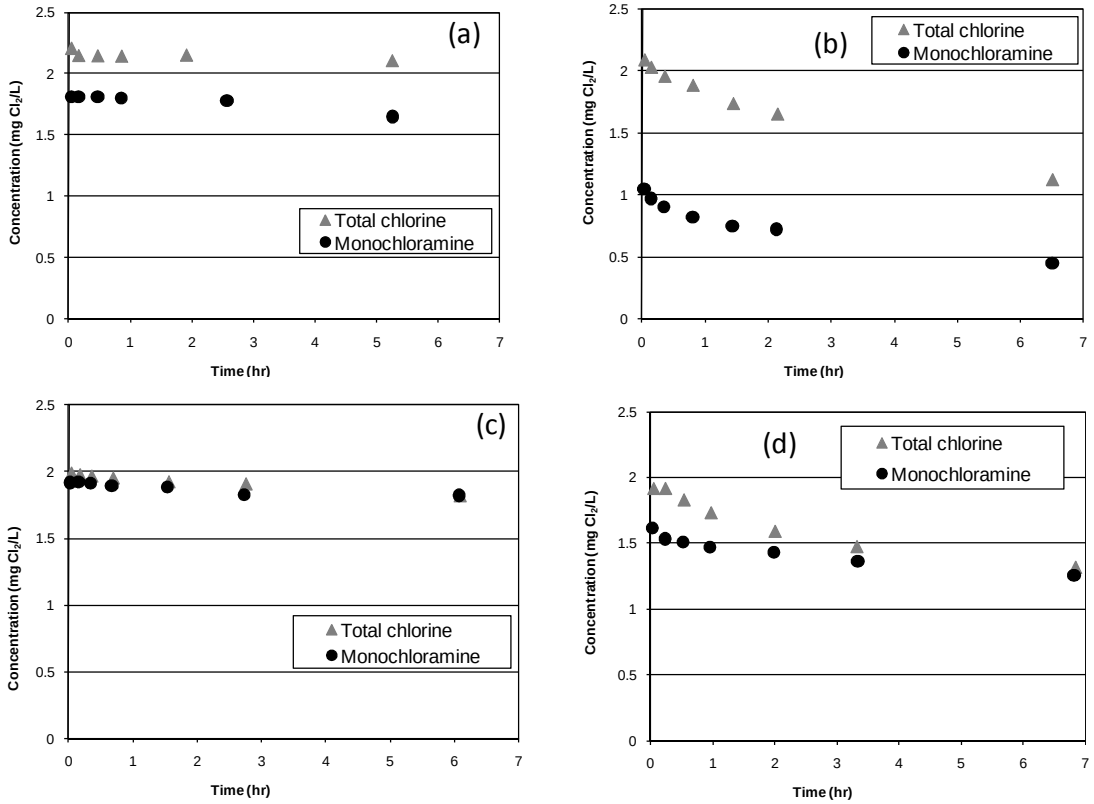

Figure 4-5: Monochloramine and total chlorine decay ($TOTCO_3$= 4 mM, Cl_2/N=3/1, 30 seconds prechlorination time) (a) pH=6.55 and Br^-=100 µg/L, (a) pH=6.55 and Br-=1000 µg/L, (a) pH=8.05 and Br^-=100 µg/L , and (a) pH=8.05 and Br^-=1000 µg/L

4.4.2. Bromochloramine decay

Different chloramine production schemes have been used to disinfect drinking water. Preformed monochloramine addition, pre-ammonia addition, and prechlorination schemes have all been used in chloramination practice. These difference schemes are expected to yield differences in monochloramine and total chlorine behavior as shown in Figure 4-6. Figure 4-6 (a) shows monochloramine and total chlorine decay over time with pre-ammonia addition prior to the chlorine addition. In the pre-ammonia chloramination addition mode, virtually no oxidation of the bromide ion by HOCl occurs, because as the chlorine is added to the solution, it will react with the ammonia to form monochloramine, because the rate constant for the reaction of HOCl with ammonia (Reaction 1 in Table 4-1) is three orders of magnitude larger than the rate constant for the reaction of HOCl with bromide ion (Reaction 11 in Table 4-1), especially at pH 8.0 where monochloramine is the dominant chloramine specie. Figure 4-6 (b) shows the monochloramine and total chlorine decay over time for the same conditions with a different chloramine addition mode of 30 seconds prechlorination time. Seven hours after ammonia addition, the concentration of monochloramine and total chlorine were comparable even though the the concentration of total chlorine was significantly higher near the start of the experiment. Seven hours after the prechlorination mode, 0.6 mg/l as Cl_2 was lost from solution, whereas only 0.37 mg/L of monochloramine was lost. The differences between the results presented for the two different addition scenarios and in the rates of disappearance of total monochloramine and total chlorine over seven hours can be explained by the reaction of monochloramine with HOBr to form bromochloramine and the subsequent decay of NHBrCl through its reaction with itself and with monochloramine.

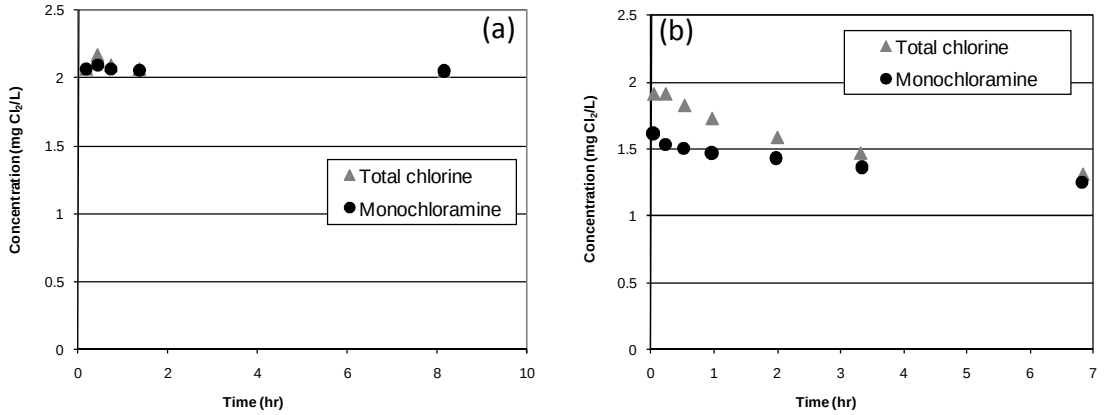

Figure 4-6: Monochloramine and total chlorine decay (pH = 8.05, $TOTCO_3$= 4 mM, Br^-=1000 µg/L, Cl_2/N=3/:1) (a) pre ammonia addition (b) 30 seconds prechlorination

Bromochloramine can form via two pathways. The first pathway is the reaction of monochloramine with bromide as shown in (Reaction 15) in Table 4-1 (Trofe *et al.* 1980). The second pathway is the reaction of monochloramine with HOBr and OBr^- (Reaction 13 and 14) in Table 4-1 (Gazda and Margerum 1994). One of these pathways will be dominant, depending on the addition mode of the chloramine. In the preformed monochloramine mode, (Reaction 15) will be dominant, because no HOBr or OBr^- is available in the system, due to the reaction of HOCl with ammonia. However, in the prechlorination mode, the bromide will be oxidized by the free chlorine to form HOBr and OBr^-. The percentage of the bromide ion that is oxidized to HOBr and OBr^- depends on the concentration of the bromide, the concentration of free chlorine, the pH, and the carbonate buffer concentration, as shown in Chapter 3.

Information on bromochloramine decay is limited. Valentine (1983) proposed that NHBrCl decomposes to regenerate OBr^- as a final product (Reaction 16). However, the modeling results presented in Figures 4-1 and 4-2 suggest that this reaction does not adequately capture the decay. To model the decomposition of bromochloramine, the

same reaction scheme responsible for dichloramine decay was assumed in which an unidentified intermediate (U) is formed that can react with either monochloramine or bromochloramine.

$$NHClBr + H_2O \rightarrow U + HCl + HBr \qquad (26)$$

$$U + NHClBr \rightarrow HOBr + N_2 + HCl \qquad (27)$$

$$U + NH_2Cl \rightarrow H_2O + N_2 + HCl \qquad (28)$$

Reaction 26 is assumed to be the rate limiting reaction in this series. Because the intermediate species U was assumed to exist at a very low concentration, only the ratio of Reaction 27 to Reaction 28 is important. To simplify the modeling effort, the ratio of rate constants for Reaction 27 to Reaction 28 were fixed to the ratio used for Reactions 9 and 10. The value of the rate constant for Reaction 27 and Reaction 28 was selected to be at least three orders of magnitude larger than the value of the rate constant of Reaction 26. Table 4-3 summarizes the reactions used in the Modified Unified Haloamine Kinetic Model V. 1.1.

Table 4-3: The Modified Unified Haloamine Kinetic Model V 1.1

No.	Reaction	Rate constant at 25 °C	Reference
1	$HOCl + NH_3 \rightarrow NH_2Cl + H_2O$	$3.07 \times 10^6\ M^{-1}S^{-1}$	Qiang and Adams (2004)
2	$NH_2Cl + H_2O \rightarrow NH_3 + HOCl$	$2.1 \times 10^{-5}\ M^{-1}S^{-1}$	Morris and Isaac (1981)
3	$NH_2Cl + HOCl \rightarrow NHCl_2 + H_2O$	$2.8 \times 10^2\ M^{-1}S^{-1}$	Margerum et al. (1978)
4	$NHCl_2 + H_2O \rightarrow NH_2Cl + HOCl$	$6.4 \times 10^{-7}\ S^{-1}$	Margerum et al. (1978)
5	$NH_2Cl + NH_2Cl \rightarrow NHCl_2 + NH_3$	K_5, pH dependent	Vikesland et al. (2001)
6	$NHCl_2 + NH_3 \rightarrow NH_2Cl + NH_2Cl$	$6.1 \times 10^4\ M^{-2}S^{-1}$	Hand and Margerum (1983)
7	$NH_2Cl + NHCl_2 \rightarrow N_2 + 3H + 3Cl^-$	$1.5 \times 10^{-2}\ M^{-1}S^{-1}$	Leao (1981)
8	$NHCl_2 + H_2O \rightarrow NOH + 2HCl$	$1.1 \times 10^2\ M^{-1}S^{-1}$	Jafvert and Valentine (1987)
9	$NOH + NHCl_2 \rightarrow N_2 + HOCl + HCl$	$2.8 \times 10^4\ M^{-1}S^{-1}$	Leao (1981)
10	$NOH + NH_2Cl \rightarrow N_2 + H_2O + HCl$	$8.3 \times 10^3\ M^{-1}S^{-1}$	Leao (1981)
11	$HOCl + Br^- \rightarrow HOBr + Cl^-$	K_{11}, pH dependent	Chapter 3
12	$HOBr + NH_3 \rightarrow NH_2Br + H_2O$	$7.5 \times 10^7\ M^{-1}S^{-1}$	Wajon and Morris (1980)
13	$HOBr + NH_2Cl \rightarrow NHBrCl + H_2O$	K_{13}, pH dependent	This work
14	$OBr^- + NH_2Cl \rightarrow NHBrCl + OH$	$2.2 \times 10^4\ M^{-1}S^{-1}$	Gazda and Margerum (1994)
15	$NH_2Cl + NH_2Cl + Br^- \rightarrow NHBrCl + Cl^- + NH_3$	K_{15}, pH dependent	Trofe et al. (1980)
16	~~$NHBrCl + NHBrCl + H_2O \rightarrow N_2 + HOBr + HBr + 2HCl$~~	Removed from the model	Valentine (1983) and Pope (2006)
17	$NH_2Br + NH_2Br \rightarrow NHBr_2 + NH_3$	pH dependent	Lei et al. (2004)
18	$NHBr_2 + NH_3 \rightarrow NH_2Br + NH_2Br$	pH dependent	Lei et al. (2004)
19	$NHBr_2 + NHBr_2 \rightarrow N_2 + 3H^+ + 3\ Br^-$	pH dependent	Lei et al. (2004)
20	$NH_2Br + NHBr_2 + H_2O \rightarrow N_2 + HOBr + 3H^+ + 3\ Br^-$	$8.9\ M^{-1}S^{-1}$	Lei et al. (2004)
21	$HOCl \leftrightarrow H^+ + OCl^-$	$pK_a = 7.5$	Connick and Chia (1959)
22	$NH_4^+ \leftrightarrow NH_3 + H^+$	$pK_a = 9.3$	Snoeyink and Jenkins (1980)
23	$HOBr \leftrightarrow OBr^- + H^+$	$pK_a = 8.8$	Haag and Hoigne (1983)
24	$H_2CO_3 \rightarrow HCO_3^- + H^+$	$pK_a = 6.3$	Snoeyink and Jenkins (1980)
25	$HCO3^- \rightarrow CO_3^{2-} + H^+$	$pK_a = 10.3$	Snoeyink and Jenkins (1980)
26	$NHBrCl + H_2O \rightarrow U + HBr + HCl$	pH, dependent	This work
27	$U + NHBrCl \rightarrow HOBr + N_2 + HCl$	$1 \times 10^{11}\ M^{-1}s^{-1}$	This work
28	$U + NH_2Cl \rightarrow H_2O + N_2 + HCl$	$3 \times 10^{10}\ M^{-1}\ s^{-1}$	This work

$k_5 = k_{H+}[H^+] + k_{H2CO3}[H_2CO_3] + k_{HCO3}[HCO_3] + k_{H2PO4}[H_2PO_4^-] + k_{H3P}[H_3PO_4]$

$k_{11} = 1517 M^{-1}s^{-1} + 2.83 \times 10^{10}\ M^{-2}S^{-1}[H^+] + 3.0 \times 10^5\ M^{-2}S^{-1}[HCO_3^-] + 2.56 \times 10^8\ M^{-2}S^{-1}[H_2CO_3] + 4.06 \times 10^5\ M^{-2}S^{-1}[NH_4^+]$

$k_{15} = 1.4 \times 10^6\ M^{-2}S^{-1}[NH_2Cl][Br^-][H^+]$

$k_{17} = 0.5\ M^{-1}S^{-1} + 5 \times 10^8\ M^{-2}S^{-1}[H^+] + 2900\ M^{-2}S^{-1}[NH_4^+] + 540\ M^{-2}S^{-1}[HCO_3^-]$

$k_{18} = 1 M^{-1}S^{-1} + 1 \times 10^9\ M^{-2}S^{-1}[H^+] + 190\ M^{-2}S^{-1}[NH_4^+] + 180\ M^{-2}S^{-1}[HCO_3^-]$

$k_{19} = 6.2 M^{-1}S^{-1} + 8.3 \times 10^4\ M^{-2}S^{-1}[OH^-] + 3.2 \times 10^3\ M^{-2}S^{-1}[CO_3^{2-}]$

NOH is the unidentified monochloramine auto-decomposition intermediate.

4.4.3. Acid catalysis effect

The analysis presented above suggests that several changes are required for improving the Modified Unified Haloamine Kinetic Model. These include estimation of the acid catalyzed rate constant for Reaction 13, removal of Reaction 16, and incorporation of the series of reactions to describe bromochloramine decay, Reactions 26-28.

The Unified Haloamine Kinetic Model of Pope (2006) and the Modified Unified Haloamine Model V. 1.0 failed to model the monochloramine and total chlorine decay over time, especially at high carbonate buffer concentration as shown in the introduction section of this chapter, which suggest that one or more of the reactions is acid catalyzed. Since the model has been shown to predict total chlorine and monochloramine decay during preformed monochloramine addition schemes, it is likely that the reaction of monochloramine and HOBr to form bromochloramine and the decay of bromochloramine are the acid catalyzed reactions. To determine the acid catalysis rate expression for these reactions a number of experiments were conducted with different carbonate buffer concentrations over a range of pH values and used in conjunction with Scientist® 3.0 software to estimate the effect of each acidic species on the rate constant. Both reactions 13 and 26 were fit simultaneously under each set of conditions selected to isolate a particular acid. Table 4-4 shows the estimated rate constant for Reaction 13 and Reaction 26 at different conditions. Figure 4-7 shows an example of a model fit for one set of conditions. Results for other conditions as well as the values of the associated rate constants are provided in Appendix 2.

Table 4-4: Estimated value for k_{13} and k_{26}

Exp. No.	pH	Carbonate buffer (mM)	Estimate k_{13} ($M^{-1}h^{-1}$)	Estimated k_{26} ($M^{-1}h^{-1}$)
1	6.55	2	$4.50x10^8$	$2.90x10^6$
2	6.55	4	$8.50x10^8$	$5.50x10^6$
3	6.55	7	$1.60x10^9$	$1.05x10^7$
4	6.55	10	$2.25x10^9$	$1.50x10^7$
5	6.55	15	$3.30x10^9$	$2.20x10^7$
6	8.05	4	$6.12x10^8$	$6.00x10^6$
7	8.05	7	$1.05x10^9$	$1.05x10^6$
8	8.05	10	$1.50x10^9$	$1.50x10^6$

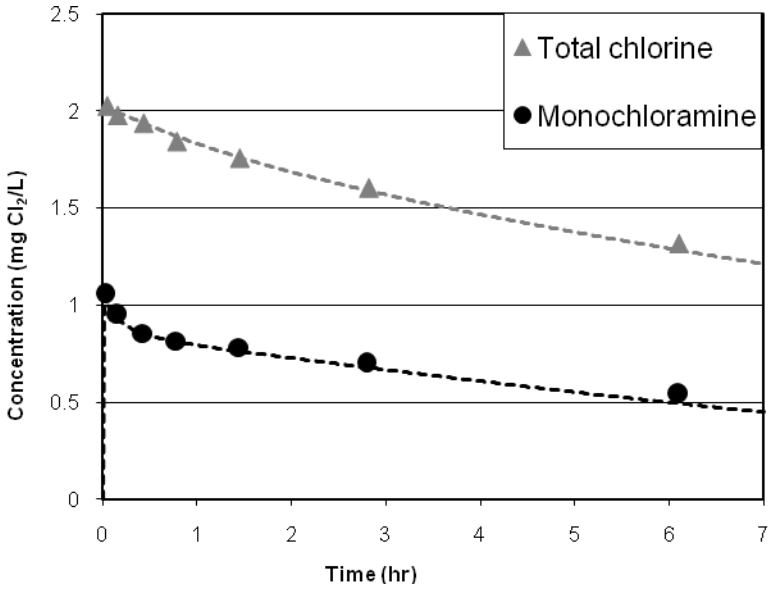

Figure 4-7: Monochloramine and total chlorine decay (pH = 6.55, $TOTCO_3$= 2 mM, Br-=1000 µg/L, Cl_2/N=3/1, 30 seconds prechlorination time) (dash lines represent the Modified Unified Haloamine Model V. 1.1 result)

The overall rate expressions of reaction 13 and reaction 26 are shown below.

$$k_{13} = k_{H_2O} + k_{H^+}[H^+] + k_{HCO_3^-}[HCO_3^-] + k_{H_2CO_3}[H_2CO_3] + k_{NH_4^+}[NH_4^+]$$

$$k_{26} = k_{H_2O} + k_{H^+}[H^+] + k_{HCO_3^-}[HCO_3^-] + k_{H_2CO_3}[H_2CO_3] + k_{NH_4^+}[NH_4^+]$$

The results showed that only the acid catalysis effect of carbonic acid and bicarbonate were important at the experiments conditions studied. The rate constant expressions of reaction 13 and 26 can be simplified to the following rate expression by assuming the acid catalysis effect of the water, hydrogen ion and ammonia is insignificant. Estimation of the contribution of H^+ to the overall rate constant will require further experiments beyond those done in this research; however, this simplification gives a good fit over the carbonate buffer range from 2-15 mM.

$$k_{13} = k_{HCO_3^-}[HCO_3^-] + k_{H_2CO_3}[H_2CO_3]$$

$$k_{26} = k_{HCO_3^-}[HCO_3^-] + k_{H_2CO_3}[H_2CO_3]$$

A pH of 8.05 with 1000 µg/L bromide concentration, 3/1 Cl_2/N ratio, and different carbonate concentrations were used to estimate the bicarbonate catalysis effect on the reaction of monochloramine with HOBr (reaction 13) and the reaction of bromochloramine decay (reaction 26) simultaneously. At pH 8.05 the dominant carbonate species is bicarbonate. Figure 4-8 and Figure 4-9 show k_{13} and k_{26} as a function of bicarbonate concentration.

After estimating the acid catalysis effect of the bicarbonate, the acid catalysis effect of the carbonic acid was determined using data collected at pH 6.6 with 1000 µg/L bromide concentration, 3/1 Cl_2/N ratio and different carbonate concentrations. The value of the bicarbonate acid catalysis effect was subtracted from the fitted value of k_{13} and $k_{26,}$ and then the acid catalysis effect of carbonic acid was estimated as shown in Figure 4-10 and Figure 4-11. The concentration of the carbonic acid was calculated as described in

Chapter 3 which was based on the pH of the solution, the known acidity constant for H_2CO_3*, and the average value of 630 for the hydrolysis of CO_2(aq) reported in Snoeyink and Jenkins (1980).

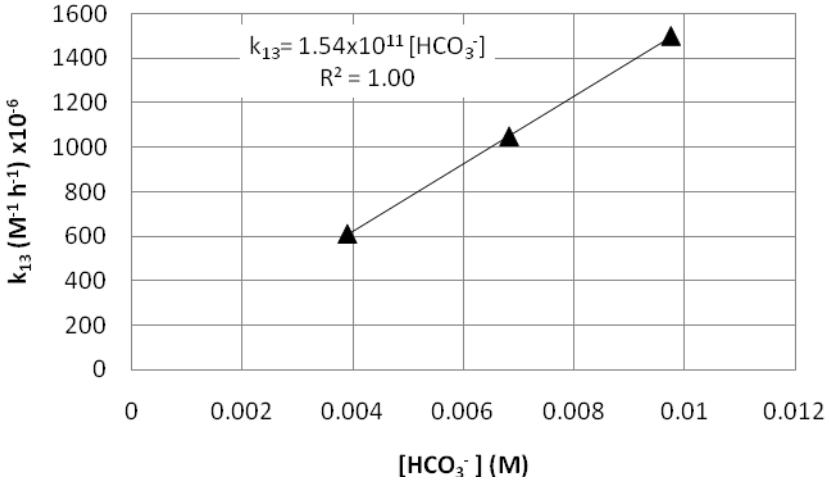

Figure 4-8: k_{13} as a function of bicarbonate concentration at pH 8.05

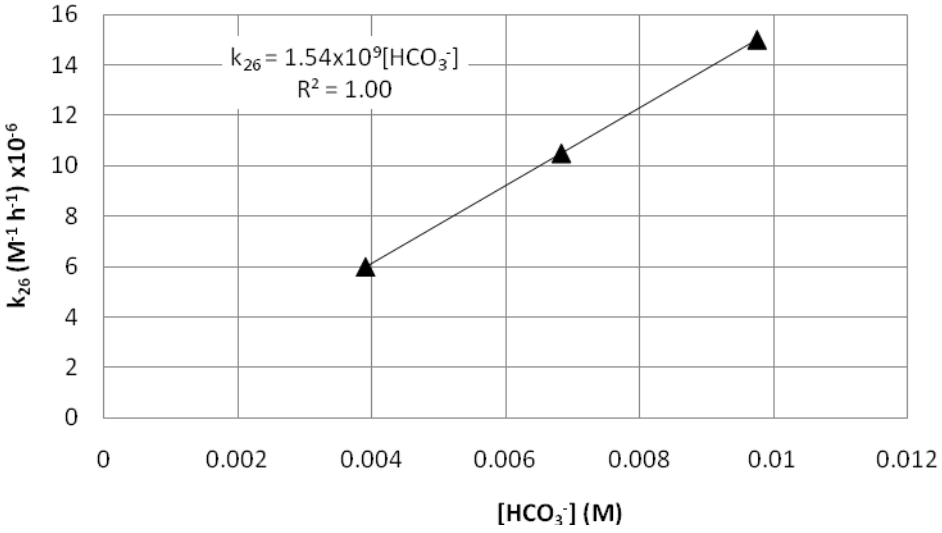

Figure 4-9: k_{26} as a function of bicarbonate concentration at pH 8.05

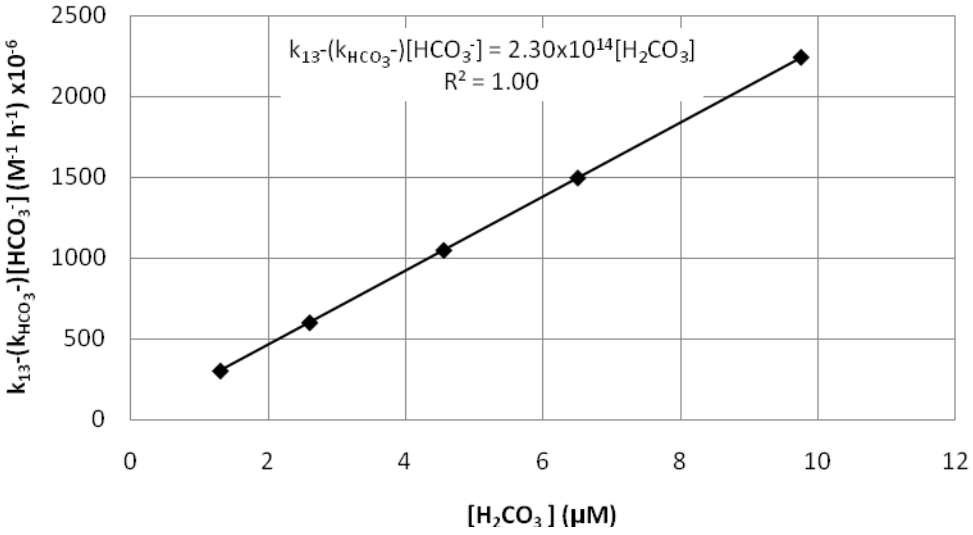

Figure 4-10: k_{13} as a function of carbonic acid concentration at pH 6.55

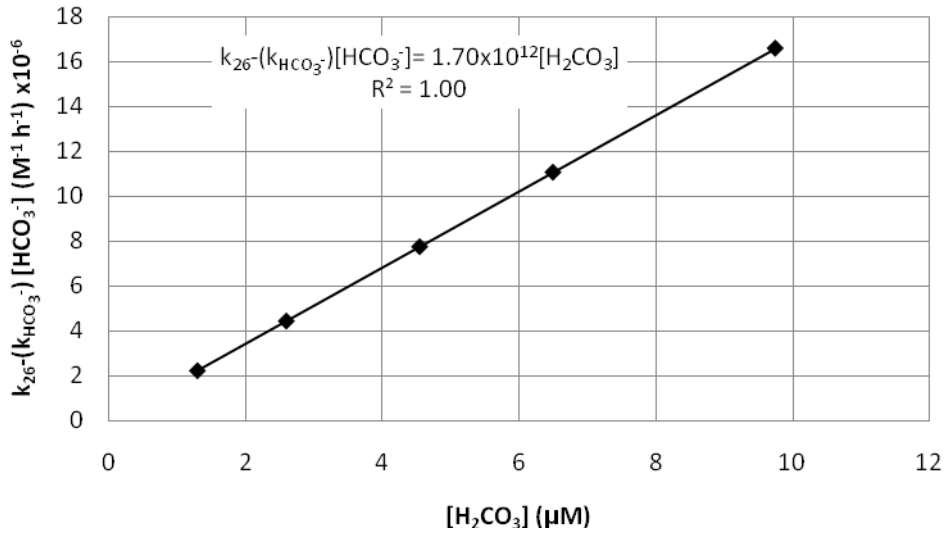

Figure 4-11: k_{26} as a function of carbonic acid concentration at pH 6.55

The equations below show k_{13} and k_{26} as functions of bicarbonate and carbonic acid concentrations.

$$k_{13} = 1.54x10^{11}[HCO_3^-] + 2.3x10^{14}[H_2CO_3]$$

$$k_{26} = 1.54x10^{9}[HCO_3^-] + 1.7x10^{12}[H_2CO_3]$$

The new reaction scheme and associated rate constants were incorporated into the Modified Unified Haloamine Kinetic Model V.1.1. Figure 4-12 and Figure 4-13 show monochloramine decay and total chlorine decay for 30-second prechlorination experiments conducted at pH 6.6 and 8.05, as well as the models results for the Unified Haloamine Kinetic Model, the Modified Unified Haloamine Kinetic Model V. 1.0, and the Modified Unified Haloamine Kinetic Model V. 1.1. The Modified Unified Haloamine Kinetic Model V. 1.1 clearly shows improvement compared to the previous versions of the model.

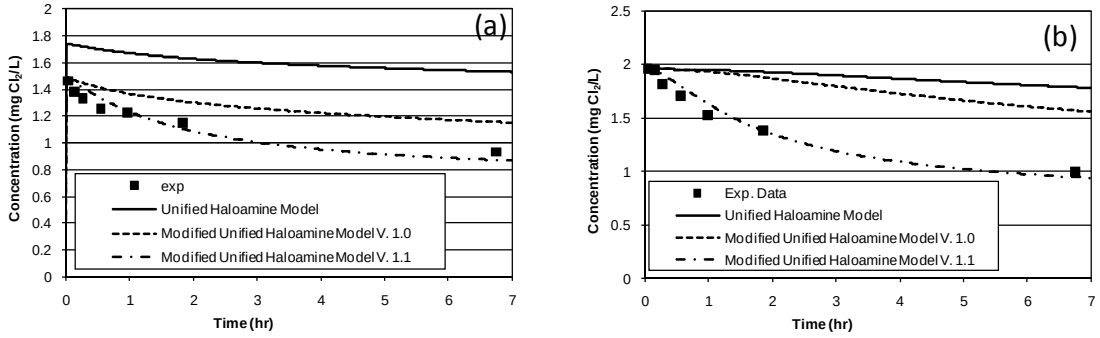

Figure 4-12: Model fitting (a) Monochloramine decay and (b) Total chlorine decay (pH = 8.05, $TOTCO_3$= 10 mM, Br-=1000 µg/L, Cl_2/N=3/1, 30 seconds prechlorination time)

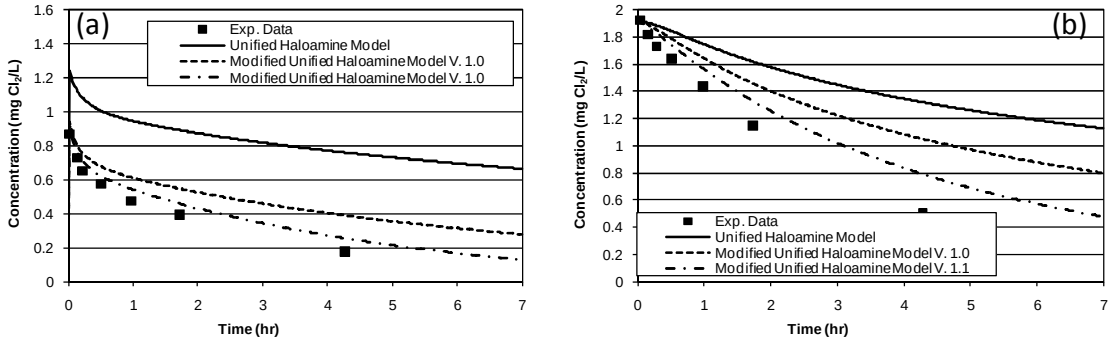

Figure 4-13: Model fitting (a) Monochloramine decay and (b) Total chlorine decay (pH = 6.55, $TOTCO_3$= 7 mM, Br-=1000µg/L, Cl_2/N=3/1, 30 seconds prechlorination time)

The monochloramine and total chlorine decay increase as the carbonate buffer concentration increases, as shown in equations k_{13} and k_{26} above. Figure 4-14 shows the monochloramine decay over time at pH 6.55 with different carbonate buffer concentrations. With a 2 mM carbonate buffer concentration, the monochloramine loss over 6 hours was less than 0.5 mg/l as Cl_2, which is 50% of the initial monochloramine concentration. With a 15 mM carbonate buffer concentration, after one hour, only 0.2 mg/l as Cl_2 was left, which means that over 80% of the initial monochloramine was lost in one hour.

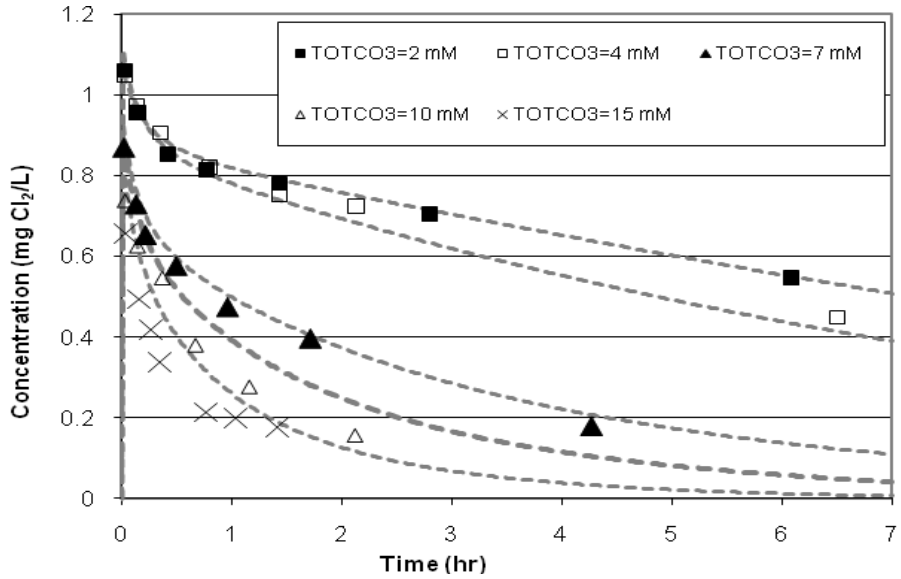

Figure 4-14: Monochloramine decay over time at pH 6.55 and different carbonate buffer concentration (dash lines represent the Modified Unified Haloamine Model V. 1.1 results)

The model accurately describes the monochloramine and total chlorine decay at carbonate buffer concentrations below 7 mM, which are typical for drinking water treatment applications. At carbonate buffer concentrations above 7 mM, the monochloramine and total chlorine decay faster than the model predictions.

It should be noted that data from experiments at pH 6.55 and 8.05 with 100 µg/L bromide, the experiment at pH 7.1, and the experiment at pH 6.55 with a 1/1 Cl_2/N ratio were not used in the calibration of k_{13} and k_{26} above, yet the model accurately predicts those kinetics. For example, Figure 4-15 shows the model prediction for pH 6.55 and 1/1 Cl_2/N ratio.

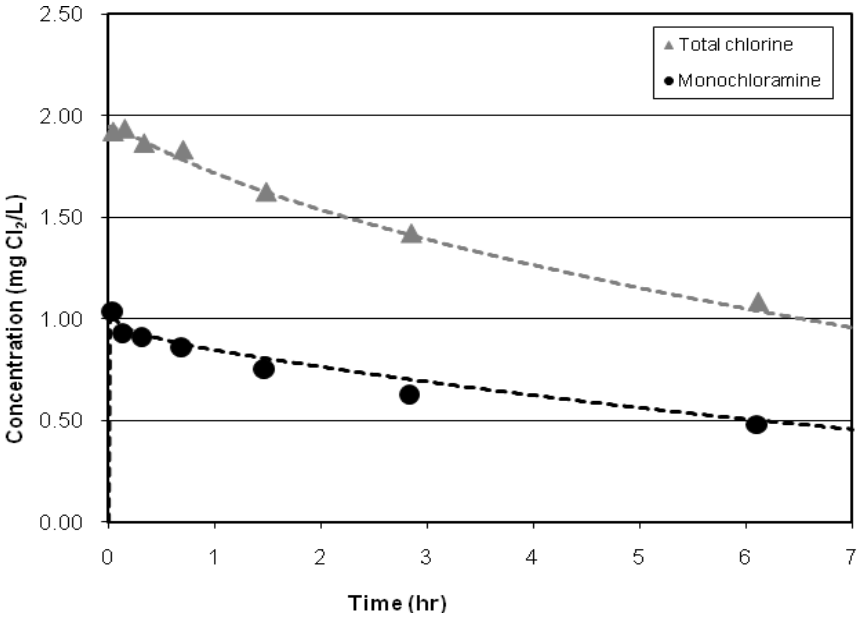

Figure 4-15: Monochloramine and total chlorine decay (pH = 6.55, $TOTCO_3$= 4 mM, Br-=1000 µg/L, Cl_2/N=1/1, 30 seconds prechlorination time) (dash lines represent model prediction)

4.5. CONCLUSION

The Modified Unified Haloamine Kinetic Model was developed to model monochloramine and total chlorine concentrations after short prechlorination times in the presence of bromide. The revised model highlights the importance of bromochloramine formation and decay during prechlorination strategies. The model includes a new bromochloramine decay scheme via the reaction with monochloramine and with itself. In addition, new acid-catalyzed rate constants for the reaction of HOCl with bromide ion and the reaction of HOBr with monochloramine were incorporated into the model.

The Modified Unified Haloamine Model V.1.1 accurately predicts monochloramine and total chlorine decay over time at carbonate buffer concentrations below 7 mM. More work is needed to accurately model monochloramine and total

chlorine decay at higher carbonate concentrations, although it is not evident that accurate modeling above 7 mM is required for most water treatment applications.

The data collected for evaluating the model revealed a number of significant findings. For example, while the monochloramine reaction with HOBr is the dominant bromochloramine formation pathway in the 30 seconds prechlorination scheme, bromochloramine formation is not significant for preformed monochloamine addition. The importance of accounting for general acid catalysis was evident by examining differences in total and monochloramine decay over long time periods (on the order of hours) under different pH conditions. Apparent conflicts between reported rate constants in the literature could often be resolved by accounting for acid catalysis.

CHAPTER 5: Effect of NOM on Monochloramine and Total chlorine Decay

5.1. INTRODUCTION

The presence of bromide in waters undergoing chloramination greatly complicates the haloamine reaction chemistry. Previous work (Chapters 3 and 4) showed that modifications to the Unified Haloamine Kinetic Model of Pope (2006) could describe the observed concentrations of total chlorine and monochloramine in the absence of natural organic matter (NOM) for waters undergoing chloramination with and without periods of prechlorination. NOM is an important reactant with haloamines and must be accounted for to fully describe the reaction chemistry in practical applications. Reactions of free chlorine, free bromine, and haloamines with NOM are also crucial from the perspective of disinfection by-product (DBP) formation and regulatory compliance with maximum contaminant levels (MCLs) for DBPs. This work extends the Unified Haloamine Kinetic Model concept by including the impact of NOM on haloamine formation and decay kinetics. Free chlorine, free bromine, and haloamines can react with NOM in two general ways. Substitution reactions result in halogen-substituted organic chemicals, some of which are regulated DBPs. Oxidation reactions yield oxidized forms of NOM and chloride or bromide. The model was extended to include reactions with NOM and to account for the formation of chlorine and bromine-substituted NOM, so that chlorine and bromine mass balances could be closed and estimates of halogenated organic chemicals formation could be made.

5.2. MATERIALS AND METHODS

5.2.1. Materials

Aldrich 4% minimum available chlorine, a reagent grade sodium hypochlorite, was used as the source of HOCl and OCl^-. Solid KBr was used as the source of the bromide ion. NH_4Cl was used as the source of ammonia. An ammonia dosing solution was prepared to have 3.33 g/L as N. Millipore ultra pure water was used in preparing all the solutions. The pH was adjusted by NaOH and HCl, and sodium carbonate was used to buffer the solutions. An ORION® 920A meter with an ORION Combination H/ATC probe were used to measure the pH, and an Agilent 8453 UV spectrophotometer was used to measure the absorbance. Two different NOM sources were used in his study, Lake Austin (Texas) and Claremore Lake (Oklahoma). Lake Austin NOM was isolated at University of Texas at Austin and Claremore Lake NOM was isolated at NIST in Boulder, Colorado. The NOM was isolated by using nonionic macroporous resins (Amberlite XAD-8 resins) (Aiken et al. 1992), Table 5-1 shows the water quality characteristics for these two waters.

Table 5-1: Water quality characteristics for Lake Austin and Claremore Lake

Parameter	Lake Austin*	Claremore Lake**
pH	8.20	7.52
DOC (mg/L)	3.74	6.40
Hydrophobic DOC (%)	50	45
SUVA (L/mg-m)	2.49	2.89
Bromide (µg/L)	168	55

* Source: Gerwe (2003).

** Measured by NIST in Boulder, Colorado

5.2.2. Methods

5.2.2.1 SUVA determination

Specific ultraviolet absorbance (SUVA) had been used to characterize the reactivity of NOM. SUVA is an indicator of the humic content of NOM. The SUVA calculation requires both the DOC and UVA measurement. The SUVA is calculated by dividing the UV absorbance of the sample (in cm^{-1}) by the DOC of the sample (in mg/L) and then multiplying by 100 cm/m. SUVA is reported in units of L/mg-m.

The NOM isolates from Lake Austin and Claremore Lake was mixed with Millipore ultrapure water to give a total organic carbon (TOC) concentration of approximately 500 mg/L. The procedures for sample preparation for dissolved organic carbon (DOC) and UV analysis were based on the recommendations of Karanfil et al. (2005). For DOC, the NOM solution was filtered through a 0.45-µm Gelman Supor 450 filter that had been first washed with 1 L of distilled-deionized water. During the filtration of a sample, the first 25 mL of filtrate was wasted before collecting the sample for DOC determination. The filter blank was determined by filtering Millipore ultra pure water; this demonstrated that there was no gain or loss of DOC during filtration. For UV_{254} determination, a Gelman GH Polypro filter was used. The same procedures as for DOC determination was used except that 100 mL of wash volume was used.

5.2.2.2 Reactive site estimation

The total reactive sites for each NOM source were estimated using the procedures of Duirk et al. (2005). The total reactive sites were estimated by adding 0.4 mM free chlorine to a 3.3 mg/L as C NOM solution in 5 mM carbonate buffered Millipore ultra pure water. The experiments were run at pH 9.0 and 22^{o}C to minimize free chlorine

decomposition. The free chlorine residual was monitored for approximately one month. The reactive site determination was assumed complete when three consecutive chlorine measurements over a period of 5-10 days did not change. A control experiment was run by adding 0.4 mM free chlorine to 5 mM carbonate buffered Millipore ultra pure water. The total reactive sites (S_T) is the difference between the average of three final free chlorine measurements in the control and in the NOM solution divided by the total organic carbon in mg-C/L, which was converted to moles using the molecular weight of carbon as shown in the equation below. (S_T) is the reactive molar percentage of total organic carbon.

$$S_T = \frac{[HOCl]_{Control\ \ final} - [HOCl]_{\ final}}{TOC} x\ 12{,}000$$

5.2.2.3 Kinetics experiments

Sodium carbonate was added to Millipore ultra pure water to buffer the solution in a 0.5-L Erlenmeyer flask covered with foil. Bromide was added and continuously mixed for five minutes, and then NOM was added. The pH was adjusted with HCl and NaOH. Then chlorine was added to have 2 mg/L as Cl_2, and ammonia was added 30 seconds later to get the target Cl_2/N ratio (3/1). This Cl_2/N ratio was based on the initial chlorine concentration; therefore, the actual Cl_2/N ratio at the start of the chloramination step was lower. The exact ammonia concentration added was used in the modeling, so no inaccuracies were introduced. This solution was then proportioned into 60-mL brown glass bottles that were capped with Teflon-lined septa with zero headspace, which were then incubated in the dark until the time of the analysis.

5.2.2.4 Total chlorine dosing solution and residual measurements

The total chlorine residual was measured using spectrophotometry to measure total chlorine at a wavelength of 530 nm using Hach DPD (N,N-diethyl-p-phenylenediamine). The Hach Total Chlorine Reagent Powder with the Hach DPD test Method 8167 is adapted from Standard Method 4500-Cl. Standards of approximately 0, 0.5, 1.5, 2.5, and 3.5 mg/L as Cl_2 were analyzed in triplicate prior to the samples to prepare the standard curve. The standards were created from the chlorine dosing solution, which was prepared with Aldrich 4% minimum available chlorine, reagent grade sodium hypochlorite. First, the exact concentration of the dosing solution was measured using Standard Method 4500-Cl B, and by spectrophotometry at a wavelength of 292nm and molar absorptivity of $362 M^{-1}cm^{-1}$ for OCl^-. Then, a primary dilution standard (PDS) was created by diluting the dosing solution to a concentration of 100 mg/L as Cl_2 with ultra pure water. Finally, the standards were prepared by diluting the PDS to the desirable concentration with ultra pure water.

The total chlorine measurement includes free chlorine (HOCl and OCl^-), free bromine (HOBr and OBr^-), chloramines (monochloramine and dichloramine), bromamines (monobromamine, dibromamine), and bromochloramine. Under typical drinking water treatment conditions (neutral pH and Cl_2/N ratios 3-5/1), virtually all chlorine and bromine are present as combined chlorine and bromine. The total chlorine measurement will measure the total chlorine concentration.

5.2.2.5 Monochloramine dosing solution and residual measurements

Preformed monochloramine was created by mixing aqueous ammonium chloride (NH_4Cl) and sodium hypochlorite (NaOCl) solutions. These solutions were formulated so that approximately equal volumes of the two, when combined, produced the desired Cl_2/N ratio. Both solutions were adjusted to pH 9 with HCl and/or NAOH. The

concentration of the chlorine solution was measured according to Standard Method 4500-Cl B (APHA, 1998) and by spectrophotometry using a molar absorptivity of 362 $M^{-1}cm^{-1}$ at λ_{max} of 292 nm for OCl^- (Furman and Margerum 1998) prior to creating preformed chloramines. The volume of ammonium solution added was adjusted to ensure the correct Cl_2/N ratio. The chlorine solution was added slowly to the ammonium solution with constant mixing in an ice bath at 1 °C. After 15 minutes of mixing, the concentration of the monochloramine solution was measured using Standard Method 4500-Cl B and by spectrophotometry using a molar absorptivity of 461 $M^{-1}cm^{-1}$ at λ_{max} of 243 nm for NH_2Cl (Kumar *et al.*, 1986) prior to dosing the samples. Two measurements were made. If these measurements differed by more than 0.1 mg/L a second pair was made. If the second pair of measurements differed by more than 0.1 mg/L the solution was discarded and remixed. An average of the two appropriate measurements was used in the calculations. All solutions were mixed with Millipre ultra pure water. This procedure was used successfully in previous chloramination research (Symons *et al.*, 1998).

The monochloramine residual was also measured using spectrophotometry to measure monochloramine at a wavelength of 655 nm using Hach Monochlor F Reagent Powder Pillows with Hach Method 10171. Monochloramine standards of approximately 0, 0.5, 1, 2, and 3.5 mg/L as Cl_2 were analyzed in triplicate prior to the samples to prepare the standard curve. This measurement only measures monochloramine (Chang and Blatchley 1999).

5.2.2.6 DOC determination

DOC was determined by UV-light promoted persulfate oxidation with infrared carbon dioxide detection using a Tekmar-Dohrmann Apollo 9000 TOC Analyzer. The DOC concentrations were measured as NPOC (non-purgeable organic carbon), in which

inorganic carbon was removed by acidification with ACS grade phosphoric acid and sparging with prepurified nitrogen (Merriam-Grave Industrial, Springvale, ME).

Dehydrated potassium hydrogen phthalate ($C_8H_5KO_4$) was used to prepare a concentrated stock (1000 mg C/L) for preparation of calibration standards in distilled deionized water. Concentrated KHP stock was acidified with 1 mL of phosphoric acid and stored at 4 ^oC for reuse up to one month. A calibration curve was generated by analyzing standards prepared as 0, 1, 2, 3, 4, and 5 mg/L as C. Calibration standards were generally prepared fresh for each run.

Glassware for organic carbon analysis was washed with Alconox, rinsed three times with tap water and three times with distilled water and soaked in a 10% nitric acid bath for 2 hours. The glassware was then rinsed 3 times with distilled deionized water. Sample vials were baked at 550 °C for two hours, brown glass bottles were baked overnight at 400 °C, and volumetric glassware was rinsed with reagent grade acetone and allowed to air-dry.

5.2.2.7 TOX determination

Total Organic Halide (TOX) was measured by Analab Corporation, Kilgore, Texas. The measurements were done based on the Standard Method 5320B (Clesceri et al., 1998). Before samples were sent to Analab 0.05 mM of sulfuric acid was added for preservation and 0.04 mM sodium sulfite was added for dechlorination. Samples were collected ten minutes after ammonia addition.

5.2.3. Experimental matrix

Experiments with different NOM sources (Lake Austin NOM and Claremore Lake NOM), different pH values, and different carbonate buffer concentrations were run to study the effect of NOM in monochloramine and total chlorine decay. Table 5-2

summarizes the experimental matrix. These experiments was designed to study the effect of different NOM sources on the decay of monochloramine and total chlorine over the pH range of 6.5-8.0 after 30 seconds of prechlorination.

Table 5-2: Experimental matrix for NOM

Exp. No.	NOM	pH	Carbonate Buffer (mM)	Bromide (µg/L)	DOC (mg/L as C)
1	Lake Austin	6.5	4	1000	2
2	Lake Austin	6.5	4	1000	5
3	Lake Austin	6.5	4	1000	10
4	Lake Austin	7	4	1000	5
5	Lake Austin	8	4	1000	2
6	Lake Austin	8	4	1000	5
7	Lake Austin	8	4	1000	10
8	Claremore Lake	6.5	4	1000	5
9	Claremore Lake	7	4	1000	5
10	Claremore Lake	8	4	1000	5
11	Lake Austin	6.5	7	1000	5
12	Lake Austin	8	7	1000	5

5.2.4. Modeling

The Modified Unified Haloamine Kinetic Model V.1.1 developed in Chapter 4 of this dissertation was used as the starting point for the modeling the concentrations of free chlorine, free bromine and haloamines in the presence of NOM. Table 5-2 lists the key reactions that are included in the model. The model is based on the Unified Haloamine Model developed by Pope (2006), the monochloramine decay model developed by Vikesland el al. (2001), the bromamine decomposition model developed by Lei et al. (2004), the bromochloramine formation and decay reactions developed by Gazda and Margerum 1994, Trofe et al. 1980, and Bousher et al. 1986, and various equilibrium expressions. In this work, the model was expanded to include substitution reactions with NOM, and the oxidation reactions of NOM were assumed to be negligible.

Table 5-3: Modified Unified Haloamine Kinetic Model V.1.1

No.	Reaction	Rate constant at 25 °C	Reference
1	$HOCl + NH_3 \rightarrow NH_2Cl + H_2O$	$3.07 \times 10^6\ M^{-1}S^{-1}$	Qiang and Adams (2004)
2	$NH_2Cl + H_2O \rightarrow NH_3 + HOCl$	$2.1 \times 10^{-5}\ M^{-1}S^{-1}$	Morris and Isaac (1981)
3	$NH_2Cl + HOCl \rightarrow NHCl_2 + H_2O$	$2.8 \times 10^2\ M^{-1}S^{-1}$	Margerum et al. (1978)
4	$NHCl_2 + H_2O \rightarrow NH_2Cl + HOCl$	$6.4 \times 10^{-7}\ S^{-1}$	Margerum et al. (1978)
5	$NH_2Cl + NH_2Cl \rightarrow NHCl_2 + NH_3$	K_5, pH dependent	Vikesland et al. (2001)
6	$NHCl_2 + NH_3 \rightarrow NH_2Cl + NH_2Cl$	$6.1 \times 10^4\ M^{-2}S^{-1}$	Hand and Margerum (1983)
7	$NH_2Cl + NHCl_2 \rightarrow N_2 + 3H + 3Cl^-$	$1.5 \times 10^{-2}\ M^{-1}S^{-1}$	Leao (1981)
8	$NHCl_2 + H_2O \rightarrow NOH + 2HCl$	$1.1 \times 10^2\ M^{-1}S^{-1}$	Jafvert and Valentine (1987)
9	$NOH + NHCl_2 \rightarrow N_2 + HOCl + HCl$	$2.8 \times 10^4\ M^{-1}S^{-1}$	Leao (1981)
10	$NOH + NH_2Cl \rightarrow N_2 + H_2O + HCl$	$8.3 \times 10^3\ M^{-1}S^{-1}$	Leao (1981)
11	$HOCl + Br^- \rightarrow HOBr + Cl^-$	K_{11}, pH dependent	This work
12	$HOBr + NH_3 \rightarrow NH_2Br + H_2O$	$7.5 \times 10^7\ M^{-1}S^{-1}$	Wajon and Morris (1980)
13	$HOBr + NH_2Cl \rightarrow NHBrCl + H_2O$	K_{13}, pH dependent	This work
14	$OBr^- + NH_2Cl \rightarrow NHBrCl + OH$	$2.2 \times 10^4\ M^{-1}S^{-1}$	Gazda and Margerum (1994)
15	$NH_2Cl + NH_2Cl + Br^- \rightarrow NHBrCl + Cl^- + NH_3$	K_{15}, pH dependent	Trofe et al. (1980)
~~16~~	~~$NHBrCl + NHBrCl + H_2O \rightarrow N_2 + HOBr + HBr + 2HCl$~~	Removed from the model	Valentine (1983) and Pope (2006)
17	$NH_2Br + NH_2Br \rightarrow NHBr_2 + NH_3$	pH dependent	Lei et al. (2004)
18	$NHBr_2 + NH_3 \rightarrow NH_2Br + NH_2Br$	pH dependent	Lei et al. (2004)
19	$NHBr_2 + NHBr_2 \rightarrow N_2 + 3H^+ + 3\ Br^-$	pH dependent	Lei et al. (2004)
20	$NH_2Br + NHBr_2 + H_2O \rightarrow N_2 + HOBr + 3H^+ + 3\ Br^-$	$8.9\ M^{-1}S^{-1}$	Lei et al. (2004)
21	$HOCl \leftrightarrow H^+ + OCl^-$	$pK_a = 7.5$	Connick and Chia (1959)
22	$NH_4^+ \leftrightarrow NH_3 + H^+$	$pK_a = 9.3$	Snoeyink and Jenkins (1980)
23	$HOBr \leftrightarrow OBr^- + H^+$	$pK_a = 8.8$	Haag and Hoigne (1983)
24	$H_2CO_3 \rightarrow HCO_3^- + H^+$	$pK_a = 6.3$	Snoeyink and Jenkins (1980)
25	$HCO3^- \rightarrow CO_3^{2-} + H^+$	$pK_a = 10.3$	Snoeyink and Jenkins (1980)
26	$NHBrCl + H_2O \rightarrow U + HBr + HCl$	pH, dependent	This work
27	$U + NHBrCl \rightarrow HOBr + N_2 + HCl$	$1 \times 10^{11}\ M^{-1}s^{-1}$	This work
28	$U + NH_2Cl \rightarrow H_2O + N_2 + HCl$	$3 \times 10^{10}\ M^{-1}\ s^{-1}$	This work

$k_5 = k_{H+}[H^+] + k_{H2CO3}[H_2CO_3] + k_{HCO3}[HCO_3] + k_{H2PO4}[H_2PO_4^-] + k_{H3P}[H_3PO_4]$

$k_{15} = 1.4 \times 10^6\ M^{-2}S^{-1}\ [NH_2Cl][Br^-][H^+]$

$k_{17} = 0.5\ M^{-1}S^{-1} + 5 \times 10^8\ M^{-2}S^{-1}\ [H^+] + 2900\ M^{-2}S^{-1}\ [NH_4^+] + 540\ M^{-2}S^{-1}\ [HCO_3^-]$

$k_{18} = 1M^{-1}S^{-1} + 1 \times 10^9\ M^{-2}S^{-1}\ [H^+] + 190\ M^{-2}S^{-1}\ [NH_4^+] + 180\ M^{-2}S^{-1}\ [HCO_3^-]$

$k_{19} = 6.2M^{-1}S^{-1} + 8.3 \times 10^4\ M^{-2}S^{-1}\ [OH^-] + 3.2 \times 10^3\ M^{-2}S^{-1}\ [CO_3^{2-}]$

$k_{11} = 1517M^{-1}s^{-1} + 2.83 \times 10^{10}\ M^{-2}S^{-1}\ [H^+] + 3.0 \times 10^5\ M^{-2}S^{-1}\ [HCO_3^-] + 2.56 \times 10^8\ M^{-2}S^{-1}\ [H_2CO_3] + 4.06 \times 10^5\ M^{-2}S^{-1}\ [NH_4^+]$

$k_{13} = 1.54 \times 10^{11}\ M^{-2}S^{-1}\ [HCO_3^-] + 2.3 \times 10^{14}\ M^{-2}S^{-1}\ [H_2CO_3]$

$k_{26} = 1.54 \times 10^9\ M^{-2}S^{-1}\ [HCO_3^-] + 1.7 \times 10^{12}\ M^{-2}S^{-1}\ [H_2CO_3]$

NOH is the unidentified monochloramine auto-decomposition intermediate.

Duirk et al. (2005) introduced a conceptual framework for free chlorine and monochloramine reactions with NOM. This framework assumes two different types of reactive sites on NOM, fast reacting and slow reacting sites. Fast reacting sites undergo reaction with monochloramine while slow reacting sites can react only with free chlorine result from monochloramine hydrolysis. Extending this framework to conditions where bromide is present and prechlorination mode used yields the reaction schematic shown in Figure 5-1. The kinetic expressions for NOM reactions introduced in this work are based on this reaction schematic.

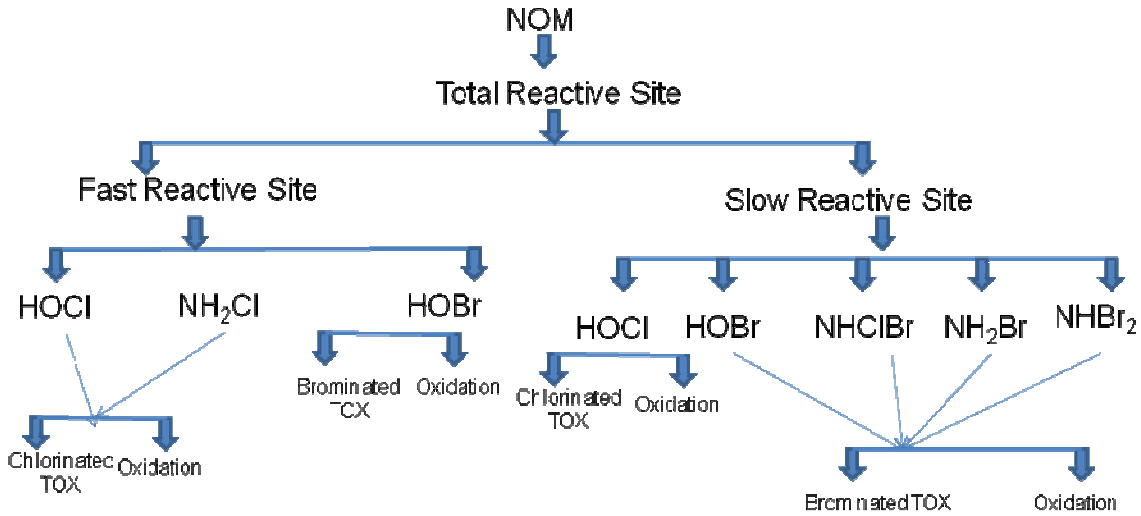

Figure 5-1: NOM reaction schematic in the presence of free chlorine, free bromine and haloamines

5.3. RESULTS AND DISCUSSION

5.3.1. Reactive site determination

The total reactive sites for each NOM source were estimated using the procedures of Duirk et al. (2005) as described in Section 5.2.2.2. Figure 5-1 and Figure 5-2 show the free chlorine residual for the samples with Lake Austin and Claremore Lake, respectively. The total reactive sites for Lake Austin and Claremore Lake are 42% and 47%, respectively. These results showed that NOM in Claremore Lake is more reactive

than Lake Austin NOM, which agreed with the SUVA shown in Table 5-1 (2.89 L/mg-m Claremore Lake SUVA vs. 2.49 L/mg-m for Lake Austin SUVA). These results match very well with the total reactive site measured by Duirk et al. (2005), who found total reactive sites of 45% and 49% for waters with a SUVA of 2.78 L/mg-m and 2.96 L/mg-m, respectively.

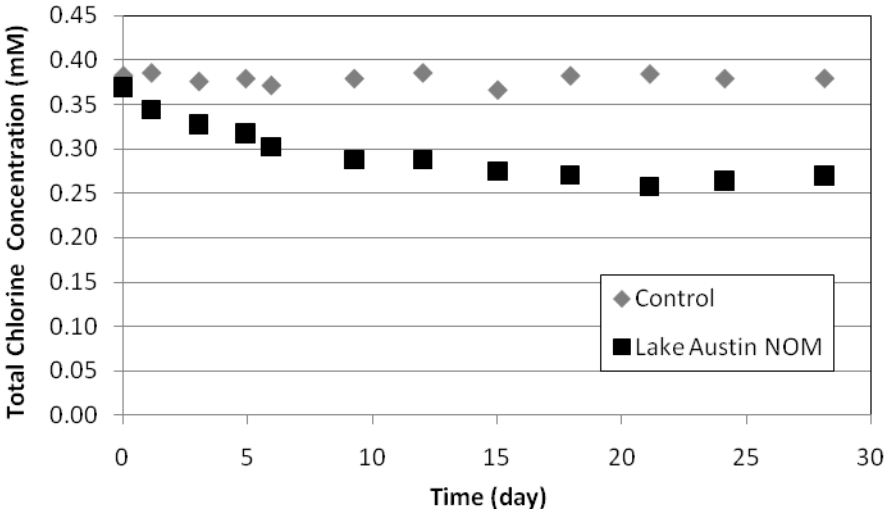

Figure 5-2: Total reactive site determination for Lake Austin NOM.

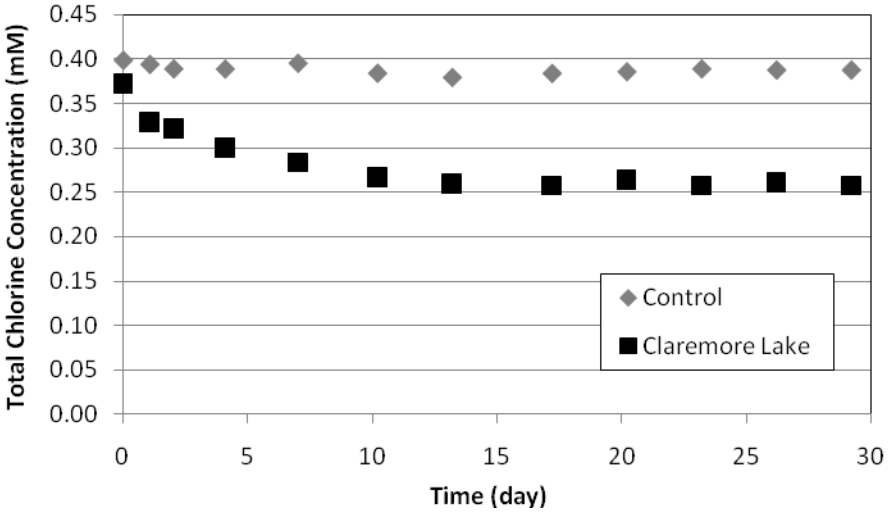

Figure 5-3: Total reactive site determination for Claremore Lake NOM.

To model monochloramine and total chlorine decay with NOM present the relative distribution of fast sites (DOC_1) and slow sites (DOC_2) must be estimated. An initial estimate of fast reacting sites was made from the Lake Austin TOX data at 1000 µg/L bromide and 5 mg/L NOM (Table 5-4). Because of the high bromide concentration, it was assumed that sufficient HOBr was formed during the prechlorination period to react with all the fast reactive sites. An average of the two measurements was taken, which yielded a fast reactive site estimate of 2.45%. The measurement at 100 µg/L bromide was excluded from the calculation because the potential HOBr formation was not large enough to guarantee that all the fast reactive sites would be consumed, while the measurement at 2 mg/L NOM was excluded because, as shown in Table 5-4, assuming all TOX formation due to fast site will lead to very high fast site fraction (6.45%) which is about two times more than what Echigo and Minear (2006) and Duirk et al. (2005) determined. This initial estimate of 2.45% was slightly above the range determined by Echigo and Minear (2006) and Duirk et al. (2005) for different NOM sources (0.3% to 2.3%). The slow reacting sites are the difference between the total reactive sites and the fast reacting sites.

Table 5-4: TOX results for Lake Austin water

pH	Bromide (µg/L)	Lake Austin NOM (mg/L as C)	TOX (µM)*	Fast-Reacting Sites (%)**
7.0	1000	5	8.38	2.01
6.5	1000	5	11.51	2.76
6.5	1000	2	10.75	6.45
6.5	100	5	7.39	1.78

*Measured after 30 sec of chlorination followed by 10 min of chloramination

** Fast-Reacting Sites = TOX(M)/TOC(M)x100

5.3.2. Model Development

The introduction of NOM affects the decay of total chlorine and monochloramine in two ways (Figure 5-3). First, the initial total chlorine and monochloramine concentrations after 30 seconds of prechlorination are lower. These lower concentrations result from the reactions between free chlorine and free bromine with the fast sites on NOM. Second, monochloramine in the presence of NOM is more stable over six hours. This stability is a result of less HOBr being available to react with monochloramine to form NHBrCl. The Modified Unified Haloamine Kinetic Model V.1.1 predicted the experimental results in NOM-free water very well. Clearly, modifications to the model are needed to account for the impact of NOM. These modifications were undertaken in two steps. First, additional reactions were introduced to the prechlorination model so that the initial concentrations for the start of chloramination were correctly predicted. Second, additional reactions were added to the chloramination model for free chlorine, free bromine, and haloamine reactions with NOM.

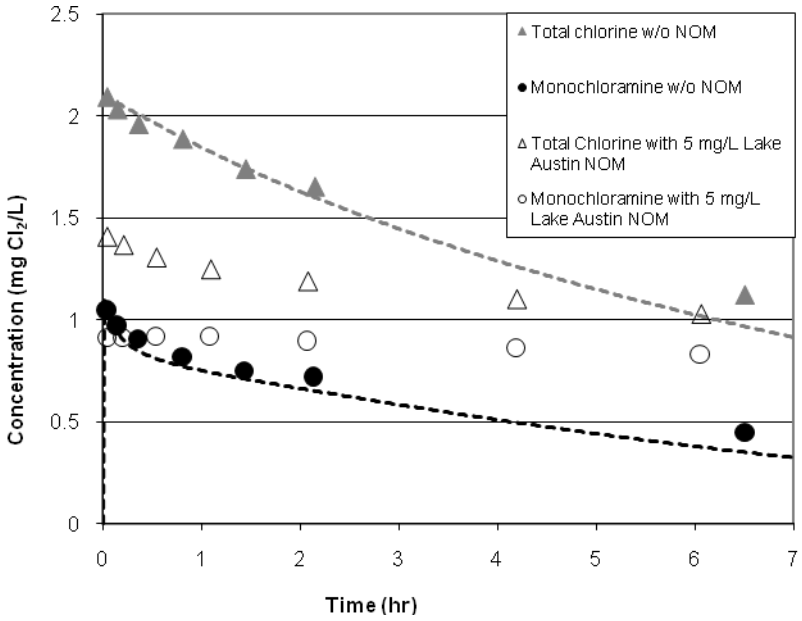

Figure 5-4: Monochloramine and total chlorine decay (pH = 6.55, TOTCO3= 4mM, Br-=1000µg/L, Cl_2/N=3/1, 30 seconds prechlorination time) (dash lines represent model results)

5.3.2.1 Prechlorination model

NOM can react with halogens (e.g., aqueous chlorine and bromine) via oxidation (i.e., cleaving carbon–carbon double bonds) and/or substitution (i.e., replacement of functional groups by a halogen molecule). Echigo and Minear (2006) studied the reaction of HOBr with NOM in water treatment processes. They used a stop-flow technique in their work and found two types of reactive sites for the reaction of HOBr with NOM. Fast reactive sites range from 0.26 to 0.92 µmol (mg C)$^{-1}$ (0.3 to 1.1 % of the NOM) at pH 7.0. The reaction between HOBr and the fast reactive sites took place in the first second, with an apparent second order rate constant ranging from 1.94×10^9 to 5.04×10^9 $M^{-1}h^{-1}$; an average value of 3.6×10^9 $M^{-1}h^{-1}$ was used in the model. In addition, they found that bromine substitution is the major pathway for the reaction between HOBr and NOM, compared to oxidation reactions that do not yield organic bromines. Also, the reaction of

HOBr with NOM was found to be much faster than that with HOCl; therefore, bromine reactions with NOM will dominate over chlorine reactions when both are present.

In modifiying the prechlorination model, only the fast-reactive sites of the NOM were assumed to react with the chlorine and bromine because of the short prechlorination time (30 seconds). In addition, the bromine and chlorine substitution onto NOM were assumed to be the only reaction pathways for the reactions between the fast reactive sites and chlorine and bromine. Also, the relative kinetics are such that the bromine reaction with the fast sites will dominate over the chlorine reaction (Echigo and Minear, 2006). As shown in Table 5-4, at 100 µg/L (1.25 µM) bromide, 7.39 µM of TOX formed, which indicates that not all the TOX was bromine-substituted organic chemicals; if the bromide concentration is exhausted, the fast sites will react with the free chlorine to form chlorine-substituted TOX. The TOX results for 100 µg/L bromide were used to estimate the reaction rate constant of free chlorine with fast reactive sites by fitting the model to the measured TOX concentration. As such the following reactions were added to the Modified Unified Haloamine Kinetic Model V.1.1 (Table 5.3) to describe prechlorination.

$$HOBr + DOC_1 \rightarrow DOC_{Br} \qquad k = 3.6x10^9 M^{-1}h^{-1}$$

$$HOCl + DOC_1 \rightarrow DOC_{Cl} \qquad k = 3x10^6 M^{-1}h^{-1}$$

When the model was run with the rate constants listed above and the initial estimate of the fast reactive sites, the concentration of free chlorine after 30 seconds of chlorination was too low to match the values measured experimentally (i.e., the initial concentrations in the chloramination step of the experiments). To address this issue, the fraction of fast reactive sites was adjusted for each NOM source, effectively decreasing

the concentration of DOC_1. The fast reactive site fraction was adjusted, rather than the rate constants, because differences were observed between the two NOM sources that could not be reconciled by adjustment of the rate constants. Therefore, the fast reactive site fraction was adjusted because it is a characteristic of each NOM source

Experiments 5 and 9 (Table 5-5) (pH 7, 5 mg/L NOM) were used to estimate the fraction of fast reactive sites; these were estimated as 1.7% for Lake Austin NOM and 2.5% Claremore Lake NOM, which is still within the range found by others (Duirk et al. 2005; Echigo and Minear 2006). Table 5-5 shows both the predicted and measured initial total chlorine and monochloramine concentrations. The model showed excellent prediction for initial total chlorine and monochloramine concentration after 30 seconds prechlorination time for the other experiments.

Table 5-5: Measured and predicted initial total chlorine and monochloramine concentration

Exp. No.	NOM	pH	Carbonate Buffer (mM)	DOC (mg/L as C)	Total chlorine (mg/L as Cl_2)		monochloramine (mg/L as Cl_2)	
					Fitted or predicted	measured	Fitted or predicted	measured
1	Lake Austin	6.5	4	2	1.80	1.70	1.00	0.99
2	Lake Austin	6.5	4	5	1.37	1.41	0.93	0.91
3	Lake Austin	6.5	4	10	1.20	1.30	0.77	0.78
4	Lake Austin	7	4	5	1.44*	1.44	1.09*	0.97
5	Lake Austin	8	4	2	1.80	1.82	1.63	1.55
6	Lake Austin	8	4	5	1.61	1.7	1.59	1.47
7	Lake Austin	8	4	10	1.55	1.78	1.52	1.50
8	Claremore Lake	6.5	4	5	1.22	1.20	0.91	0.86
9	Claremore Lake	7	4	5	1.23*	1.21	1.08*	0.91
10	Lake Austin	6.5	7	5	1.37	1.42	0.90	0.83
11	Lake Austin	8	7	5	1.27	1.48	1.27	1.30

* Fitted total chlorine and monochloramine all other are prediction

The different NOM sources yielded different initial total chlorine concentrations form the same conditions, as shown if Table 5-5. The initial concentrations for Claremore Lake NOM were less than the initial concentrations for Lake Austin NOM. This difference results from both more total reactive sites and a higher percentage of fast reactive sites in Claremore Lake NOM than in Lake Austin NOM (i.e., the DOC_1 concentration was higher for Claremore Lake NOM).

5.3.2.2 Chloramination model

The presence of ammonia and the subsequent formation of haloamines greatly increase the number of potential reactions with NOM. To keep the complexity of the model at a manageable level, a number of simplifying assumptions were made in modifying the model:

1. Only free chlorine, free bromine, and monochloramine react with the fast reactive sites. These three species are the dominant species for reaction times of less than 1 minute, when the reaction with fast reactive sites occurs. For prechlorination period only free chlorine and free bromine are available, while in the preformed monochloramine addition mode monochloramine will be the dominant specie over the first minute.
2. Monochloramine does not directly react with slow reactive NOM, in keeping with the work of Duirk et al. (2005).
3. Bromine-substituted haloamines, free chlorine, and free bromine react with the slow reactive sites, which is consistent with the work of Duirk et al. (2007) and Echigo and Miner (2006).
4. The reaction of a dihaloamine with NOM leads to substitution of one halogen onto the NOM and a monohaloamine product.

5. Bromochloramine reacts with NOM by substituting a bromine atom onto the NOM and generating monochloramine as a product, based on the work of Valentine (1986).
6. All halogen reactions with NOM result in the substitution of a halogen on NOM (i.e., oxidation reactions are negligible).
7. All bromine-substituted haloamines have the same reaction rate constant with NOM, based on Duirk et al. (2007) who indicated that the reactions are so fast that it is difficult to distinguish individual rate constants.

Table 5-6 shows the reactions with the slow reactive NOM sites added to the Modified Unified Haloamine Kinetic Model V.1.1 to develop the Modified Unified Haloamine Kinetic Model V.2. This model includes all the reactions in Table 5.3, plus the reactions with the fast and slow reactive NOM sites. The rate constant for HOCl reacting with DOC_2 was adopted from Duirk et al. (2007), who gave a range for this rate constant. The value used is the average reported for waters with similar SUVA to Lake Austin and Claremore Lake. Echigo and Minear (2006) also gave a range for the rate constant of the HOBr reaction with DOC_2; the average value was used here. Scientist®3.0 software was used to fit the model to the experimental results at pH 7.0 and 5 mg/L NOM to estimate the rate constants for the reaction between slow sites on the NOM and the bromine-substituted haloamines. Fitting was performed by minimizing the squared difference between the measured and fitted total chlorine and monochloramine concentration over time. Independent estimates of the rate constant for Lake Austin NOM and Claremore Lake NOM yielded the same value ($1.0x10^4$ $M^{-1}h^{-1}$). The rate constant of bromine-substituted haloamines with the slow sites is four orders of magnitude less than the rate of HOBr reaction with the slow sites (Table 5-6); however, after ammonia addition most of the HOBr will react with ammonia and monochloramine to form

bromine-substituted haloamines. Within a few minutes of ammonia addition, the concentration of bromine-substituted haloamines will be more than four orders of magnitude greater than free bromine (HOBr) concentration, so even though the rate constants of bromine-substituted haloamines are much lower than the rate constant of HOBr, they still an play important role in total chlorine and monochloramine decay and in bromine speciation. Figure 5-5 shows the fit of the model to the data.

Table 5-6: Reaction of NOM in the chloramination model

Reaction	Rate constant ($M^{-1}h^{-1}$)	Reference
$HOCl+DOC_2 \rightarrow DOC_{Cl}$	$k = 6.0x10^5$	Duirk et al. (2005)
$HOBr+DOC_2 \rightarrow DOC_{Br}$	$k = 3.6x10^9$	Echigo and Minear (2006)
$NH_2Br + DOC_2 \rightarrow DOC_{Br} + NH_3$	$k = 1.0x10^4$	This work
$NHBr2 + DOC_2 \rightarrow DOC_{Br} + NH_2Br$	$k = 1.0x10^4$	This work
$NHBrCl + DOC_2 \rightarrow DOC_{Br} + NH_2Cl$	$k = 1.0x10^4$	This work

DOC_{Cl} is the chlorine-substituted TOX and DOC_{Br} is the bromine-substituted TOX in mole halite

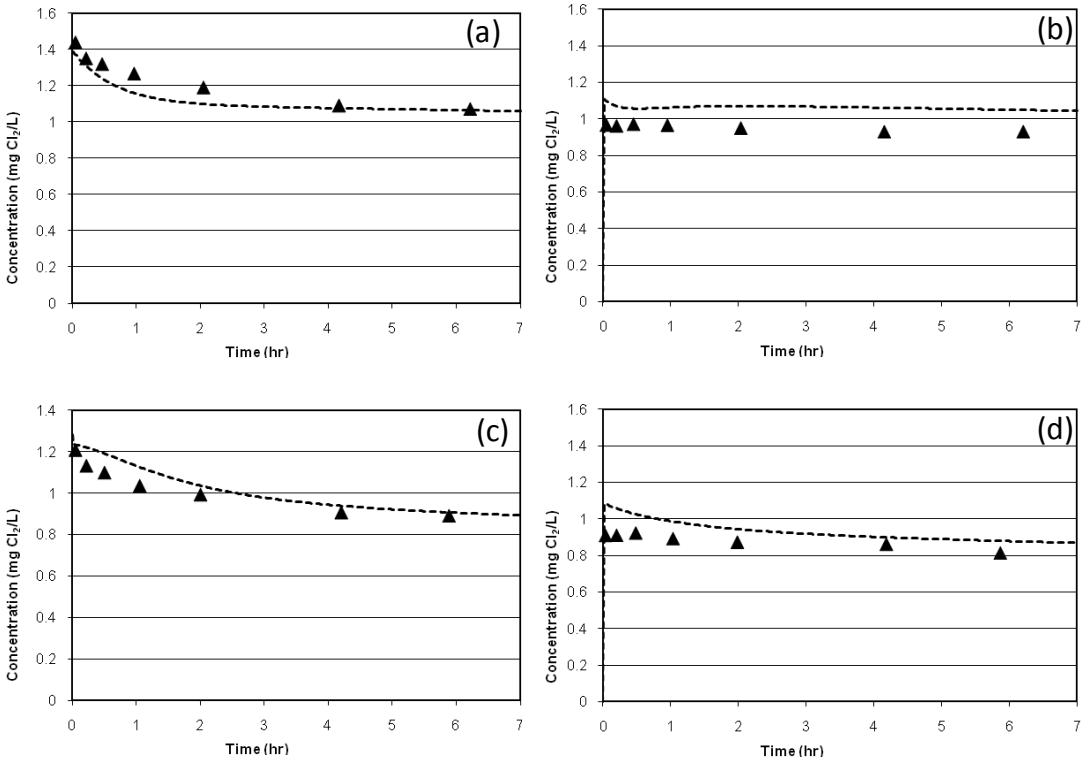

Figure 5-5: Model fitting (pH = 7.0, TOTCO3= 4mM, Br-=1000µg/L, /=3/1, NOM= 5 mg/L as C, and , 30 seconds prechlorination time) (dash lines represent model results) (a) total chlorine with Lake Austin NOM, (b) monochloramine with Lake Austin NOM, (c) total chlorine with Claremore Lake NOM, and (d) monochloramine with Claremore Lake NOM,

5.3.3. Model Testing

The model was tested by predicting the results of several other experiments. At a NOM concentration of 5 mg/L, the model predicted the experimental results for monochloramine at pH 6.5 for Lake Austin water very well (Figures 5-6), both with respect to initial concentrations and the decay over time. The model predicted a more rapid decay of total chlorine than was observed experimentally. This rapid decay may be due to the use of only reactions with the fast sites during the prechlorination modeling. If the fast sites are exhausted before the end of the prechlorination step, the predicted HOBr

concentration could be higher than the actual concentration, which could lead the model to predict more rapid total chlorine decay than observed experimentally. At pH 8 (Figure 5-7), little decay occurred over the course of the experiment and the model predicted these observations very well.

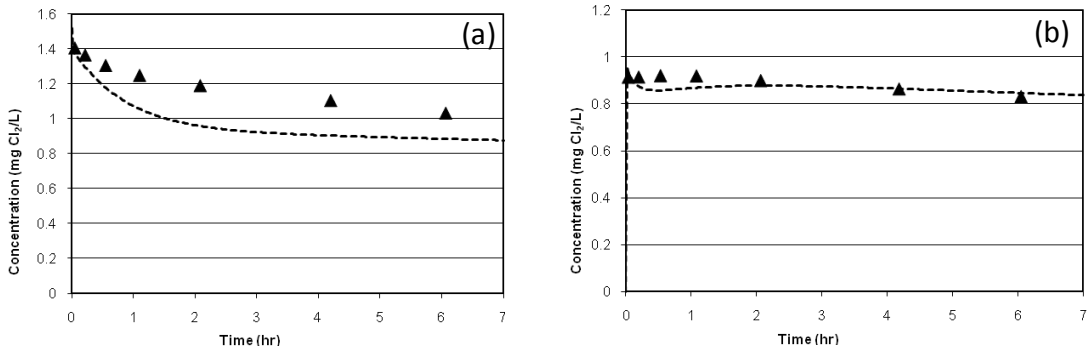

Figure 5-6: (a) Total chlorine decay and (b) monochloramine decay (pH = 6.5, TOTCO3= 4mM, Br-=1000µg/L, Cl_2/N=3/1, 5 mg/L as C Lake Austin NOM, 30 seconds prechlorination time) (dash lines represent model prediction)

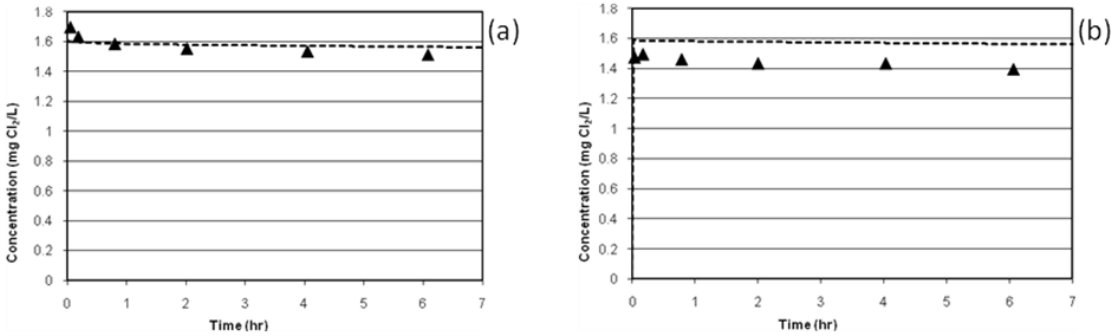

Figure 5-7: (a) Total chlorine decay and (b) monochloramine decay (pH = 8.0, TOTCO3= 4mM, Br-=1000µg/L, Cl_2/N=3/1, 5 mg/L as C Lake Austin NOM, 30 seconds prechlorination time) (dash lines represent model prediction)

Predictions for NOM concentrations of 2, 5 and 10 mg/L at pH 6.5 for Lake Austin NOM are shown for total chlorine and monochloramine, in Figure 5-8. The data for 5 mg/L were shown in Figure 5-6. As note above, the model had some difficulty predicting the total chlorine concentration at 5 mg/L NOM. This difficulty increased at the lower NOM concentration and diminished at the higher NOM concentration.

Predictions of monochloramine decay were quite good, although as with total chlorine the model did predict more rapid decay of monochloramine at 2 mg/L NOM than was experimentally observed.

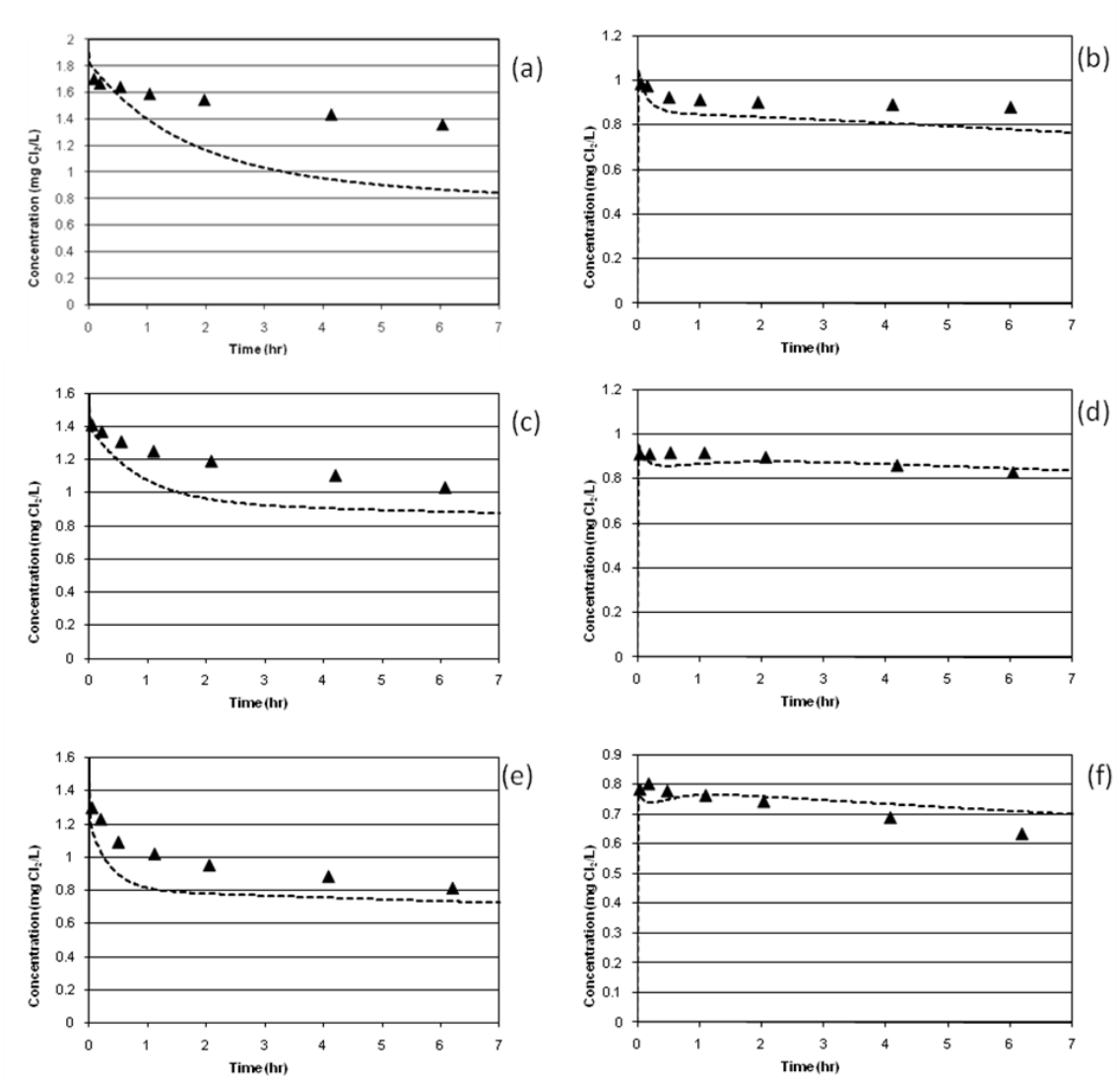

Figure 5-8 Model prediction (pH = 6.5, $TOTCO_3$= 4 mM, Br-=1000 µg/L, Cl_2/N=3/1, and , Lake Austin NOM, 30 seconds prechlorination time) (dash lines represent model prediction) (a) total chlorine with 2 mg/L NOM, (b) monochloramine with 2 mg/L NOM, (c) total chlorine with 5 mg/L NOM, (d) monochloramine with 5 mg/L NOM, (e) total chlorine with 10 mg/L NOM, (f) monochloramine with 10mg/L NOM

For Claremore Lake (Figure 5-9), the model showed excellent predictions at pH 6.5 for both total chlorine and monochloramine. Claremore Lake NOM yield lower initial

total chlorine and monochloramine comparred to Lake Austin NOM at the same conditions as shown in Table 5-5. This difference is due to the more fast reactive sites in Claremore Lake NOM (Claremore Lake fast sites are 2.5% and Lake Austin NOM fast sites are 1.7%). As shown in Figure 5-8 (c) and 5-9 the prediction for total chlorine decay for Claremore Lake NOM is more accurate than the prediction for Lake Austin NOM. This more accurate prediction may result from the higher concentraiton of fast reactive sites in Claremore Lake NOM, which reduces the likelihood of exhausting the fast reactive sites during prechlorination.

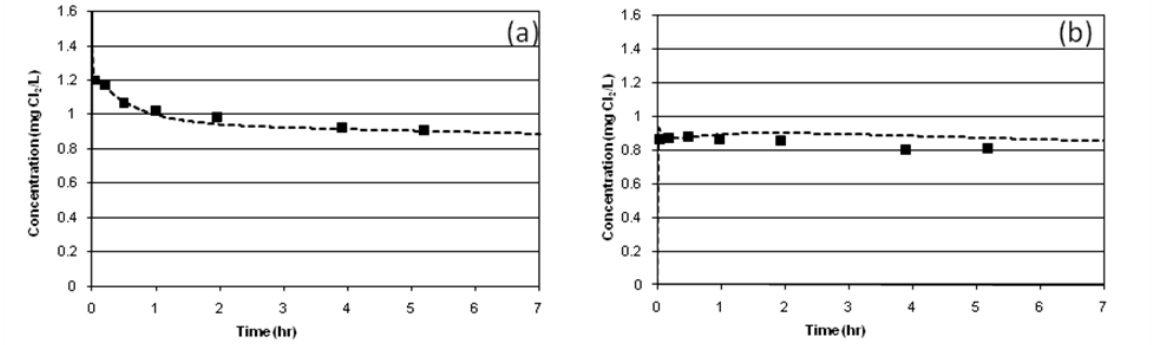

Figure 5-9: (a) Total chlorine decay and (b) monochloramine decay (pH = 6.5, $TOTCO_3$= 4 mM, Br-=1000 µg/L, Cl_2/N=3/1, 5 mg/L as C Claremore Lake NOM, 30 seconds prechlorination time) (dash lines represent model prediction)

The ability of the model to predict the measured TOX concentrations (Table 5-4) was also examined. The sum of the DOC_{Cl} (the chlorine-substituted TOX) and DOC_{Br} (the bromine-substituted TOX) concentrations predicted by the model was compared to the measured TOX values (Table 5-7). The model showed good prediction for TOX formation with 5 mg/L NOM, while the model under estimate the TOX formation with 2 mg/L. The good agreement with three of the four TOX measurements confirms that the assumption of 100% halogen substitution in reactions with DOC_1 and DOC_2 is reasonable.

Table 5-7: Measured and predicted TOX concentration

pH	Bromide (µg/L)	NOM (mg/L)	Measured TOX (µM)	Predicted TOX (µM)	Error %
7.0	1000	5	8.38	9.01	7.5
6.5	1000	5	11.51	10.33	-10.3
6.5	1000	2	10.75	4.61	-57.2
6.5	100	5	7.39	6.95	-5.96

5.4. EFFECT OF NOM ON HALOAMINE DECAY

The presentce of NOM affects the decay of total chlorine and monochloramine after a short prechlorination time. As shown in Figure 5-10, the initial concentration of total chlorine with 5 mg/L Lake Austin NOM was 30% less than without NOM, illustrating the importance of of reactions between NOM and free bromine and free chlorine. The initial concentration of monochloramine did not change very much because at a short time (30 seconds) and with a high bromide concentration (1000 µg/L), the main TOX formation pathway is through the reaction of HOBr with NOM. In addition, the decay of total chlorine and monochloramine over time was less rapid in the presence of NOM. This stability results from less HOBr being available to react with monochloramine to form bromochloramine, which in turn promotes faster total chlorine and monochloramine decay, as shown in Chapter 4.

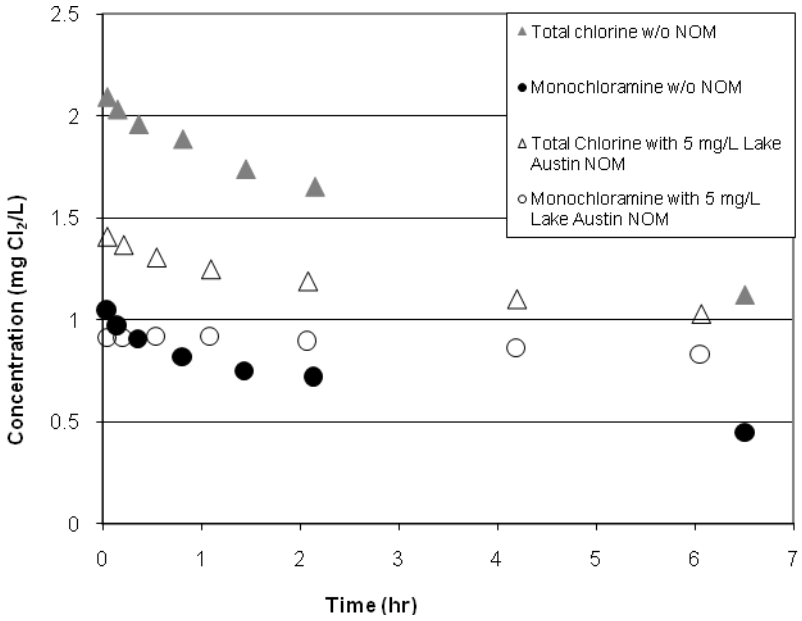

Figure 5-10: Monochloramine and total chlorine decay (pH = 6.55, TOTCO3= 4mM, Br^-=1000µg/L, Cl_2/N=3/1, 30 seconds prechlorination time)

5.5. CONCLUSION

The Modified Unified Haloamine Kinetic V.2 (Table 5-8) was developed by adding eight reactions with NOM encompassing two NOM fractions reacting with free chlorine, free bromine, and haloamines. With the addition of this relatively small number of reaction equations, the model showed good predictions for monochloramine and total chlorine decay over time after a short prechlorination period in the presence of bromide and NOM over the pH range of 6.5-8.0, carbonate buffer range of 2-10 mM, and NOM range of 2-10 mg/L as C. In addition, the model showed good predictions for TOX formation in limited testing.

Table 5-8: Modified Unified Haloamine Kinetic Model V.2

No.	Reaction	Rate constant at 25 °C	Reference
1	$HOCl + NH_3 \rightarrow NH_2Cl + H_2O$	$3.07 \times 10^6\ M^{-1}S^{-1}$	Qiang and Adams (2004)
2	$NH_2Cl + H_2O \rightarrow NH_3 + HOCl$	$2.1 \times 10^{-5}\ M^{-1}S^{-1}$	Morris and Isaac (1981)
3	$NH_2Cl + HOCl \rightarrow NHCl_2 + H_2O$	$2.8 \times 10^2\ M^{-1}S^{-1}$	Margerum et al. (1978)
4	$NHCl_2 + H_2O \rightarrow NH_2Cl + HOCl$	$6.4 \times 10^{-7}\ S^{-1}$	Margerum et al. (1978)
5	$NH_2Cl + NH_2Cl \rightarrow NHCl_2 + NH_3$	K_5, pH dependent	Vikesland et al. (2001)
6	$NHCl_2 + NH_3 \rightarrow NH_2Cl + NH_2Cl$	$6.1 \times 10^4\ M^{-2}S^{-1}$	Hand and Margerum (1983)
7	$NH_2Cl + NHCl_2 \rightarrow N_2 + 3H + 3Cl^-$	$1.5 \times 10^{-2}\ M^{-1}S^{-1}$	Leao (1981)
8	$NHCl_2 + H_2O \rightarrow NOH + 2HCl$	$1.1 \times 10^2\ M^{-1}S^{-1}$	Jafvert and Valentine (1987)
9	*NOH* $+ NHCl_2 \rightarrow N_2 + HOCl + HCl$	$2.8 \times 10^4\ M^{-1}S^{-1}$	Leao (1981)
10	*NOH* $+ NH_2Cl \rightarrow N_2 + H_2O + HCl$	$8.3 \times 10^3\ M^{-1}S^{-1}$	Leao (1981)
11	$HOCl + Br^- \rightarrow HOBr + Cl^-$	K_{11}, pH dependent	This work
12	$HOBr + NH_3 \rightarrow NH_2Br + H_2O$	$7.5 \times 10^7\ M^{-1}S^{-1}$	Wajon and Morris (1980)
13	$HOBr + NH_2Cl \rightarrow NHBrCl + H_2O$	K_{13}, pH dependent	This work
14	$OBr^- + NH_2Cl \rightarrow NHBrCl + OH$	$2.2 \times 10^4\ M^{-1}S^{-1}$	Gazda and Margerum (1994)
15	$NH_2Cl + NH_2Cl + Br^- \rightarrow NHBrCl + Cl^- + NH_3$	K_{15}, pH dependent	Trofe et al. (1980)
16	~~$NHBrCl + NHBrCl + H_2O \rightarrow N_2 + HOBr + HBr + 2HCl$~~	Removed from the model	Valentine (1983) and Pope (2006)
17	$NH_2Br + NH_2Br \rightarrow NHBr_2 + NH_3$	pH dependent	Lei et al. (2004)
18	$NHBr_2 + NH_3 \rightarrow NH_2Br + NH_2Br$	pH dependent	Lei et al. (2004)
19	$NHBr_2 + NHBr_2 \rightarrow N_2 + 3H^+ + 3\ Br^-$	pH dependent	Lei et al. (2004)
20	$NH_2Br + NHBr_2 + H_2O \rightarrow N_2 + HOBr + 3H^+ + 3\ Br^-$	$8.9\ M^{-1}S^{-1}$	Lei et al. (2004)
21	$HOCl \leftrightarrow H^+ + OCl^-$	$pK_a = 7.5$	Connick and Chia (1959)
22	$NH_4^+ \leftrightarrow NH_3 + H^+$	$pK_a = 9.3$	Snoeyink and Jenkins (1980)
23	$HOBr \leftrightarrow OBr^- + H^+$	$pK_a = 8.8$	Haag and Hoigne (1983)
24	$H_2CO_3 \rightarrow HCO_3^- + H^+$	$pK_a = 6.3$	Snoeyink and Jenkins (1980)
25	$HCO_3^- \rightarrow CO_3^{2-} + H^+$	$pK_a = 10.3$	Snoeyink and Jenkins (1980)
26	$NHBrCl + H_2O \rightarrow U + HBr + HCl$	pH, dependent	This work
27	$U + NHBrCl \rightarrow HOBr + N_2 + HCl$	$1 \times 10^{11}\ M^{-1}s^{-1}$	This work
28	$U + NH_2Cl \rightarrow H_2O + N_2 + HCl$	$3 \times 10^{10}\ M^{-1}\ s^{-1}$	This work
29	$HOBr + DOC_1 \rightarrow DOC_{Br}$	$1 \times 10^6\ M^{-1}\ s^{-1}$	Echigo and Minear (2006)
30	$HOCl + DOC_1 \rightarrow DOC_{Cl}$	$833\ M^{-1}\ s^{-1}$	This work
31	$NH_2Cl + DOC_1 \rightarrow DOC_{Cl}$	$5.6\ M^{-1}\ s^{-1}$	Duirk (2005)
32	$HOBr + DOC_2 \rightarrow DOC_{Br}$	$1 \times 10^6\ M^{-1}\ s^{-1}$	Echigo and Minear (2006)
33	$HOCl + DOC_2 \rightarrow DOC_{Cl}$	$167\ M^{-1}\ s^{-1}$	Duirk (2005)
34	$NH_2Br + DOC_2 \rightarrow DOC_{Br} + NH_3$	$2.78\ M^{-1}\ s^{-1}$	This work
35	$NHBr_2 + DOC_2 \rightarrow DOC_{Br} + NH_2Br$	$2.78\ M^{-1}\ s^{-1}$	This work
36	$NHBrCl + DOC_2 \rightarrow DOC_{Br} + NH_2Cl$	$2.78\ M^{-1}\ s^{-1}$	This work

$k_5 = k_{H^+}[H^+] + k_{H2CO3}[H_2CO_3] + k_{HCO3}[HCO_3] + k_{H2PO4}[H_2PO_4^-] + k_{H3P}[H_3PO_4]$

$k_{15} = 1.4 \times 10^6\ M^{-2}S^{-1}\ [NH_2Cl][Br^-][H^+]$

$k_{11} = 1517 M^{-1}s^{-1} + 2.83 \times 10^{10}\ M^{-2}S^{-1}\ [H^+] + 3.0 \times 10^5\ M^{-2}S^{-1}\ [HCO_3^-] + 2.56 \times 10^8\ M^{-2}S^{-1}\ [H_2CO_3] + 4.06 \times 10^5\ M^{-2}S^{-1}\ [NH_4^+]$

$k_{13} = 1.54 \times 10^{11}\ M^{-2}S^{-1}\ [HCO_3^-] + 2.3 \times 10^{14}\ M^{-2}S^{-1}[H_2CO_3]$

$k_{17} = 0.5\ M^{-1}S^{-1} + 5 \times 10^8\ M^{-2}S^{-1}\ [H^+] + 2900\ M^{-2}S^{-1}\ [NH_4^+] + 540\ M^{-2}S^{-1}\ [HCO_3^-]$

$k_{18} = 1 M^{-1}S^{-1} + 1 \times 10^9\ M^{-2}S^{-1}\ [H^+] + 190\ M^{-2}S^{-1}\ [NH_4^+] + 180\ M^{-2}S^{-1}\ [HCO_3^-]$

$k_{19} = 6.2 M^{-1}S^{-1} + 8.3 \times 10^4\ M^{-2}S^{-1}\ [OH^-] + 3.2 \times 10^3\ M^{-2}S^{-1}\ [CO_3^{2-}]$

$k_{26} = 1.54 \times 10^9\ M^{-2}S^{-1}[HCO_3^-] + 1.7 \times 10^{12}\ M^{-2}S^{-1}[H_2CO_3]$

NOH is the unidentified monochloramine auto-decomposition intermediate.

CHAPTER 6: Conclusions and Engineering Significance

6.1. CONCLUSIONS

This research focused on understanding better and modeling more accurately haloamine chemistry in the presence of bromide and NOM with or without a prechlorination step. Several key issues were investigated:

1. The oxidation rate of bromide by free chlorine during short periods of chlorination.
2. The formation rate of bromochloramine from the reaction of monochloramine and HOBr: This reaction is the dominant bromochloramine formation pathway upon ammonia addition after prechlorination.
3. A new scheme of bromochloramine decay.
4. The impact of NOM on haloamine decay over a broad range of pH, carbonate buffer concentrations and NOM.
5. Incorporation of Br into organic chemicals.

The hypobromous acid formation rate was found to be an acid-catalyzed reaction, which confirms the finding of Kumar et al. (1987). A new value of the acid catalysis effect of hydrogen ion was estimated. New terms were introduced to the hyprobromous acid formation rate including the acid catalysis effect of bicarbonate, carbonic acid, and ammonium ion. In addition, the hypobromous acid formation rate played a very important role in the initial concentration of monochloramine after a short time of prechlorination. The new rate constant for the reaction of HOCl with bromide ion to form hypobromous acid proposed by this study was used in the Modified Unified Haloamine

Kinetic Model and shows excellent prediction for TOTOBr (HOBr and OBr^-) formation, TOTOCl (HOCl and OCl^-) decay, and initial monochloramine concentration after 30 seconds of prechlorination.

The bromochloramine formation rate from the reaction of hypobromous acid and monochloramine was found to be an acid-catalyzed reaction. The monochloramine reaction with HOBr is the dominant bromochloramine formation pathway; therefore, accurate description of this reaction rate is crucial to the performance of the model. Both a new rate constant and its dependency on common acid-catalyzing species were determined in this research.

In addition, a new scheme for bromochloramine decay was developed. The old scheme of bromochloramine decay, proposed by Valentine (1983), consisted of bromochloramine reacting only with itself, but no rate constant was proposed. Pope, (2006) estimated a rate constant for the Valentine bromochloramine reaction, but this rate constant failed to model the experimental results. In this research, bromochloramine decay was modeled similarly to the well-established dichloramine decay scheme: bromochloramine decays through reactions with monochloramine and with itself. The rate constants for this new decay scheme were also estimated in this work. The new acid-catalysis rate constant for bromochloramine formation and the new scheme and rate constants for bromochloramine decay help described the rapid total chlorine and monochloramine decay observed under some conditions, especially at high carbonate concentration.

In sequential chlorination/chloramination, the presence of NOM will lead to lower initial total chlorine and monochloramine concentrations at the start of chloramination because NOM will react with free chlorine and and free bromine to form TOX. In addition, the presence of NOM will lead to more stable total chlorine and

monochloramine decay over time because less HOBr is available to react with monochloramine to form bromochloramine, leading to slower total chlorine and monochloramine decay.

Thirty seconds of prechlorination will lead to the same bromide speciation and to the same bromate control level as 5 minutes at below neutral pH values, but allows less time for other DBP formation. Considering the *Chlorine Ammonia Process* for pretreatment before ozonation, both 30 seconds and 5 minutes of prechlorination will reduce the available free bromide to react with ozone in the ozonation step and should reduce the bromate formation. At higher pH, the Modified Haloamine Kinetic Model V.2 can be used to estimate the minimum prechlorination time required to control bromate formation.

6.2. ENGINEERING SIGNIFICANCE

The Modified Unified Haloamine Kinetic Model V.2 provides a fundamental framework for understanding haloamine chemistry in the presence of bromide and NOM with or without a prechlorination step. The model can be used in a variety of applications; however, the motivating application for this research was an interest in understanding bromide sequestration better during chlorine and chloramine preoxidation in advance of ozonation. Application of the model to several such scenarios is summarized below.

The first scenario considers a water with 4 mg/L NOM (as DOC) with the NOM characteristics of Lake Austin water, pH 7, and a bromide concentration of 100 µg/L, which is the average concentration found in U.S. waters by Amy et al. (1994). Figure 6-1 shows the model predictions for bromine speciation after 10 minutes of chloramine contact under four different modes of pretreatment or chloramine addition. With

prechlorination of either 30 seconds or 5 minutes, the dominant bromine species is TOX. A very small amount of bromide is present and negligible concentrations of bromine-substituted haloamines. Prechlorination simulates the *Chlorine Ammonia Process* for sequestering bromide prior to ozonation. The literature suggests that bromide is sequestered in bromamines in this process (Buffle et al., 2004), but the model indicates that bromine-substituted organic chemicals are the likely sequestering agent. HOBr forms very rapidly in the presence of free chlorine and reacts very rapidly with NOM; therefore, the estimated speciation makes sense in light of the known kinetics. Unfortunately, this performance is quite undesirable from the viewpoint of limiting overall DBP formation, although it may reduce bromate formation during ozonation.

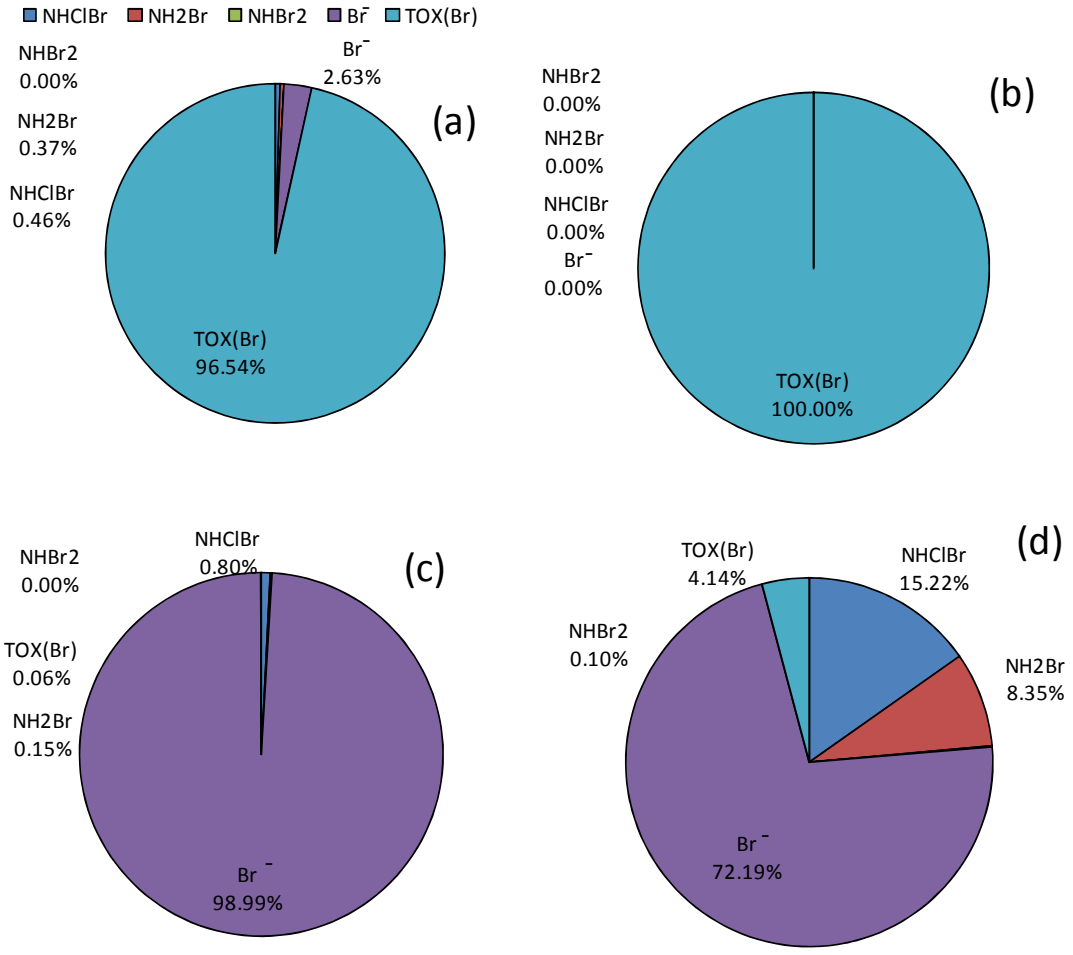

Figure 6-1: model prediction for bromide speciation (pH=7.0, Br^- =100 µg/L, NOM=4 mg/L, Cl_2/N=3/1) (a) 30 seconds prechlorination time, (b) 5 minutes prechlorination time, (c) Preformed monochloramine, and (d) Simultaneous chlorine and ammonia addition

The use of pre-formed monochloramine causes an opposite problem: essentially none of the bromide is sequestered in other chemicals. With pre-formed monochloramine, very little free chlorine is available to react with bromide to form HOBr. The absence of HOBr prevents the formation of bromine-substituted haloamines and organic chemicals. Over the reaction timeframe of the simulation, the rate of monochloramine reactions with bromide is simply too slow to have much impact on the bromide concentration.

With simultaneous chlorine and ammonia addition, significant concentrations of bromochloramine and monobromamine are predicted, as well as a much lower concentration of TOX than with prechlorination. Unfortunately, under these operating conditions, a significant fraction of the bromide (72%) that was not sequestered would be available to react subsequently with ozone to form bromate. A comparison of the four modes of treatment indicates that simultaneous addition of chlorine and ammonia is the most promising from the perspective of sequestering bromine in haloamines, rather than organic chemicals. Further investigation of this conclusion is needed, however, because simultaneous addition of chlorine and ammonia was not investigated in this research. Confirmation of the model under these operating conditions would increase the confidence in the conclusion drawn from the simulations.

The model can also be used to explore operating conditions that promote more sequestration of bromide. Figure 6-2 shows bromide speciation with simultaneous chlorine and ammonia addition at four different operation conditions, consisting of variations in chlorine dose and Cl_2/N ratios. Figure 6-2 (a) represents the same operating condition as in Figure 6-1(d). Increasing the chlorine dose from 2 to 3 mg/L with the same Cl_2/N ratio (Figure 6-2 (b)) had a negligible effect on the bromine speciation because with the same moderate Cl_2/N most of free chlorine will react with ammonia to form monochloramine and only a small amount will remain to react with bromide to form bromine-substituted haloamines. Maintaining the same chlorine dose (2 mg/L), but increasing the Cl_2/N ratio from 3/1 to 5/1 (Figure 6-2(c)) causes a substantial increase in the bromochloramine concentration and a corresponding decrease in the bromide concentration. The opposite effect was seen when the Cl_2/N ratio was decreased to 1/1 (Figure 6-2(d)). Higher Cl_2/N ratios favor the formation of HOBr relative to monochloramine, because at higher Cl_2/N more free chlorine is available to react with

bromide and form HOBr which in turn reacts with monochloramine to form a higher concentration of bromochloramine.

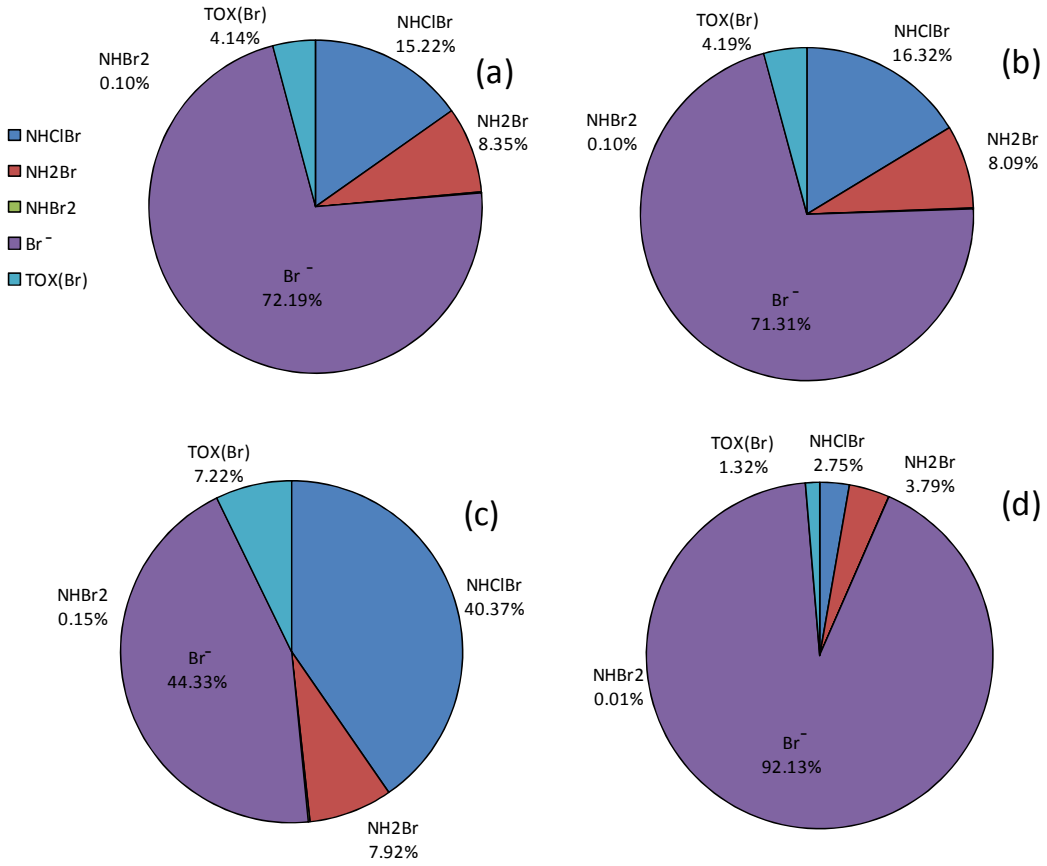

Figure 6-2: model prediction for bromide speciation (Simultaneous chlorine and ammonia addition ,pH=7.0, Br=100 µg/L, NOM=4 mg/L) (a) $TOTCl_2$= 2mg/L and Cl_2/N = 3/1, (b) $TOTCl_2$= 3 mg/L and Cl_2/N = 3/1 (c) $TOTCl_2$= 2 mg/L and Cl_2/N = 5/1, and (d) $TOTCl_2$= 2 mg/L and Cl_2/N = 1/1

Figure 6-3 shows the main changes to operating conditions that promote more sequestration of bromide. Figure 6-3 (a) and (b) show the effect of increasing the Cl_2/N ratio from 3/1 to 5/1 at pH 7. At a 5/1 Cl_2/N ratio, the free bromide concentration decreased from 72% to 44%, and the bromochloramine concentration increased from 15% to 40%, which should lead to less bromate formation during subsequent ozonation. The lower bromide concentration results from higher free chlorine concentration

available to react with bromide ion to form HOBr. Figure 6-3 (a) and Figure 6-3 (c) show the effect of lowering the pH from 7.0 to 6.5. At pH 6.5 the free bromide concentration decreased from 72% to only 18%. The lower bromide concentration results from the approximate doubling of the rate constant for the reaction between HOCl and bromide to form HOBr due to acid catalysis. Comparing the two approaches, increasing the Cl_2/N ratio (Figure 6-3 (b)) and lowering the pH (Figure 6-3 (c)) show that the second approach led to a lower free bromide concentration and higher bromochloramine concentration, which should lead to lower bromate formation during ozonation.

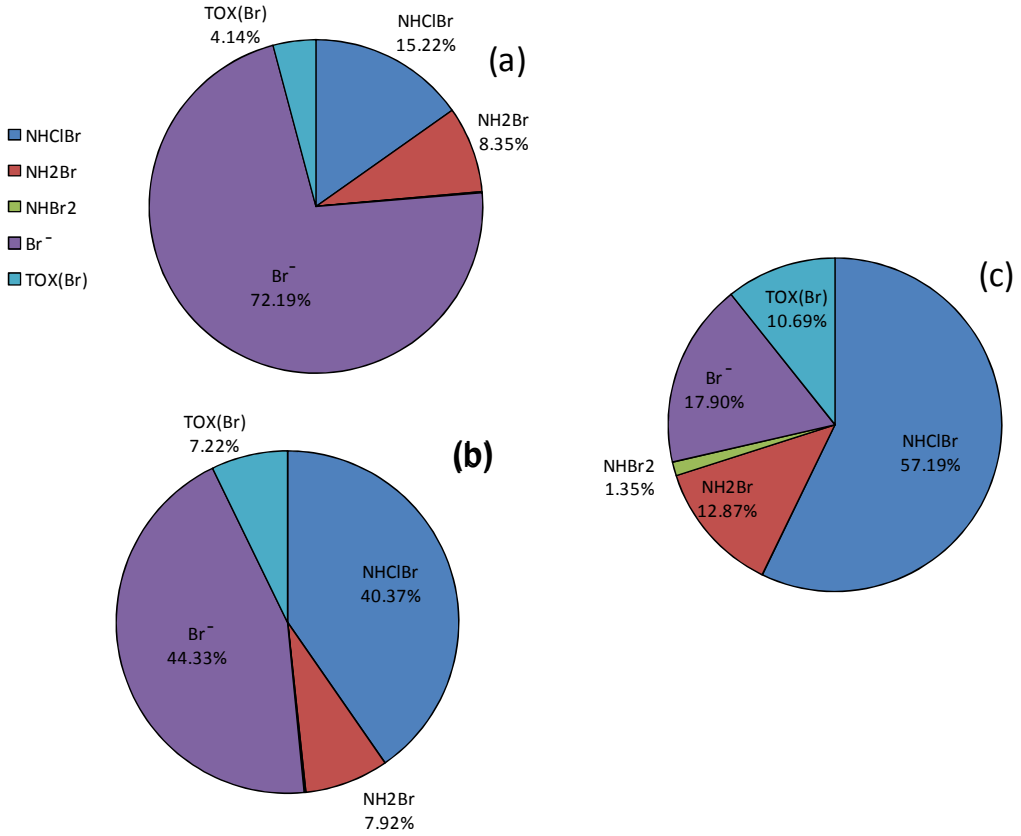

Figure 6-3: model prediction for bromide speciation (Simultaneous chlorine and ammonia addition ($TOTCl_2$= 2 mg/L, Br=100 µg/L, NOM=4 mg/L) (a) pH-7.0 and Cl2/N = 3/1, (b) pH=7.0 and Cl_2/N = 5/1 and (c) pH=6.5 and Cl_2/N = 3/1

The model was also compared to the pilot scale data of Krasner et al. (2007); the goal of their pilot-scale experiments was to evaluate alternative bromate control strategies. The raw water used in the pilot scale study came from two treatment plants in Southern California (Jensen and Mills). Krasner et al. ran their pilot plant (2.25-gpm facility) at pH 7.0, 200-300 µg/L bromide concentration, a chlorine dose of 0.5 and 1.0 mg/L, a 4/1 Cl_2/N ratio, and a TOC concentration 0f 3-4 mg/L. They tested operating modes involving both prechlorination and simultaneous chlorine and ammonia addition. Figure 6-4 shows that the prechlorination operating mode resulted in the least bromate formation; 1 minute and 5 minutes of prechlorination had the same bromate concentration after ozonation. These results agree very well with Modified Unified Haloamine Kinetic Model V.2 (Figure 6-1) in which 30 seconds and 5 minutes of prechlorination led to similar bromide speciation. The THM concentration with 1 minute of prechlorination, however, was only 57% of that with 5 minutes of prechlorination.. Simultaneous addition of chlorine and ammonia was not quite as effective as prechlorination, which is to be expected based on the comparison presented in Figure 6-1. Nevertheless, the bromate concentration after ozonation was well below the MCL. In contrast, the bromate control strategy of ammonia addition alone was not effective, and the bromate MCL was exceeded during ozonation.

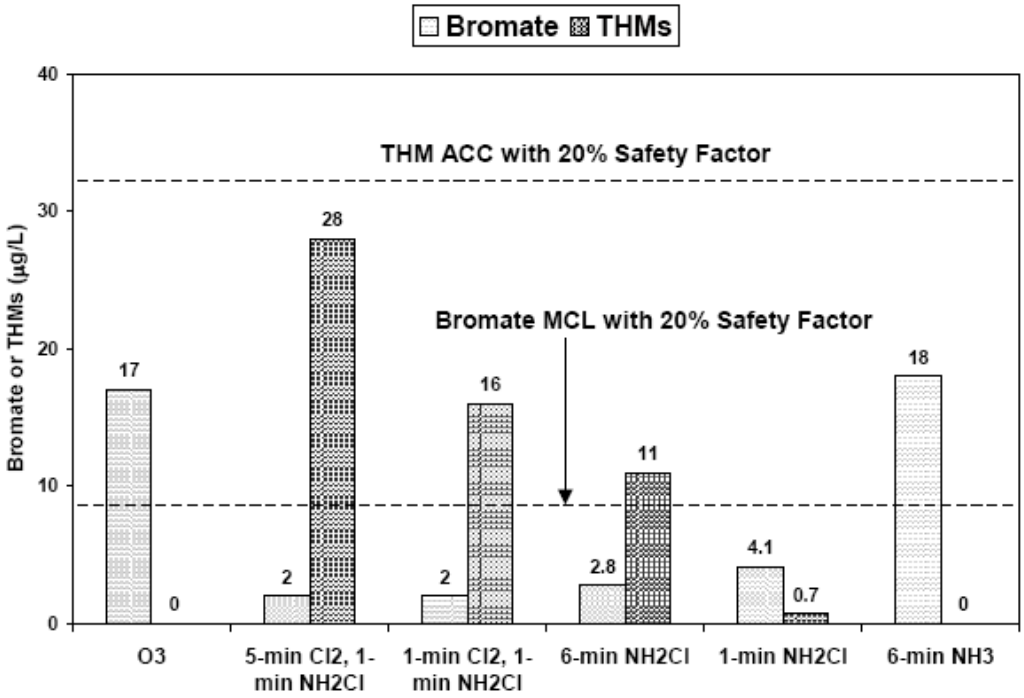

Figure 6-4: Effect of chloramine addition mode on bromate and THMs formation (pH=7.0, Cl_2/N= 4/1 and bromide = 200 µg/L) (Krasner et al., 2007)

Appendix -1: Brønsted p and q estimation

Species	p	q
H_2O	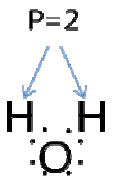	
H_3O^+	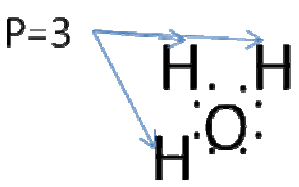	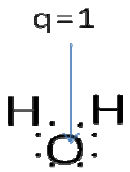
NH_4^+	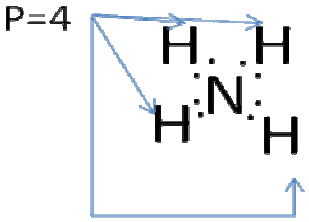	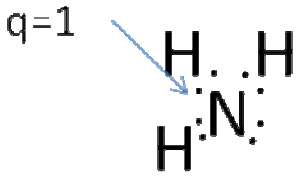
H_2CO_3	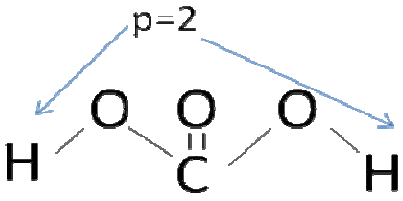	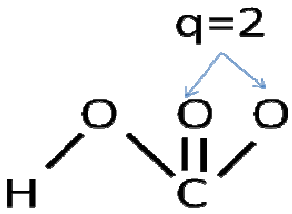
HCO_3^-	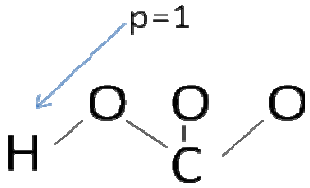	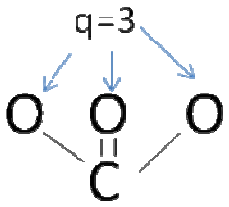

p: is the number of equivalent acidic protons in the acid.

q: is the number of equivalent basic sites in its conjugate base.

Appendix -2: Experimental Result and Model Prediction

This appendix shows the experimental results for all the experiments run in this research. In addition, this appendix shows the model predictions for each experiment. The Modified Unified Haloamine Kinetic Model V.1.1 was used to predict total chlorine and monochloramine decay in the experiments in the absence of NOM. The Modified Unified Haloamine Kinetic Model V.2 was used to predict total chlorine and monochloramine decay in the experiments with NOM.

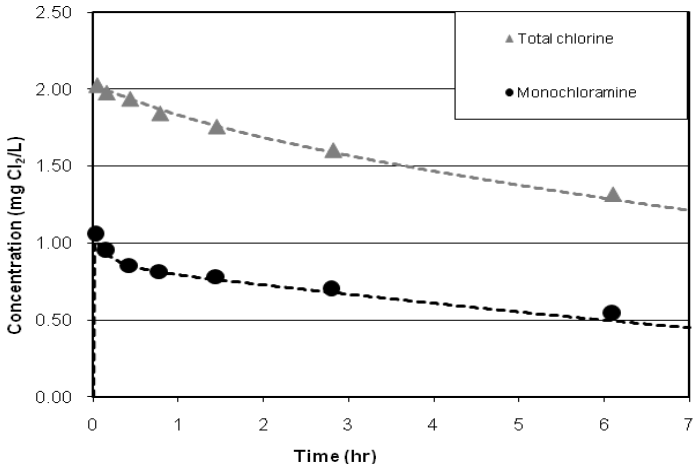

Monochloramine and total chlorine decay (pH = 6.55, $TOTCO_3$= 2 mM, Br^-=1000 µg/L, Cl_2/N=3/1, 30 seconds prechlorination time) (dash lines represent model predictions)

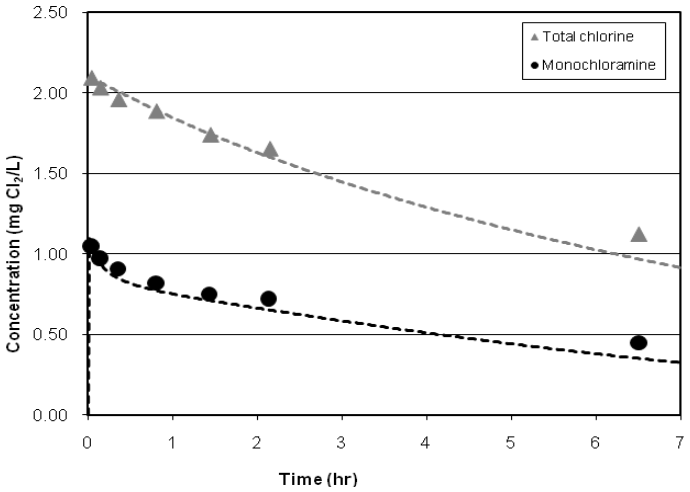

Monochloramine and total chlorine decay (pH = 6.55, $TOTCO_3$= 4 mM, Br^-=1000 µg/L, Cl_2/N=3/1, 30 seconds prechlorination time) (dash lines represent model predictions)

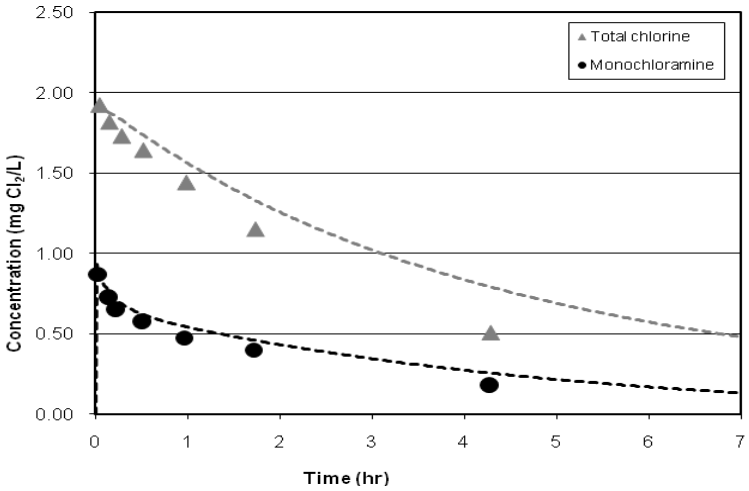

Monochloramine and total chlorine decay (pH = 6.55, $TOTCO_3$= 7 mM, Br^-=1000 µg/L, Cl_2/N=3/1, 30 seconds prechlorination time) (dash lines represent model predictions)

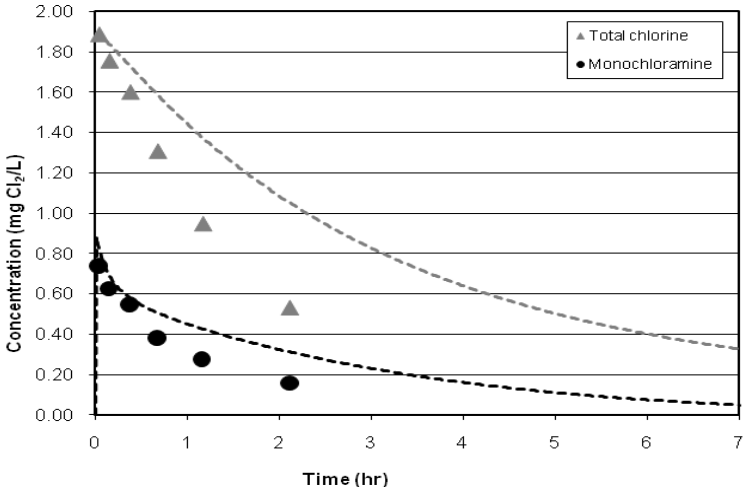

Monochloramine and total chlorine decay (pH = 6.55, $TOTCO_3$= 10 mM, Br^-=1000 µg/L, Cl_2/N=3/1, 30 seconds prechlorination time) (dash lines represent model predictions)

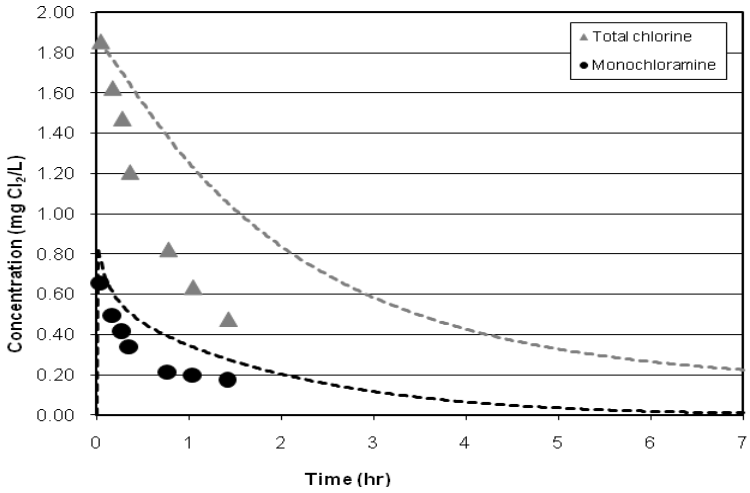

Monochloramine and total chlorine decay (pH = 6.55, $TOTCO_3$= 15 mM, Br^-=1000 µg/L, Cl_2/N=3/1, 30 seconds prechlorination time) (dash lines represent model predictions)

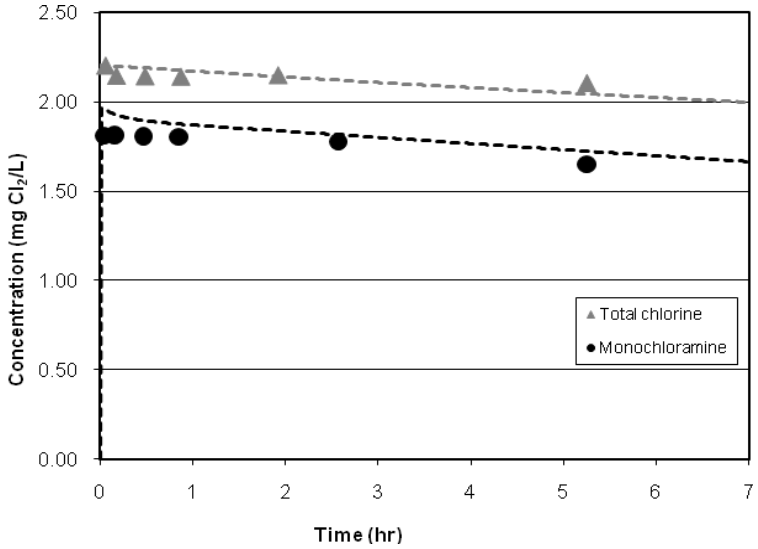

Monochloramine and total chlorine decay (pH = 6.55, $TOTCO_3$= 4 mM, Br-=100 µg/L, Cl_2/N=3/1, 30 seconds prechlorination time) (dash lines represent model predictions)

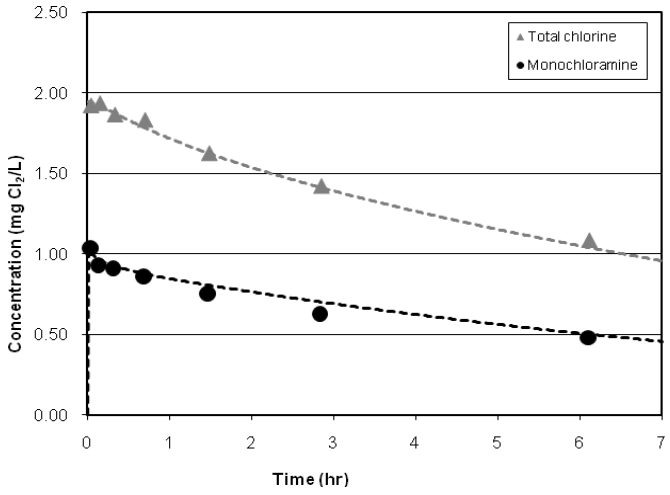

Monochloramine and total chlorine decay (pH = 6.55, $TOTCO_3$= 4 mM, Br^-=1000 µg/L, Cl_2/N=1/1, 30 seconds prechlorination time) (dash lines represent model predictions)

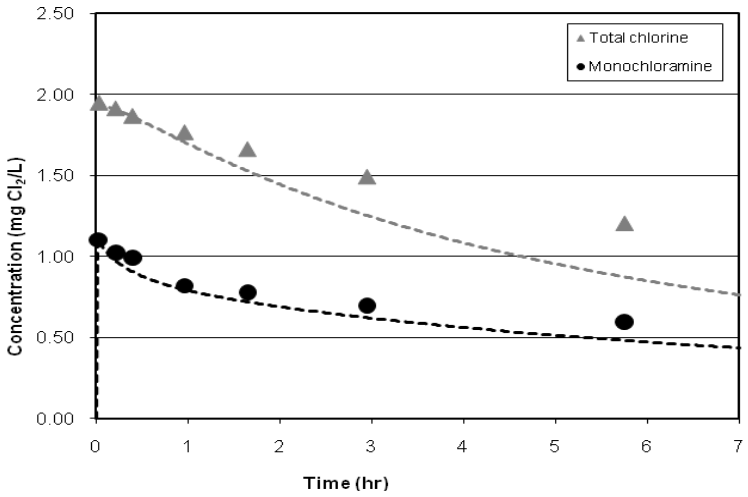

Monochloramine and total chlorine decay (pH = 7.05, $TOTCO_3$= 4 mM, Br^-=1000 µg/L, Cl_2/N=3/1, 30 seconds prechlorination time) (dash lines represent model predictions)

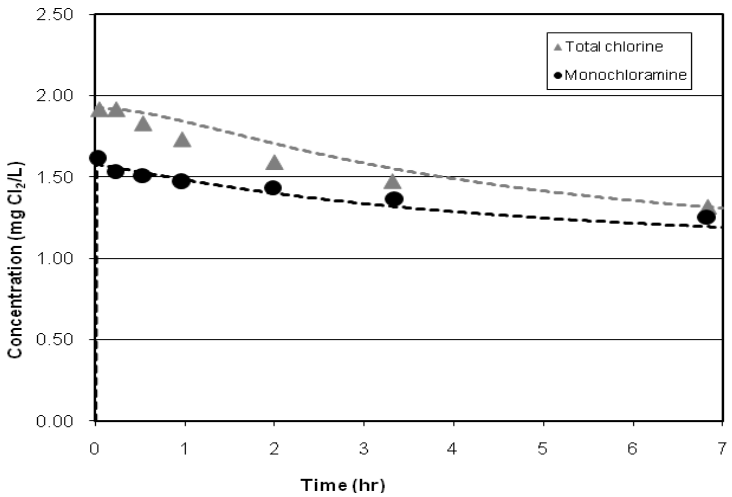

Monochloramine and total chlorine decay (pH = 8.05, $TOTCO_3$= 4 mM, Br^-=1000 µg/L, Cl_2/N=3/1, 30 seconds prechlorination time) (dash lines represent model predictions)

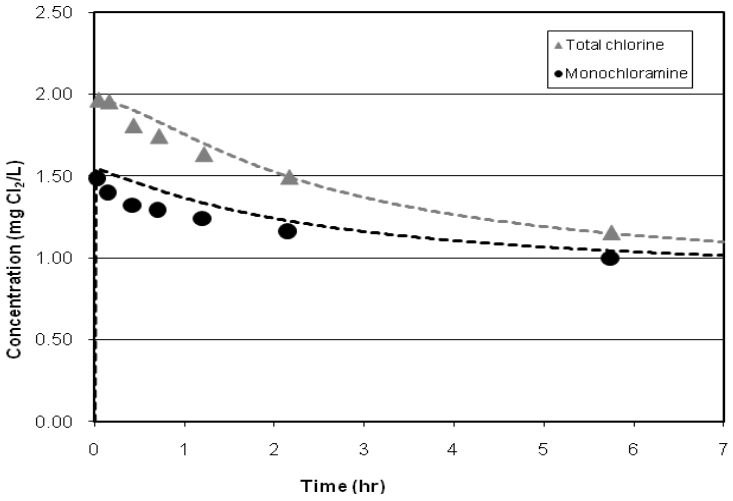

Monochloramine and total chlorine decay (pH = 8.05, $TOTCO_3$= 7 mM, Br^-=1000 µg/L, Cl_2/N=3/1, 30 seconds prechlorination time) (dash lines represent model predictions)

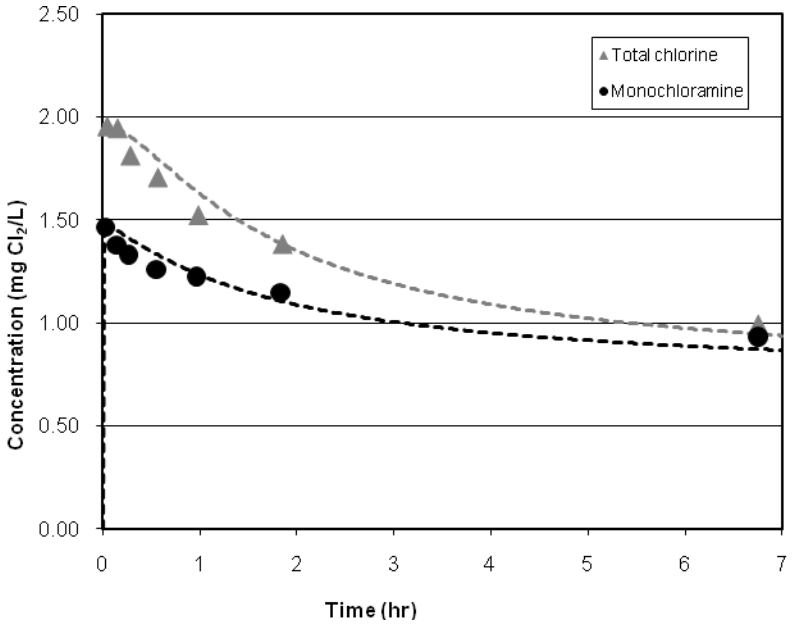

Monochloramine and total chlorine decay (pH = 8.05, $TOTCO_3$= 10 mM, Br^-=1000 µg/L, Cl_2/N=3/1, 30 seconds prechlorination time) (dash lines represent model predictions)

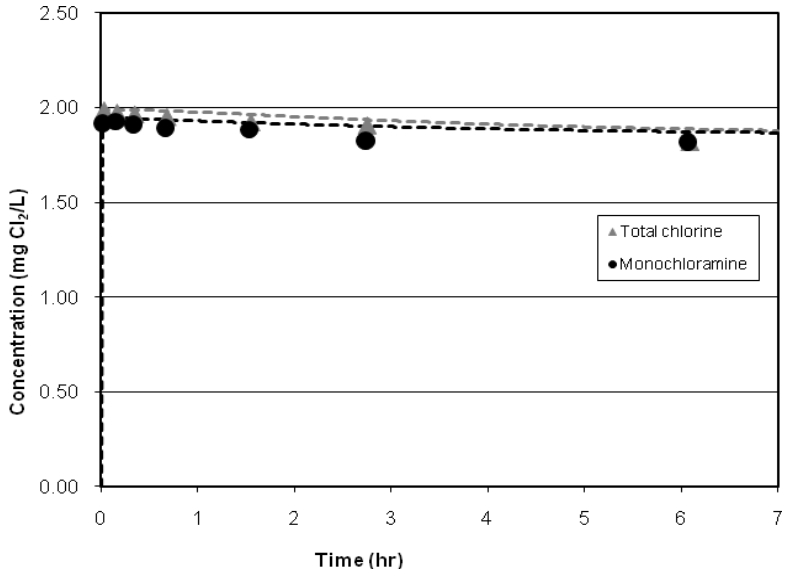

Monochloramine and total chlorine decay (pH = 8.05, $TOTCO_3$= 4 mM, Br^-=100 µg/L, Cl_2/N=3/1, 30 seconds prechlorination time) (dash lines represent model predictions)

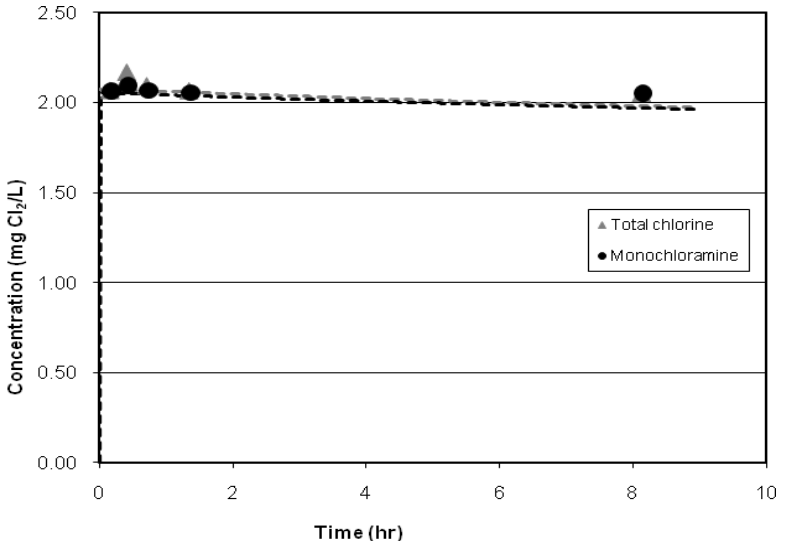

Monochloramine and total chlorine decay (pH = 8.05, $TOTCO_3$= 4 mM, Br^-=100 µg/L, Cl_2/N=3/1, seconds pre-Ammonia) (dash lines represent model predictions)

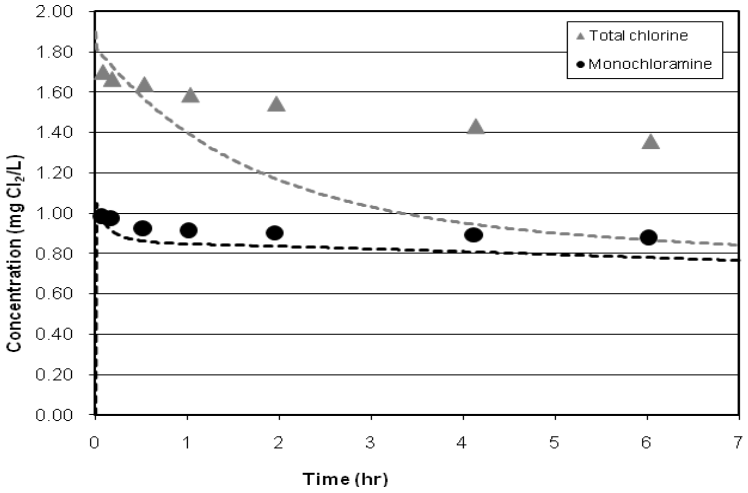

Monochloramine and total chlorine decay (pH = 6.50, $TOTCO_3$= 4 mM, Br^-=1000 µg/L, Cl_2/N=3/1, 2 mg/L Lake Austin NOM, 30 seconds prechlorination time) (dash lines represent model predictions)

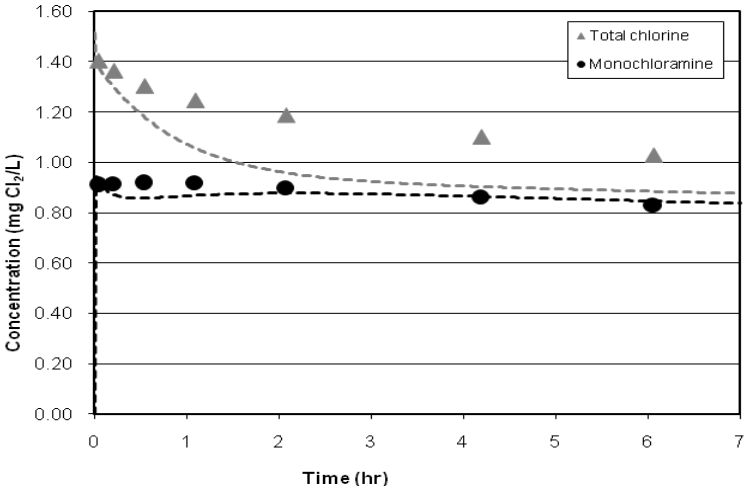

Monochloramine and total chlorine decay (pH = 6.50, $TOTCO_3$= 4 mM, Br^-=1000 µg/L, Cl_2/N=3/1, 5 mg/L Lake Austin NOM, 30 seconds prechlorination time) (dash lines represent model predictions)

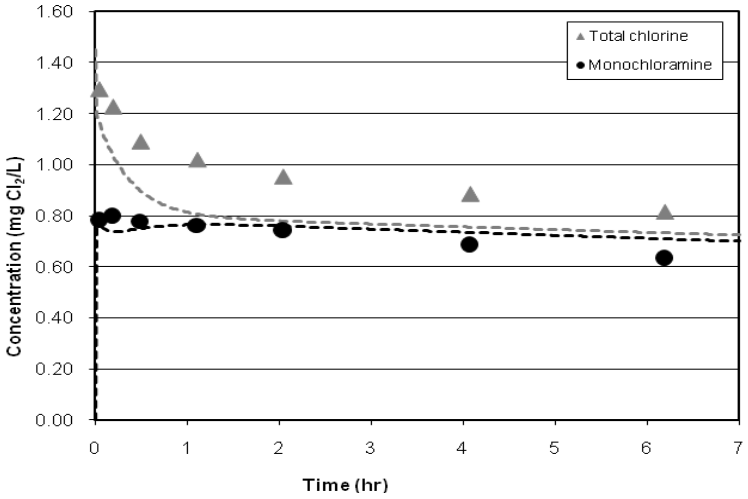

Monochloramine and total chlorine decay (pH = 6.50, $TOTCO_3$= 4 mM, Br^-=1000 µg/L, Cl_2/N=3/1, 10 mg/L Lake Austin NOM, 30 seconds prechlorination time) (dash lines represent model predictions)

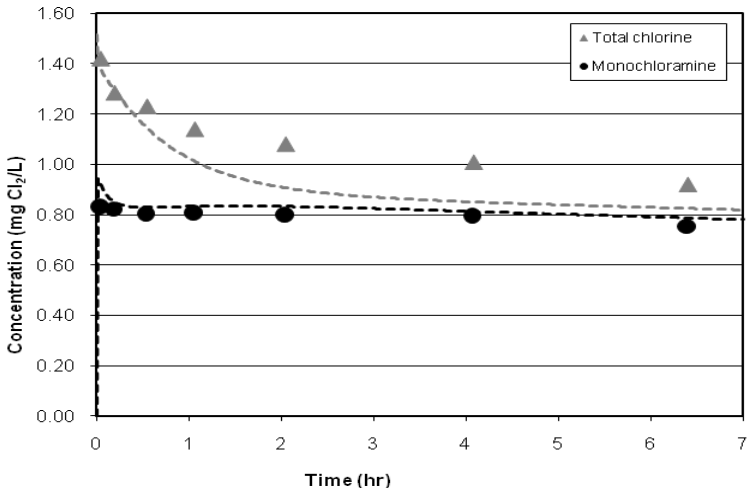

Monochloramine and total chlorine decay (pH = 6.50, $TOTCO_3$= 7 mM, Br^-=1000 µg/L, Cl_2/N=3/1, 5 mg/L Lake Austin NOM, 30 seconds prechlorination time) (dash lines represent model predictions)

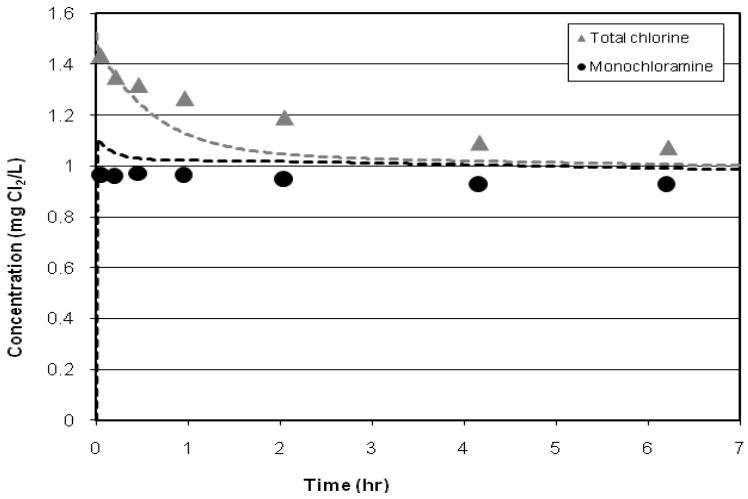

Monochloramine and total chlorine decay (pH = 7.0, $TOTCO_3$= 4 mM, Br^-=1000 µg/L, Cl_2/N=3/1, 5 mg/L Lake Austin NOM, 30 seconds prechlorination time) (dash lines represent model predictions)

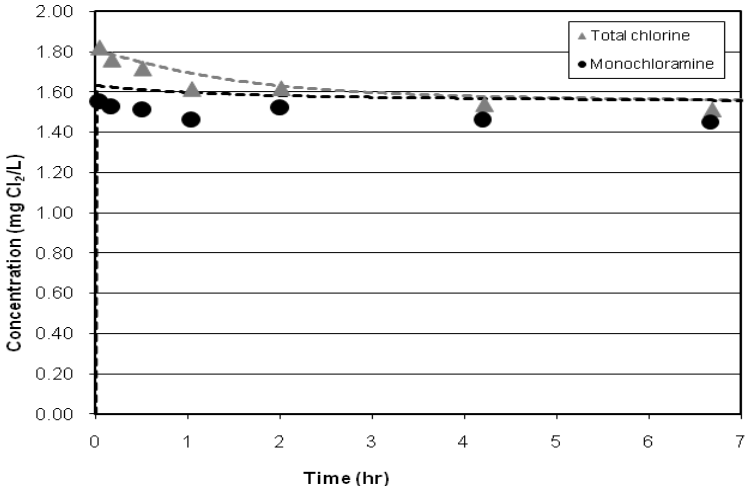

Monochloramine and total chlorine decay (pH = 8.0, $TOTCO_3$= 4 mM, Br^-=1000 µg/L, Cl_2/N=3/1, 2 mg/L Lake Austin NOM, 30 seconds prechlorination time) (dash lines represent model predictions)

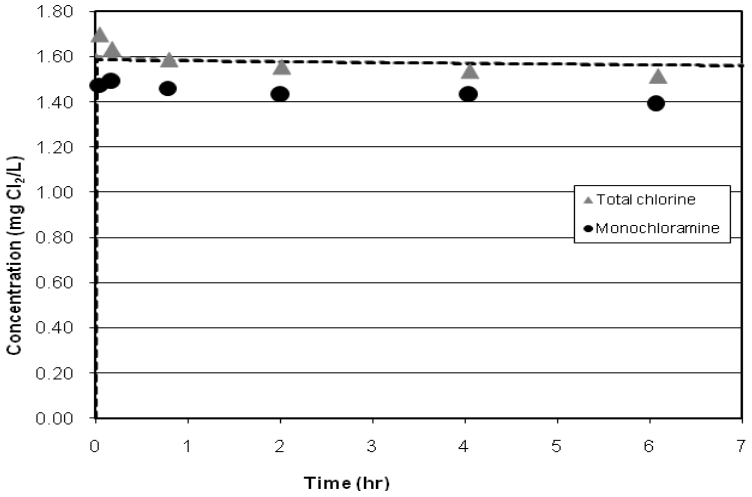

Monochloramine and total chlorine decay (pH = 8.0, $TOTCO_3$= 4 mM, Br^-=1000 µg/L, Cl_2/N=3/1, 5 mg/L Lake Austin NOM, 30 seconds prechlorination time) (dash lines represent model predictions)

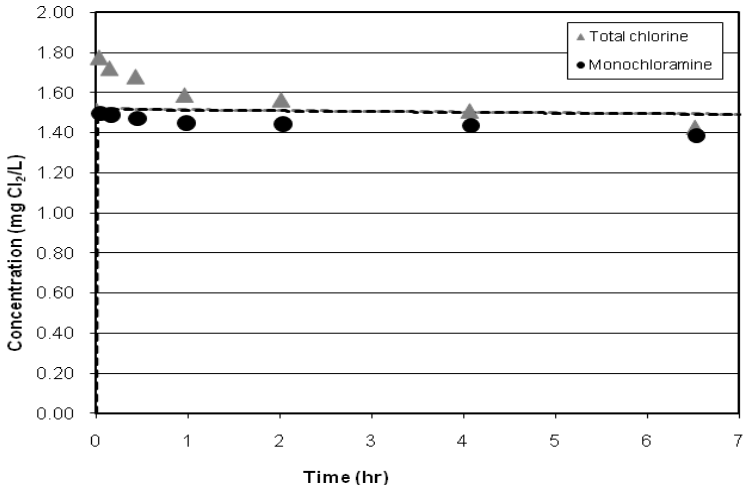

Monochloramine and total chlorine decay (pH = 8.0, $TOTCO_3$= 4 mM, Br^-=1000 µg/L, Cl_2/N=3/1, 10 mg/L Lake Austin NOM, 30 seconds prechlorination time) (dash lines represent model predictions)

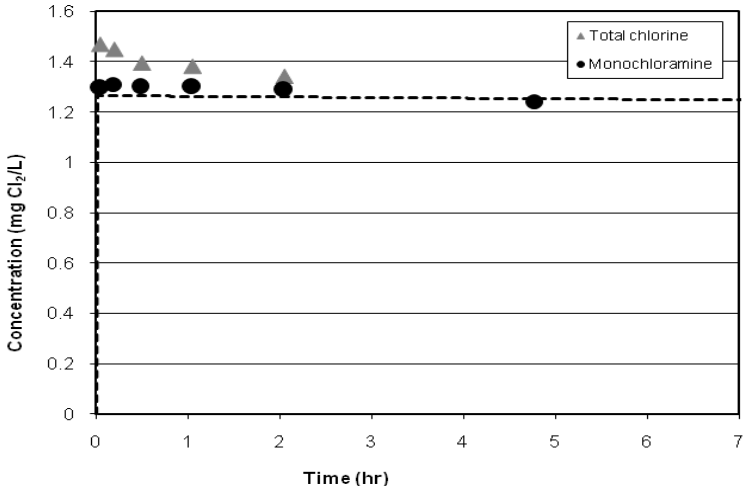

Monochloramine and total chlorine decay (pH = 8.0, $TOTCO_3$= 7 mM, Br^-=1000 µg/L, Cl_2/N=3/1, 5 mg/L Lake Austin NOM, 30 seconds prechlorination time) (dash lines represent model predictions)

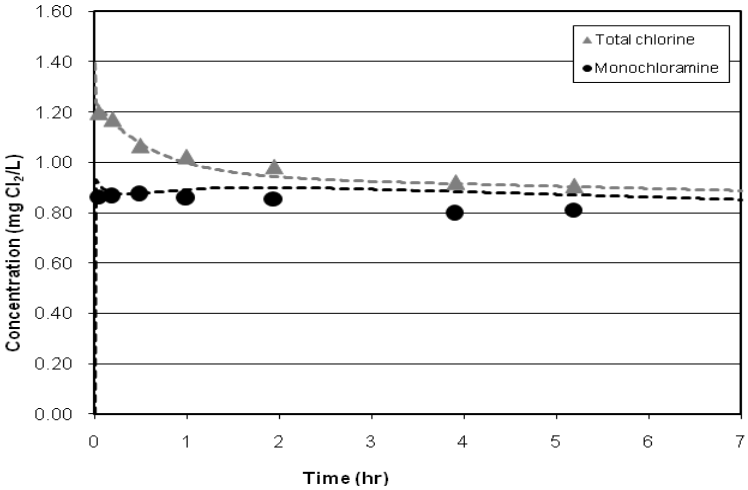

Monochloramine and total chlorine decay (pH = 6.5, $TOTCO_3$= 4 mM, Br^-=1000 µg/L, Cl_2/N=3/1, 5 mg/L Claremore Lake NOM, 30 seconds prechlorination time) (dash lines represent model predictions)

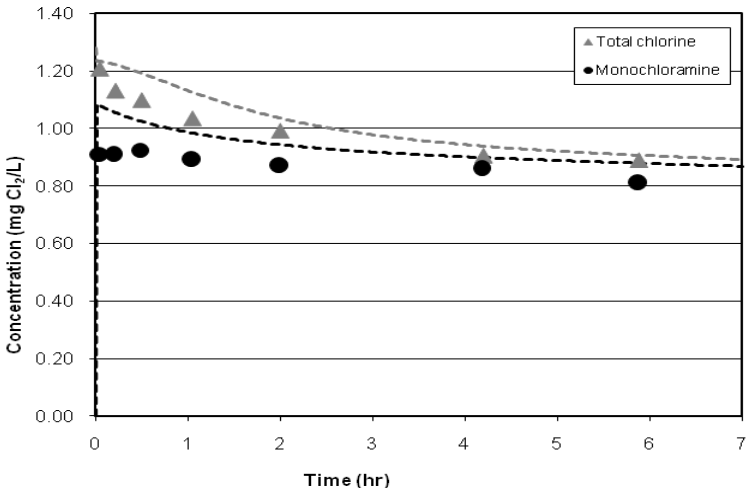

Monochloramine and total chlorine decay (pH = 7.0, $TOTCO_3$= 4 mM, Br^-=1000 µg/L, Cl_2/N=3/1, 5 mg/L Claremore Lake NOM, 30 seconds prechlorination time) (dash lines represent model predictions)

References

Aiken, G. R.., D. M. McKnight, K. A. Thorn, and E. M. Thurman. 1992. Isolation of Hydrophilic Organic Acid from Water Using Nonionic Macroporous Resins. *Organic Geochemistry* 18(4): 567-573.

Bousher, A., P. Brimblecombe, and D. Midgley. 1986. Rate of Hypobromite Formation in Chlorinated Seawater. *Water Research* 20(7): 865-870.

Bousher, A., P. Brimblecombe, and D. Midgley. 1989. Kinetics of Reactions in Solutions Containing Monochloramine and Bromide. *Water Research* 23(8): 1049-1058.

Bousher, A., P. Brimblecombe, and D. Midgley. 1990. Bromate Production in Chlorinated Waters: Reaction of Monochloramine and Hypobromite. *Water Research* 24(10): 1285-1294.

Brønsted, J. N. 1924. *Acid and Basic Catalysis*. University of Copenhagen, Denmark

Buffle, M.O, S. Galli, and U. Von Gunten. 2004. Enhanced Bromate Control during Ozonation: The Chlorine-Ammonia Process. *Environ. Sci. & Technol*., 38: 5187-5195.

Chang, E. E., Y. P. Lin, and P. C. Chiang. 2001. Effect of Bromide on the Formation of THMs and HAAs. *Chemosphere*., 43: 1029-1034.

Chen, Zhuo and R. L. Valentine. 2006. Modeling the Formation of N-Nitrosodimethylamine (NDMA) from the Reaction of Natural Organic Matter (NOM) with Monochloramine. *Environ. Sci. & Technol*., 40: 7290-7297.

Deborde, M., U. Van Gunten. 2008. Reaction of Chlorine with Inorganic and Organic Compounds During Water Treatment—Kinetics and Mechanisms: A Critical Review. *Water Research. 42: 13-51*

Diehl, A.C., G.E. Speitel Jr., J.M. Symons, S.W. Krasner, C.J. Hwang, and S.E. Barrett. 2000. Factors Affecting Disinfection By-Product Formation During Chloramination. *Jour. AWWA.* 92(6): 76-90.

Duirk, Stephen E. (2003). Mechanisms and Modeling of Monochloramine Loss, Natural Organic Mater Oxidation, and Disinfectant By-Product Formation in Water. PhD Dissertation, The University of Iowa.

Duirk, S.E., B. Gombert, J. Choi, and R.L. Valentine. 2002. Monochloramine Loss in the Presence of Humic Acid. *J. Environ. Monit.*, 4: 85-89.

Duirk, S.E., B. Gombert, J.P. Croué, and R.L. Valentine. 2005. Modeling Monochloramine Loss in the Presence of Natural Organic Matter. *Water Research* 39 (14): 3418-3431.

Duirk, S.E., and R.L. Valentine. 2006. Modeling Dichloroacetic Acid Formation from the Reaction Between Monochloramine and Natural Organic Matter. *Water Research* 40 (14): 2667-2674.

Duirk, S.E., and R.L. Valentine. 2007. Bromide Oxidation and Formation of Dihaloacetic Acid in Chloraminated Water. *Environ. Sci. & Technol.* 41 : 7047-7053.

Echigo, S., S. Itoh, T. Natsui, T. Araki, and R.Ando. 2004. Contribution of brominated organic disinfection by-products to the mutagenicity of drinking water. *Environ. Sci. & Technol.* 50 (5): 321-328.

Echigo, S. and R. A. Minear 2006. Kinetics of the Reaction of Hypobromous Acid and Organic Matters in Water Treatment Poocesses. *Environ. Sci. & Technol.* 53 (11): 235-243.

Farkas, L., M. Lewis, and R. Bloch. 1949. The Reaction Between Hypochlorite and Bromides. *Journal of the American Chemical Society* . 71 1988-91

Gadza, M., L.E. Dejarmi, T.K. Chowdury, R.G. Cooks, and D.E. Margerum. 1993. Mass Spectrometric Evidence for the Formation of Bromochloramine and N-Bromo-N-chloromethylamine in Aqueous Solution. *Environ. Sci. Technol.*, 27(3): 557-561.

Gadza, M. and D.E. Margerum. 1994. Reactions of Monochloramine with Br_2, Br_3^-, HOBr, and OBr^-: Formation of Bromochloramines. *Inorganic Chemistry*, 33/118-123.

Gerwe, C.E. (2003). Natural Organic Matter (NOM) Adsorption onto and Coprecipitation with Solids Formed During Softening. PhD Dissertation, The University of Texas at Austin.

Haag, W. R. and J. Hoigne. 1983. Ozonation of Bromide-Containing Waters: Kinetics of Formation of Hypobromous Acid and Bromate. *Environ. Sci. & Technol.*, 17(5), 261-267.

Hach Company, *Water Analysis Handbook*, 4th Edition, Loveland, CO, 2003.

Hand, V. C. and D.W. Margerum. 1983. Kinetics and Mechanisms of the Decomposition of Dichloramine in Aqueous Solution. *Anal. Chem.*, 22(10), 1449-1456.

Hofmann, R. and R.C. Andrews. 2001. Ammonical Bromamines: A Review of their Influnce on Bromate Formation Durnig Ozonation. *Wat. Res.*, 35(3), 599-604.

Hwang, C.J., M.J. Sclimenti, and S.W. Krasner. 2000. Disinfection By-Product Formation Potential of Natural Organic Matter Fractions of a Low-Humic Water. In *Natural Organic Matter and Disinfection By-Products: Characterization and Control in Drinking Water*. Edited by S.E. Barrett, S.W. Krasner, and G.L. Amy. Washington, D.C.: ACS.

Inmam, G.W., and J.D. Johnson. 1984. Kinetics of Monochloramine Disproportionation-Dibromamine Formation in Aqueous Ammonia Solutions. *Environ. Sci. & Technol*., 18(4):219-224.

Isaac, R.A., and J.C. Morris. 1983. Transfer of Active Chlorine and Chloramine to Nitrogenous Organic Compounds. 1. Kinetics. *Environ. Sci. & Technol*., 17(12):738-742.

Jacangelo, J.G., N.L. Patania, K.M. Reagan, E.M. Aieta, S.W. Krasner, and M.J. McGuire. 1989. Ozonation: Assessing Its Role in the Formation and Control of Disinfection By-products. *Jour. AWWA*, 81(8): 74-84.

Jafvert, Chad T. (1985). A Unified Chlorine-Ammonia Speciation and Fate Model. PhD Dissertation, The University of Iowa.

Jafvert, C.T. and R.L. Valentine. 1987. Dichloramine Decomposition in the Presence of Excess Ammonia. *Wat. Res.*, 21(8), 967-973.

Jafvert, C.T., and R.L. Valentine. 1988. General Acid Catalysis of Monochloramine Disproportionation. *Environ. Sci. & Technol*., 22:691-696.

Jafvert, C.T., and R.L. Valentine. 1992. Reaction Scheme for the Chlorination of Ammoniacal Water. *Environ. Sci. & Technol*., 26:577-586.

Kranser, S. W., R. Yates, C. J. Gabelich, and S. Liang. 2007. Evaluation of Alternative Bromate Control Stratefies. *Proceedings - Annual Conference, American Water Works Association.*

Kumar, K. and D.W. Margerum. 1987 "Kinetics and Mechanism of General-Acid-Assisted Oxidation of Bromide by Hypochlorite and Hypochlorous Acid," *Inorganic Chemistry, 26*(16): 2706-2711.

Leao, S. F. 1981. Kinetics of Combined Chlorine: Reaction of Substitution and redox. Ph.D. Dissertation, University of California, Berkely, CA.

Leenheer, J.A. and J.P. Croue. 2003. Characterizing Dissolved Aquatic Organic Matter. *Environ. Sci. & Technol.*, 37(1), 18A-26A.

Lei, H. (2003). Bromamine Decomposition and Cyanogen Bromide Formation in Drinking Water from Monobromamine and Formaldehyde. PhD Dissertation, The University of Illinois at Urbana-Champaign.

Lei, H., B.J. Marinas, and R.A. Minear. 2004. Bromamine Decomposition Kinetics in Aqueous Solutions. *Environ. Sci. & Technol.*, 38(7), 2111-2119.

Pope, P. G.; Martin-Doole, Melanie; Speitel, Gerald E., Jr.; Collins, M. Robin. Relative significance of factors influencing DXAA formation during chloramination. *Journal - American Water Works Association* (2007), 99(9), 144-156.

Pope, P. G. (2006). Haloacetic Acid Formation and Control During Chloramination. PhD dissertation, The University of Texas at Austin.

Qiang, Z., and C.D. Adams. 2004. Determination of Monochloramine Formation Rate Constant with Stopped-Flow Spectrophometry. *Environ. Sci. & Technol*., 38: 1435-1444.

Qualls, R. G. and J. D. Johnson. 1983. Kinetics of the Short-Term Consumption of Chlorine by Fulvic Acid. *Environ. Sci. & Technol.* 17 (11): 692-698.

Scientist®3.0. Version 3.0. Software Package. Micromath. Salt Lake City, UT.

Snoeyink, Vernon L. and D. Jenkins. 1980. *Water Chemistry*. Jon Wiley & Sons, New York.

Speitel, G.E. Jr. 1999. Control of Disinfection By-Product Formation Using Chloramines. In: *Formation and Control of Disinfection By-Products in Drinking Water*, P.C. Singer (ed.), American Water Works Association, Denver, CO.

Symons, J.M., S.W. Krasner, L.A. Simms, and M Sclimenti. 1993. Measurement of THM and Precursor Concentrations Revisited: The Effect of Bromide Ion. *Jour. AWWA* 85(1): 51-62.

Symons, J.M., G.E. Speitel Jr., C.J. Hwang, S.W. Krasner, S.E. Barrett, A.C. Diehl, R. Xia. 1998. *Factors Affecting Disinfection By-Product Formation During Chloramination*. Report No. 90728 American Water Works Association Research Foundation, Denver, CO.

Teefy, S., C. Peña, B. Grntry, I. Najm, and A. Mofidi. 2008. Comparison of Bromate Control Strategies: pH Suppression vs. Chloramine Addition. *Proceedings - American Water Association WQTC Conference.*

Trofe, T.W., G.W. Inman, and J.D. Johnson. 1980. Kinetics of Monochloramine Decomposition in the Presence of Bromide. *Environ. Sci. & Technol.*, 14(5): 544-549.

Valentine, R.L. 1983. The Dissapearance of Chloramines in the Presence of Bromide and Nitrite. Ph.D. Dissertation. University of California-Berkley.

Valentine, R.L. 1986. Bromochloramine Oxidation of N,N-Diethyl-p-phenylenediamine in the Presence of Monochloramine. *Environ. Sci. & Technol*., 20(2):166-170.

Valentine, R.L., Brandt, K.I., and Jafvert, C.T. 1986. A Spectrophotometric Study of the Formation of an Unidentified Monochloramine Decomposition Product. *Wat. Res*., 20(8) : 1067-1074.

Valentine, R.L., K. Ozekin, and P.J. Vikesland. 1998. *Monochloramine Decomposition in Distribution System and Model Waters*. Report No. 90721 American Water Works Association Research Foundation, Denver, CO.

Vikesland, P.J., K. Ozekin, and R.L. Valentine. 1998. Effect of Natural Organic Matter on Monochloramine Decomposition: Pathway Elucidation through the Use of Mass and Redox Balances. *Environ. Sci. & Technol*., 32(10):1409-1416.

Vikesland, P.J., K. Ozekin, and R.L. Valentine. 2001. Monochloramine Decay in Model and Distribution System Waters. *Water Research* 35(7): 1766-1776.

Von Gunten, U. and J. Hoigné. 1994. Bromate Formation During Ozonation of Bromide-Containing Water: Interaction of Ozone and Hydroxyl Radical Reactions. *Environ. Sci. Technol* 28: 1234-1242.

Wert, E. C., J. J. Neemann, D. Johnson, D. Rexing, and R. Zegers. 2007. Pilot-Scale and Full-Scale Evaluation of the Chlorine-Ammonia Process for Bromate Control During Ozonation. *Ozone: Sci. and Eng.* 29: 363-372.

Westerhoff P., P. Chao, and H. Mash. 2004. Reactivity of Natural Organic Matter with Aqueous Chlorine and Bromine. *Water Research. 38: 1502-1513*

Yang, X. and Shang, C. 2004. Chlorination Byproduct Formation in the Presence of Humic Acid, Model Nitrogenous Organic Compounds, Ammonia, and Bromide, *Environ. Sci. & Technol*., 38(19):4995-5001.

Vita

Abdalrahman Daham Alsulaili was born in Jahra, Kuwait on July 29, 1979. After completing his work at Alwaha High School, he attended Kuwait University. He received the degree of Bachelor of Science in Civil Engineering with Class Honors from Kuwait University in January 2002. In January 2002, he entered graduate school at the Kuwait University in the Civil Engineering program, and he received his Master's Degree in July 2004. In 2005, he was awarded a scholarship from Kuwait University to perform his doctoral studies at the University of Texas at Austin with an invitation to return to Kuwait University as a professor.

Permanent address: Kuwait, Alwaha, Block 3, Street 1, House 9

This dissertation was typed by author.